Active Surface Deformation Technology for Management of Marine Biofouling

by

Phanindhar Shivapooja

Department of Biomedical Engineering
Duke University

Date: _____

Approved:

_____
Gabriel P. López, Co-Supervisor

_____
William Monty Reichert, Co-Supervisor

_____
Daniel Rittschof

_____
Stefan Zauscher

_____
Ashutosh Chilkoti

Dissertation submitted in partial fulfillment of
the requirements for the degree of Doctor
of Philosophy in the Department of
Biomedical Engineering in the Graduate School
of Duke University

2016

ABSTRACT

Active Surface Deformation Technology for Management of Marine Biofouling

by

Phanindhar Shivapooja

Department of Biomedical Engineering
Duke University

Date: _____

Approved:

_____
Gabriel P. López, Co-Supervisor

_____
William Monty Reichert, Co-Supervisor

_____
Daniel Rittschof

_____
Stefan Zauscher

_____
Ashutosh Chilkoti

An abstract of a dissertation submitted in partial
fulfillment of the requirements for the degree
of Doctor of Philosophy in the Department of
Biomedical Engineering in the Graduate School of
Duke University

2016

Abstract

Biofouling, the accumulation of biomolecules, cells, organisms and their deposits on submerged and implanted surfaces, is a ubiquitous problem across various human endeavors including maritime operations, medicine, food industries and biotechnology. Since several decades, there have been substantial research efforts towards developing various types of antifouling and fouling release approaches to control bioaccumulation on man-made surfaces. In this work we hypothesized, investigated and developed dynamic change of the surface area and topology of elastomers as a general approach for biofouling management. Further, we combined dynamic surface deformation of elastomers with other existing antifouling and fouling-release approaches to develop multifunctional, pro-active biofouling control strategies.

This research work was focused on developing fundamental, new and environment-friendly approaches for biofouling management with emphasis on marine model systems and applications, but which also provided fundamental insights into the control of infectious biofilms on biomedical devices. We used different methods (mechanical stretching, electrical-actuation and pneumatic-actuation) to generate dynamic deformation of elastomer surfaces. Our initial studies showed that dynamic surface deformation methods are effective in detaching laboratory grown bacterial biofilms and barnacles. Further systematic studies revealed that a threshold critical

surface strain is required to debond a biofilm from the surface, and this critical strain is dependent on the biofilm mechanical properties including adhesion energy, thickness and modulus. To test the dynamic surface deformation approach in natural environment, we conducted field studies (at Beaufort, NC) in natural seawater using pneumatic-actuation of silicone elastomer. The field studies also confirmed that a critical substrate strain is needed to detach natural biofilm accumulated in seawater. Additionally, the results from the field studies suggested that substrate modulus also affect the critical strain needed to debond biofilms. To sum up, both the laboratory and the field studies proved that dynamic surface deformation approach can effectively detach various biofilms and barnacles, and therefore offers a non-toxic and environmental friendly approach for biofouling management.

Deformable elastomer systems used in our studies are easy to fabricate and can be used as complementary approach for existing commercial strategies for biofouling control. To this end, we aimed towards developed proactive multifunctional surfaces and proposed two different approaches: (i) modification of elastomers with antifouling polymers to produce multifunctional, and (ii) incorporation of silicone-oil additives into the elastomer to enhance fouling-release performance.

In approach (i), we modified poly(vinylmethylsiloxane) elastomer surfaces with zwitterionic polymers using thiol-ene click chemistry and controlled free radical polymerization. These surfaces exhibited both fouling resistance and triggered fouling-

release functionalities. The zwitterionic polymers exhibited fouling resistance over short-term (~hours) exposure to bacteria and barnacle cyprids. The biofilms that eventually accumulated over prolonged-exposure (~days) were easily detached by applying mechanical strain to the elastomer substrate. In approach (ii), we incorporated silicone-oil additives in deformable elastomer and studied synergistic effect of silicone-oils and surface strain on barnacle detachment. We hypothesized that incorporation of silicone-oil additive reduces the amount of surface strain needed to detach barnacles. Our experimental results supported the above hypothesis and suggested that surface-action of silicone-oils plays a major role in decreasing the strain needed to detach barnacles. Further, we also examined the effect of change in substrate modulus and showed that stiffer substrates require lower amount of strain to detach barnacles.

In summary, this study shows that (1) dynamic surface deformation can be used as an effective, environmental friendly approach for biofouling control (2) stretchable elastomer surfaces modified with anti-fouling polymers provides a pro-active, dual-mode approach for biofouling control, and (3) incorporation of silicone-oils additives into stretchable elastomers improves the fouling-release performance of dynamic surface deformation technology. Dynamic surface deformation by itself and as a supplementary approach can be utilized biofouling management in biomedical, industrial and marine applications.

Dedication

I would like to dedicate this dissertation to my parents. I am thankful to my mother and father, Aruna and Chandra Mouli Shivapooja, for their endless love, support and encouragement throughout my life. I should thank my brother, Shashidhar Shivapooja, who always helps me and has been my best cheerleader. Lastly, I would also like to dedicate this dissertation to my almost-one-year-old adorable niece, Shanvi Shivapooja.

Contents

List of Tables

List of Figures

Acknowledgements

I express my deepest appreciation to Dr. Gabriel P. López, academic adviser and research mentor. I started working in Dr. López's lab as an early-stage graduate student researcher at University of New Mexico. His guidance and trust in my abilities allowed me to expand my horizons and boosted my confidence to do PhD at Duke University. Dr. Lopez always encouraged me to explore new innovative ways to solve scientific problems, which nurtured my thinking process and interest towards research. I am sincerely thankful to Dr. Lopez for always keeping me on my toes; reviewing my progress; and giving thorough feedback whenever needed. His straightforwardness and humor kept me comfortable to talk to him. Dr. Lopez has been a shining example to me on how to become a truly amazing scientist while maintaining high ethical standards.

I would like to thank Dr. Xuanhe Zhao for his research collaboration, enthusiasm and active support. Collaboration with Dr. Zhao had a great, unique and positive influence on the way I conducted my research. His mentorship taught me to enhance research productive by designing experiments in a way so that that every minute spent in the lab is directed towards achieving project goals. I would also like to thank Zhoa's student (now Prof.), Qiming Wang, with whom I worked very closely.

I would to like to thank Dr. Daniel Rittschof for all his collaboration, help and wisdom that benefited my research at Duke. I appreciate his generosity for offering me a

summer tuition fellowship at the Duke University Marine Laboratory, so that I could spend time with him and get trained on conducting field studies of our newly developed technology for marine biofouling management. Dr. Rittschof always delivered quick and thorough reviews for our co-authored manuscripts. Research collaboration with Dan's lab has been a great help to advance my PhD research and to spend time at Beaufort, NC. I would also like to extend my appreciation to Beatriz Orihuela who works in Dan's lab and provided me technical assistant while conducting laboratory experiments.

I would also like to thank Dr. Stefan Zauscher for allowing me to use various instruments in his lab for all these years. He has been always there to greet me and ask about the progress of my research. He always coined interesting questions about my research, which made me to think deeper about the fundamental concepts related to polymer science and surface chemistry. I would also like to thank Dr. Zauscher for giving me the opportunity to work as a teaching assistant and as a guest lecturer for his graduate course - theoretical and applied polymer science.

Dr. Monty Reichert has been my department adviser and encouraged me to join the CBTE certificate program. He provided all the external support that I needed to fulfill my degree requirements. He gave valuable suggestions whenever I reached out to him, and has been an active member of my research committee. I am deeply thankful for Dr. Reichert's support and encouragement.

I would like to thank all the post-doctorate researchers and the graduate students in Lopez lab at Duke University. I have always enjoyed working with all of them; it was an honor to be part of such an active, competitive and hard-working research laboratory. I would also like to thank my friend Padma Priya who encouraged me to join Duke University. I'm greatly thankful to my dearest friends, Naresh and Raj who always stood by my side and boosted me with their encouragement. Finally, I would like to thank the Office of Naval Research and National Science Foundation's Research Triangle Material Research Science and Engineering Center for the financial support of this research for all these years. Once again, I would like to convey my sincere regards to Dr. López, who financially supported me through his research grants for all the years I worked with him.

1. Chapter 1: Introduction, scope of research and specific aims

This dissertation will be publicly available after a one-year embargo period.

1.1 Biofouling

Biofouling or biological fouling is often defined as the unwanted accumulation and growth of biomolecules, cells, organisms, and their deposits on man-made surfaces.[1-4]. It is a worldwide problem, encountered in an extremely wide range of situations, and is generally problematic in all human endeavors where water based liquids are in contact with other materials. Marine biofouling in particular has been known since mankind began sailing the seas due to the adverse impact to shipping throughout the ages. Biofouling is a complex phenomenon and often involves 'biofilm' formation as a key step. Biofilms (slimes) are formed on surfaces by agglomeration of micro-fouling organism (e.g., bacteria, unicellular algae, barnacle larvae and *Ulva* spores) that are held together by extracellular polymeric substances [1, 3]. Biofilm have various adverse effects on the performance and lifetime of man-made surfaces [5]. In marine environments, the buildup of biofilms on vessels occurs very rapidly (within hours) and involves complex growth mechanisms, mainly due to the presence of robust and diverse range of fouling species that prefer surface colonization. Marine biofilms further promotes the attachment and growth of larger macro-fouling organisms (e.g., barnacles and mussels), which have a much higher economic impact on the naval

industry [6]. Biofouling currently costs more than $1 billion per annum to the US Navy alone [7]. It leads to significant maintenance and time costs in various other industries also, such as petroleum and natural gas refining, paper manufacturing, food processing, underwater construction, and desalination [8-10]. Undesired infectious biofilms are often observed on medical devices and implants and can be formed by plethora of bacterial species that opportunistically infect hosts, causing health issues that can require expensive medical intervention [7, 10]. For example, there are more than one million cases of catheter-associated urinary tract infections reported each year in the US hospitals and nursing homes, many of which can be attributed to biofilm-associated bacteria [11]. Hence, biofouling in general is a serious problem, affecting a multitude of industrial processes and maritime equipment. As a result, there is currently a huge array of research enterprises aimed towards prevention and control of biofouling on man-made materials.

1.2 Scope of Research

The control of biofouling on submerged surfaces in marine environments is a considerable challenge: fouling organisms are opportunists and have evolved many mechanisms to attach and proliferate on a range of surfaces in the natural, often turbulent, marine environment. This research was focused on developing fundamental, new and environment-friendly approaches for biofouling management with emphasis on marine model systems and applications, but which also provided fundamental

insights into the control of infectious biofilms. One of the central goals for this work was to develop and investigate the use active surface deformation of elastomers as a technology to promote easy release of accumulated fouling species. This research demonstrated that dynamic surface deformation can be generated using different types of external stimuli (e.g., electro-actuation and pneumatic-actuation), which produced controlled surface strain and facilitated the de-bonding of fouling species. One of the unique advantages of the dynamic surface deformation is the applicability of this technology as a complementary approach to existing and developing coating technologies used for biofouling management in marine settings, and other approaches contemplated in the medical settings [12]. The scope of this research further extended to demonstrating multifunctional approaches for biofouling management, by combining the dynamic surface deformation with other anti-fouling or fouling-release strategies such as tethered anti-fouling polymer brushes and incorporation of diffusible silicone-oil additives. While, the various studies presented in this work were focused on marine biofouling, the concepts, approaches and technologies developed have direct implications for managing biofouling in other areas as well (e.g., industrial piping and medical devices).

1.3 Specific Aims

1.3.1 Specific Aim 1: Dynamic actuation of elastomer surfaces to detach biofilms and barnacles

This work explored the use of dynamic change in surface area and topology of soft deformable elastomers for fouling release. In order to generate controlled surface deformation, we first employed the use of electro-actuation of substrate-bonded elastomer film, a mechanism previously reported by Zhao *et al.* [13]. The studies were conducted using laboratory grown model marine bacteria biofilms and electro-actuation of silicone-based coatings. The preliminary results obtained from these studies, led to a new hypothesis that a critical surface strain is required to de-bond biofilm from the substrate. This hypothesis was extensively investigated in fundamental studies, in which elastomers were stretched to varied amount of strain to detach two different types of biofilms of varying thickness. A second objective of this aim was focused towards the use of soft-robotic inspired, pneumatic-actuation (i.e., using pressure in elastomeric chambers to selectively actuate specific surface regions of a device) of elastomers as an alternative means to generate surface strain to detach both model bacterial biofilms and adult barnacles. The detailed discussion of the approaches and findings of these studies are presented in Chapter 3.

Another objective of this aim included the use of dynamic surface deformation for marine fouling release in the field environment. This work was conducted at the field-test site of the Duke University Marine Laboratory (Beaufort, NC). In brief, the

samples for this study were comprised of silicone elastomers of two different substrate moduli that were submerged in the natural marine environment for prolonged time-periods (weeks), and then pneumatically actuated to varied amounts of surface strain. The release of natural biofilms accumulated in the field environment was compared with that of laboratory–grown biofilms, and also the influence of elastomer modulus on biofilm detachment was investigated. The detailed discussion of the approaches and experimental findings of this study are presented in Chapter 4.

Specific Aim 1 Hypotheses Addressed:

(1) Biofilm detachment using electro-actuation is caused by surface deformation and not due to the applied voltage.

(2) Surface deformation has to reach a certain critical amount of strain to detach biofilm.

(3) Dynamic surface deformation of elastomers by pneumatic actuation can effectively detach both crustacean and non-crustacean fouling species.

1.3.2 Specific Aim 2: Chemical modification of dynamic elastomer surfaces to develop multi-functional biofouling management systems

This work integrated polymer brushes that have fouling-resistant properties with the elastomer networks that are capable of dynamic deformation and fouling release. Such bifunctional surfaces enable the use of both fouling-resistant and fouling-release strategies for biofouling management. In our work, poly(vinylmethylsiloxane) elastomers were successfully modified with zwitterionic polymer brushes using UV-

assisted thiol-ene click chemistry [14] and controlled radical polymerization [15]. The systematic studies and findings of this research are presented in Chapter 5. The results obtained from these studies supported our hypothesis that zwitterionic polymers grafted from silicone surfaces can resist biofouling over the short-term; when fouling eventually occurs, the deformation of the silicone substrate facilities fouling-release. Other previously used methods for grafting polymer brushes to silicones would likely not be as effective, because they rely on surface oxidation of the silicone to form an inelastic silica interfacial layer. As a whole, this new approach provides both new applications of cutting edge chemistry, as well as a new paradigm for highly effective dual-mode control of biofouling, which can be implemented with a wide range of fouling-resistant surfaces that eventually all succumb to fouling in real world applications.

Specific Aim 2 Hypotheses Addressed:

(1) ARGET-ATRP can be used to graft polymer brushes from vinyl containing cross-linked elastomer surfaces by functionalizing them with a thiol-based ATRP initiator.

(2) PVMS grafted with zwitterionic polymers will imbue fouling resistant properties to the elastomer.

(3) Dynamic deformation of zwitterionic polymer modified silicones will detach biofilms that accumulate over prolonged exposure and will also regenerate the anti-fouling properties of zwitterionic polymers.

1.3.3 Specific Aim 3: Incorporation of silicone-oil additives in stretchable silicone elastomers to improve fouling-release performance

This study investigated the combined effects of surface deformation and silicone-oil additives for biofouling management using silicone elastomers. It hypothesized that silicone-oil additives incorporated into stretchable elastomers can reduce the amount of substrate strain needed to detach barnacles.

Non-reactive silicone-oil additives of various types and compositions are often used in silicone elastomers because they elute to surface of the coating and serve as a slip agent, and thereby reduce the adhesion of fouling organisms such as barnacles [16, 17]. Moreover, recent studies have shown the silicone-oils can also interfere with the curing process of the biological adhesive secreted by various fouling organisms and lower their adhesive strength [18]. Hence, this study attempted to explore the benefit of using both silicone-oil additives and surface deformation on barnacle detachment. Another objective of this study was to investigate the effect of silicone-oil additives on elastomer modulus because barnacle adhesion strength is also dependent on substrate modulus [19]. Specifically, we decoupled the effect of surface activity of silicone-oils and the change in modulus (due to silicone-oil additives) on barnacle adhesion strength. The

findings of the studies conducted for this aim are presented in Chapter 6. The results support the hypothesis that use of silicone-oil additives in the silicone elastomers can significantly lower the substrate strain required to detach barnacles. We also showed that change in modulus due to silicone-oil increases the strain required to detach barnacles, while surface activity of silicone-oil additives significantly reduces the barnacle adhesion strength. The combined effect of silicone-oils and substrate deformation provides an effective, and two-pronged strategy for biofouling management.

Specific Aim 3 Hypothesis Addressed:

(1) Incorporation of silicone-oil additives into elastomers reduces the amount of substrate strain required to detach barnacles in dynamic surface deformation approaches.

2. Chapter 2: Marine biofouling: background, significance and control strategies

Biofouling in a marine environment is a highly dynamic process. Surfaces, upon submersion in these environments, become colonized by a wide range of fouling organisms, resulting in the formation of complex biofilms as well as macrofouling [2]. This chapter presents an overview of various factors that influence surface colonization, which in turn promote the buildup of problematic biofilms and macrofouling. The economic and ecological impacts of marine biofouling and the methods used for biofouling control are also discussed.

2.1 Marine biofouling

2.1.1 Key steps involved in surface colonization and biofilm growth

Marine biofouling involves a vast diversity of fouling organisms. It is reported that more than 4,000 species have been identified on fouled structures worldwide [20]. Biofouling occurs over length scales from molecular dimensions to centimeters (see Figure 1). Surfaces submerged in seawater are rapidly conditioned (within minutes) by organic molecules and matter from the marine environment [21]. The initial steps in attachment of fouling organisms involves the location of a surface by the organism, exploration of the surface, and then adhesion, which occur at length scales specific to the organisms. The dimensions of fouling organisms during their settling stages (bacteria, cells, spores, or larvae) are typically 500 nm to 100 μm (see Figure 1), but the recognition

of surface cues through the relevant sensory structures probably occurs at much smaller length scales (i.e., at the subcellular and molecular level). These complex events eventually result in the formation of early-stage biofilms (slime), and can consist of bacteria, larvae, spores and soft fouling unicellular algae, which can be co-agglomerated by polymeric substances secreted by the organisms. Colloidal models [22-24] and movement tracking [25, 26] are examples for methods employed by researchers to understand the settlement behavior of micro-foulers, however, the exact bio-interfacial mechanisms that direct initial attachment to substrata is still unclear for most marine organisms.

Slimy biofilms in their later stage can result in macro-fouling, which includes the attachment of more complex fouling organisms comprising of both "soft" and "hard" foulers such as mussels, tubeworms, macro-algae and barnacles [2]. It should be noted that the colonization of different fouling species is often synergistic. For example — bacterial biofilms are important, but not necessary, initiators for the successful settlement of marine invertebrates [27]. Thus, biofouling is a highly heterogeneous and dynamic process that provides ecological advantages for the biofilm mode of life.

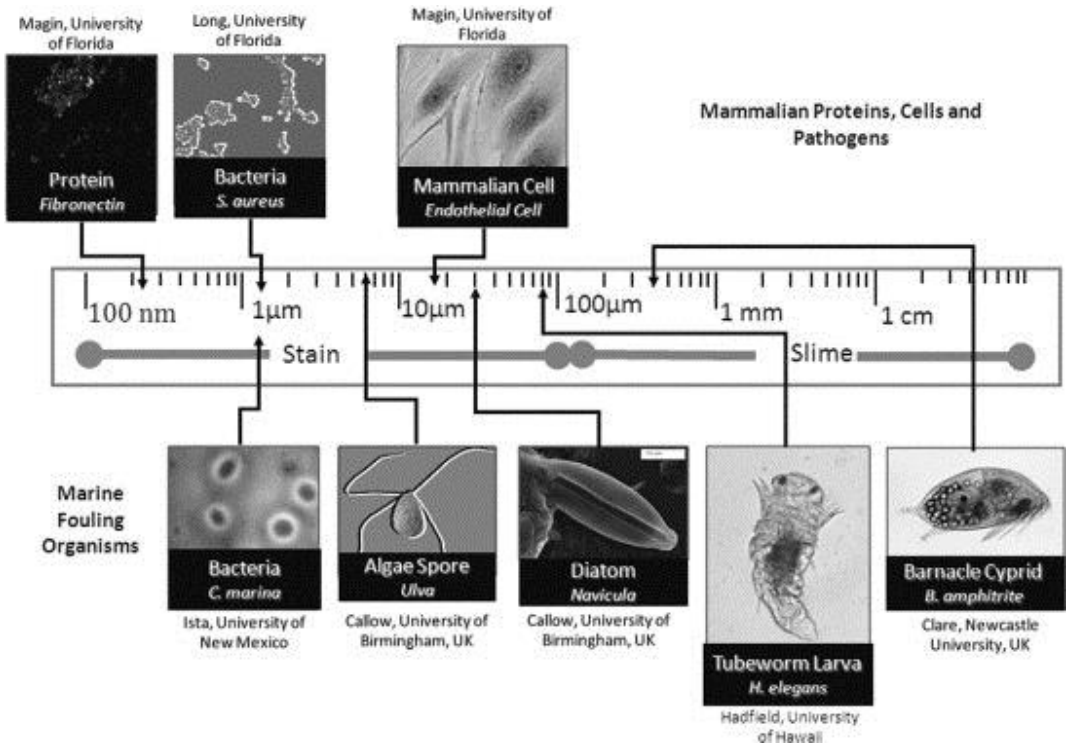

Figure 1: Schematic demonstrating the hierarchy of fouling organisms. Cells and compounds relevant to biomedical applications are shown above the scale axis. Marine organisms are shown below the scale. Reproduced with permission from Magin *et al.* 2010 [28]. Copyright Elsevier 2015.

2.1.2 Effect of substrate properties on initial attachment of fouling organisms

Surface charge, chemistry and energy

The settlement of fouling organisms is often influenced by the physico-chemical properties of the substrate on which they adhere. A systematic search and classification of non-fouling surfaces carried out by Whitesides and co-workers concluded that hydrogen bond acceptors promote non-fouling properties [22, 29, 30]. This has been shown not to be a universal rule [31], but the pioneering work by Whitesides and co-workers guided later studies such as those of polysaccharides [32],

oligo(ethylene glycol)s [22] and zwitterions [33] for anti-fouling properties. Self-assembled monolayer (SAM) surfaces provide an elegant and reproducible way of systematically modifying surface energy, surface wettability and surface chemistry and have been used by researchers to screen/develop new materials with better antifouling properties [34]. One other major advantage is that the complexity to disentangle surface chemistry and elastic properties is reduced, since in contrast to polymeric bulk materials, the elastic modulus of the SAM-coated surface is dominated by the substrate.

Physical properties, such as surface charge have a significant effect on the settlement and adhesion of fouling species. For instance, Rosenhahn *et al.* [35] demonstrated that electrostatic interactions directly influence adhesion of *Ulva* spores. They showed number and strength of adherent spores was dependent on the sign (positive or negative) and density of charge implanted into poly(tetrafluoroethylene) (PTFE) surfaces; with the negatively charged surface showing a reduction in settlement as compared to uncharged and positively charged PTFE substrates. This behavior was attributed to the surface negative charge (≈ - 19 mV) carried by *Ulva* spores. In case of barnacle larvae, as reported by Petrone *et al.* [36], the settlement was much higher on the negatively charged surfaces (-COOH) SAM surfaces and relatively much lower on positively charged ($N(CH_3)_3^+$) SAM surfaces. Based on the above two examples, it can be implied that settlement behavior of the microbial fouling species is influenced by the sign (positive or negative) and density of the surface charge on both, the substrata and

the fouling species. Surface charge is also known to influence the adhesion strength of the microbes on the surfaces. For example, Ederth *et al.* [37] investigated the settlement behavior of *Ulva* spores onto cationic oligopeptide self-assembled monolayers (SAMs) and suggested that settlement of spores to be stimulated by positive charge (i.e., lysine- and arginine-rich) oligopeptide SAMs, but the attachment was in an anomalous fashion; meaning the spores were "pseudo-settled" and are relatively easily detachable from the surfaces, as they do not undergo the full settlement process [38].

Another physicochemical parameter affecting bacterial adhesion and biofilm formation is surface energy, commonly measured with the help of contact angles measurements of water (and other polar and non-polar organic solutions). There are various approaches to calculate the surface free energy from the contact angle measurements, a comprehensive review on these approaches has been provided by Hejda *et al.* and others [39, 40]. The interfacial tension of water with a solid has a profound effect on the interaction of the submerged surface with macromolecules and colloids. This has been discussed in a comprehensive review by Vogler [41], where he makes reference to the so-called "Berg Limit" which defines the transition from an attractive to an inert or repulsive regime of surface energies and contact angles at 30 dyn cm^{-1} or $\theta_{water} \approx 65°$. At lower surface tensions (or higher contact angles) the surfaces become attractive to adhesion, whereas at higher (lower) values the interaction becomes negligible [41]. Baier *et al.* published similar observations much earlier for protein,

bacterial and tissue adhesion [42-44]. For bacterial adhesion, Baier *et al.* reported that the biomass on a surface does not depend linearly on the surface energy of the polymer substrate, but that there is a range of surface energies (20–30 mJ m^{-2}), where adhesion is minimal [43]. At higher surface tension (at > 30 dyn cm^{-1}) they observed again an increase in bacterial adhesion. In contradiction to Baier's conclusions, bacterial settlement studies by Absolom *et al*. [45] revealed that the adhesion of four different bacterial strains (*Staphylococcus aureus*, *Staphylococcus epidermidis*, *Escherichia coli*, and *Listeria monocytogenes*) on a range of solid substrates (Teflon®, polyethylene, polystyrene, and acetylated and sulfonated polystyrene) follow a linear relationship between surface energy and bacterial adhesion. There are also other notable studies in the literature that showed results that are in contradiction to Baier's theory. In this context, our research group (Ista and Lopez *et al.*) has previously reported that attachment of model fouling bacterium, *Cobetia marina*, proceeded linearly with respect to decreasing surface energy on a series of SAMs surfaces composed of methyl terminated thiolates (CH_3) diluted with either hydroxyl (OH) or carboxylic acid (COOH) terminated thiolates [46]. A systematic change of wettability using varying compositions of mixed mercaptoundecanol (–OH terminated) and dodecanethiol (–CH_3 terminated) SAMs on gold, indicated that *Ulva* zoospores avoided settling on hydrophilic surfaces [46-48]. The increase of *Ulva* zoospore adhesion with increasing contact angle depends on the surface composition of the mixed –OH/–CH_3 terminated alkanethiol SAM [47].

However, although more cells settled on the hydrophobic CH_3-rich SAMs, they were less strongly adhered than to the hydrophilic surfaces [48]. To add to the confusion, if water contact angles are a good indicator for bioadhesion, we note that the diatom Amphora adhered more strongly to the hydrophobic methyl-terminated SAM and less strongly to the hydrophilic hydroxyl-terminated SAM [48]. Also, in the field studies, the effect of surface energy was found to differ based on the fouling species. For example, bryozoans preferentially settled on surfaces with low energy (10–30 $mN \cdot m^{-1}$), barnacles on surfaces with high energy (30–35 $mN \cdot m^{-1}$) and hydroids in equal proportion on surfaces of all energies [49, 50]. In general, the settlement and adhesion of fouling organisms may decrease or increase with increasing surface energy of substrates, depending on the physical and chemical properties of bacteria, substrates, and water solutions [46, 51].

Surface roughness

Substrate roughness and porosity may also play a role in the settlement of fouling organisms on immersed surfaces as the surface irregularities generated increase the surface area that can be potentially colonized. The valleys of rough surfaces may also be penetrated by marine bioadhesives, which cure to create a secure mechanical lock. Thus, it may be considered that, the rougher a coating surface becomes, the more likely it is to be fouled [52]. Moreover, surface irregularities may provide a suitable environment for the development of bacteria and other marine organisms as they are

protected in these confined areas from exterior aggressions, shear and abrasion, thus making their removal by a hydrodynamic action difficult [52]. In contrast to this notion, Brennan *et al.* have proposed and developed engineered surface-roughness, which are analogous to micro-topographies observed on sharks, and provides a bio-inspired, non-toxic approach for biofouling control [28, 53].

2.1.3 Diversified dispersal stages and adhesion mechanism of fouling species

More than four thousand fouling organisms have been identified worldwide [54]. Among them, bacteria, diatoms, and algae spores are the main microorganisms that settle on ship hulls, while barnacles, tubeworms, bryozoans, mussels, and algae are the most common macro-organisms. The problem of biofouling and its control is also attributed to the diverse dispersal stages of various fouling organisms, rather than the adult forms. Larvae of invertebrates and spores of algae can quickly find and bind to a surface as a key part of the organism's life cycle. This adhesion process can take place within seconds, under water, to a wide range of substrates, over a wide range of temperatures and salinities, and in conditions of turbulence. This phase of initial, or first-contact, adhesion to a substrate has been observed for a diverse range of single- and multi-cellular fouling organisms [55]. In certain cases the adhesion is effectively permanent; in other cases adhesion needs to be temporary as the organism moves around on a surface to find the most appropriate settlement site. An understanding of

the cellular and molecular processes and materials involved underpins much of contemporary basic research in marine fouling.

Biological adhesives consist of biomolecular materials that, typically, are protein complexes involved in firm underwater attachment. The interaction between an adhesive material (secreted by the foulant) and the substrate involves two main steps – (i) wetting of the substrate by the adhesive, and (ii) curing of the adhesive. The wetting process determines the area of contact between the adhesive and the substrate. The curing process determines the microstructure of the solidified film, thus influencing both the mechanical properties and the adhesive strength. The molecular and curing properties of the adhesives secreted by foulants have been recently studied for a few species, notably mussels and barnacles. The protein glues of the blue mussel comprises a dihydroxyphenylalanine (DOPA)-rich family of polypeptides, which cross-link through an oxidative phenolic tanning-type process [56]. In case of barnacles, the cement produced by mature adult barnacles consists of a complex of hydrophobic proteins that are unrelated to the blue mussel proteins, and are cross-linked via cysteine residues [18, 57]. It is generally believed that representatives of all the phyla of marine foulants use sticky materials with permanent or temporary adhesive capabilities, but adhesion mechanisms and detailed molecular characteristics of these glues are, thus far, largely unknown.

2.1.4 Environmental factors

Several environmental factors influence the settlement of marine fouling on surfaces, including salinity, pH, temperature, nutrient levels, shear, and the intensity of solar radiation. These factors vary seasonally, spatially, and with depth [54]. Colonization and succession of biofouling communities are highly affected by seasonality, with less fouling in winter, generally, due to the reduction in seawater temperature, sunlight, and the numbers of spores and larvae [6]. From spring to late summer, seawater temperature and nutrient levels increase, leading to a higher fouling pressure. Fewer variations of the water temperature and the light intensity are observed in marine tropical and subtropical oceans than in polar areas, resulting in high pressure of fouling throughout the year [58]. Generally, the same major groups of organisms are responsible for fouling worldwide, but the dominant species involved tend to vary from region to region.

2.2 Impact and consequences of marine biofouling

Accumulations of micro- and macro-organisms generate surface roughness and irregularities, which increase the frictional resistance of a boat moving through water and consequently increase fuel consumption and emission of greenhouse gases. Schultz *et al.* showed that even slime films can lead to significant increases in hydrodynamic resistance and fuel consumption [59]. It is estimated that antifouling coatings provide the shipping industry with annual fuel savings of $60 billion and reduced emission of

carbon dioxide and sulfur dioxide of 384 million and 3.6 million tons per annum, respectively [60].

Treatment of biofouling necessitates an increase of the frequency of dry-docking operations, either because of the need of hull cleaning, coating replacement or hull repair [61]. Transport of fouling organisms on hull vessels is also a major issue that can lead to the introduction of invasive species into non-native environments [62]. The impacts of this phenomenon can be ecological and evolutionary, and can lead to direct and indirect competition with native species, to higher trophic levels, and to changes of ecosystem processes.

Parts of the ship other than the hull are also affected by biofouling, such as external cooling pipes, bridge kneel, sea chest, bow thrusters, anchor lockers, propellers and ballast systems. For instance, sea water can also come into contact with the interior of vessels during its use as a coolant for a ship's power plant; it leads to buildup of biofouling on heat transfer equipment and results in drastic reductions in its performance, up to 30% in a matter of months [63]. Biofouling is huge problem for various other maritime equipment as well, including under-water sensors [64], buoys [65], sonar devices [66], offshore structures [67], oil platforms [68], underwater cables [69] and marinas [5]. For example, in case of oceanographic sensors biofouling leads to reduced sensitivity and quality of measurements [9, 64]. Biofouling is also known to

increase the rate of corrosion of metal by acid-producing, peroxide producing and sulfate reducing bacteria in the slimy biofilm-matrix [70, 71].

2.3 Methods to control biofouling

Surface coatings that are being used for biofouling management are broadly categorized in to antifouling coatings and fouling-release coatings. Antifouling coatings function by the release of broad-spectrum biocides, which kill the fouling organisms and thereby inhibit biofouling. Fouling-release coatings do not prevent organisms from attaching, but dramatically reduce their adhesion strength so that the attached species are easily removed by the hydrodynamic shear forces generated by movement of a ship through the water, by water jets, or by gentle 'grooming' devices. In both cases the objective is to achieve the desired result (i.e., control biofouling). Below, I present a comprehensive overview of existing and emerging technologies related to antifouling and fouling-release coatings.

2.3.1 Conventional approaches

Antifouling coatings

Biocide-based antifouling coatings are currently widely used on ship-hulls. Since antiquity, antifouling coatings have been developed to prevent the settlement of fouling organisms. Pitch, tar, wax or heavy metal-based (lead, arsenic) coatings were the earliest techniques used to prevent biofouling [72]. During the late 1970s, antifouling research and development efforts were mainly focused on the successful tributyltin-based (TBT)-

based self-polishing acrylic-based copolymer systems. However, due to the emergence of environmental issues associated with TBT compounds, tin-free compounds are currently being used as biocides. Following the ban of TBT-based products in antifouling paints, alternatives containing copper-based The key property of a good antifouling biocide with respect to the environment is that it is effective in preventing fouling of the painted surface without persisting at concentrations greater than those that can cause detrimental environmental effects [73].

The current biocide-based antifouling coatings can be divided into three categories according to their release mechanism: contact leaching coatings (insoluble matrix), controlled depletion polymer coatings (soluble matrix) and self-polishing copolymer coatings [54, 74]. In contact leaching coatings, the polymer matrix, is mainly comprise of vinyl, epoxy, acrylic or chlorinated rubber polymer .The toxicants or particles can be incorporated in the coatings and released gradually (see Figure 2a), leaving empty pores that the seawater can permeate through to dissolve the inner toxicant particles. In this case, the release rate gradually decreases over time, reducing the protection effect [74]. The short lifetime (12–24 months) of contact leaching coatings has limited their application. In order to circumvent this problem, soluble matrix coatings were developed by incorporating a large proportion of seawater-soluble binder based on rosin and its derivatives. Once in contact with seawater, the biocides and soluble resins are dissolved and released (see Figure 2b). Controlled depletion polymer

coatings adopt a similar mechanism by using more resistant synthetic organic resins to control the hydration and dissolution of soluble binder. The lifetime can be extended up to 36 months [20, 74].

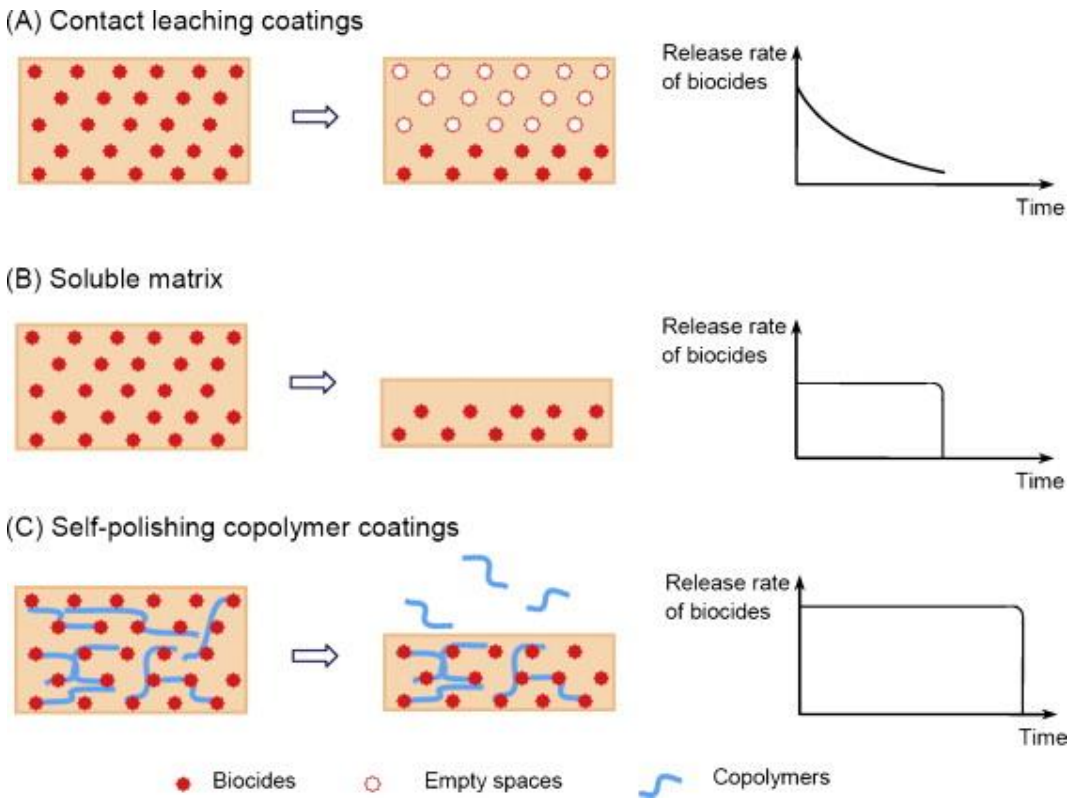

Figure 2: Schematic illustration of the behavior of biocide-based antifouling system. (A) Contact leaching coatings, (B) soluble matrix coatings and (C) self-polishing copolymer coatings. Reprinted with permission from Rittschof et al. 2014 [75]. Copyright: Elsevier 2015.

Self-polishing copolymer coatings erode and release the biocide over a sustained period of time (see Figure 2c). Self-polishing coatings use an acrylic or methacrylic copolymer matrix that can be hydrolyzed in seawater to facilitate biocide release and to

keep the surface polished to reduce drag [54]. The attached fouling organisms are removed together with the matrix decomposed by hydrolysis. The release rate of biocides can be controlled by the degree of polymerization and hydrophilic properties of the copolymer binders [75]. Self-polishing coatings have an extended lifetime up to 5 years and currently account for 80% of the market for antifouling paints. Hybrid self-polishing coatings are another type of system, which combines the hydrolyzable self-polishing copolymer technology with the resin-based controlled depletion technology [74]. The biocide release relies on both hydrolysis and hydration mechanisms. Their antifouling effectiveness generally lasts between 3 and 5 years.

Fouling-release coatings

Fouling-release coatings are biocide-free coatings, which rely on 'non-sticky' surface properties [76]. These coatings minimize the adhesion strength between a fouling organism and the substrate, so that the organism can be removed by hydrodynamic stress during navigation or by a simple mechanical cleaning. Moreover, the smoothness of fouling-release coatings enables them to reduce the drag of the vessel and therefore reduce fuel consumption and greenhouse gas emissions. Commercial fouling release coatings are mainly composed of silicones or fluoropolymers [20]. Both these materials exhibit low surface energy and high smoothness, but fluoropolymers are non-porous and relatively hard (higher modulus) as compared to silicones. Due to the lower modulus of silicones, external forces applied to detach foulants can deform the

silicone and result in a peeling mode of adhesive failure, which generally requires less energy than release from fluoropolymers [77]. In the case of silicones, the backbone of the polymer chains, typically poly(dimethylsiloxane) (PDMS), is made of alternating silicon and oxygen atoms (see Figure 3), and are relatively flexible and allows the pedant non-polar methyl groups to be arranged on the surface.

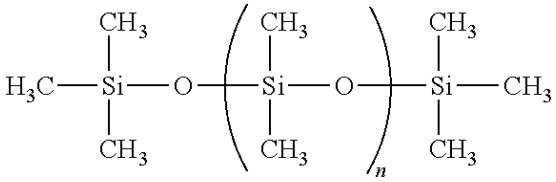

Figure 3: Chemical structure of poly(dimethylsiloxane) polymer backbone.

Current fouling-release coatings are generally deployed as a duplex system composed of a fouling-release top-coat and a tie-coat applied on an anticorrosive epoxy primer (see Figure 4). The topcoat is based on cross-linked PDMS elastomers and usually contains oil additives to enhance their slipperiness. The tie-coat is required to promote the adhesion between the nonstick, fouling-release topcoat and the epoxy primer. These non-polar, low surface energy (~20-30 mN m^{-1}), hydrophobic polymers would be expected to show low adhesion toward polar molecules (including adhesive proteins) because of reduced opportunities for hydrogen-bonding and polar interactions [76, 78, 79].

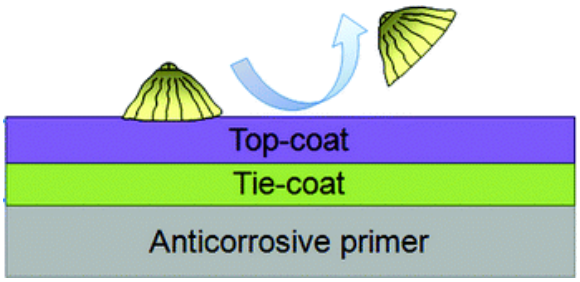

Figure 4: Schematic illustration of a typical FR duplex coating system. Reproduced with permission from Andre et al. 2012 [112]. Copyright: ACS Publications 2015.

Although PDMS exhibits the desired combination of low surface energy and low modulus (to minimize the work of adhesion), such coatings suffer from some disadvantages. Because of their low surface energy, they are difficult to bond to a substrate without an appropriate tie coat. They are less durable (i.e., more easily damaged) than other types of coatings and they frequently 'fail' to brown slimes dominated by diatoms that attach strongly to hydrophobic surfaces [76]. The fouling-release technology is also most effective when applied to frequently used, fast-moving (>15 knot) vessels and is less suitable for vessels that spend long periods in port or which are operated at lower speeds. To improve the durability and fouling-release properties of silicone-based coating numerous synthetic pathways have been attempted in the literature including the incorporation of silicone-oil additives [16, 80] and nano-fillers (e.g., $CaCO_3$, SiO_2) [81]. Fouling-resistant synthetic polymer compounds, such as zwitterionic compounds, have also been introduced into the silicone-matrix [82], with the general aim to create a dynamic and compositional surface complexity that deters

settlement of fouling organisms while reducing the interfacial bonding of adhesive biopolymers.

2.3.2 Emerging approaches

Current technologies employ two basic strategies for non-biocidal coatings — fouling-resistant (deterrence of initial attachment) and fouling release (weaken adhesion strength so the organisms can be easily removed) surfaces. Both strategies, in principle, leave the fouling organisms unharmed and without releasing toxic chemicals into the organism or the marine environment. This section highlights few of the significant research efforts that are directed towards the discovery or improvement of non-toxic, non-fouling coatings as alternatives to those currently used commercially.

Biomimetic surface topography

Surface micro-topographies (see Figure 5a-b) of marine animals (e.g., shark skin and mollusk shells) are speculated to deter biofouling by inhibiting the attachment of barnacles, zoospores and algae [83, 84]. Inspired by this approach, engineering surface micro-topographical surfaces (see Figure 5c) with various feature sizes and geometry have be studied by researchers to enable physical disruption of the adhesion of marine organisms and thus provides a non-toxic antifouling strategy [28, 85-87]. For example, engineered microtopographies (circular pillars with 2 μm feature size in dia., height and periodicity) on PDMS surfaces that mimicked shark skin have been shown to reduce the settlement of *Ulva* spores by 77% [85]. Similarly, Petronis *et al.* [87] showed that pyramid

like microstructures (30-90 μm in dia. and 20-70 μm in height) on PDMS surface inhibited barnacle cyprid settlement by 67% in comparison to smooth PDMS surfaces. In a comprehensive review provided by Magin *et al.* [28] it was concluded the width and spacing of topographical features necessary to deter biofouling must be tailored to the size of the organism.

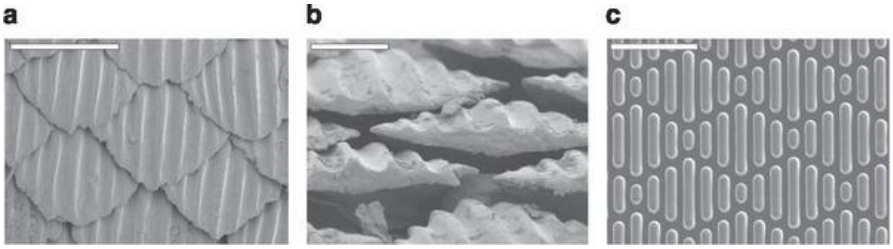

Figure 5: The scanning electron micrographs show the skin denticles of spinner shark in face (a**) and end (**b**) views and (**c**) image of Sharklet AF topography moulded in PDMS. Scale bars are (**a**) 500 μm, (**b**) 250 μm and (**c**) 20 μm. Reproduced with permission from Callow et al. 2011 [76]. Copyright: Nature Publishing Group 2015.**

The change in wettability of a surface due to microtopographical roughness is also likely to be a contributing factor to antifouling properties. The topic of wetting and dewetting on rough surfaces has been thoroughly reviewed by Quéré and colleagues [88]. The application of surface roughness to alter wettability for antifouling coatings especially superhydrophobic coatings has also been reviewed extensively [52, 89, 90]. Long and others have reported recently different engineered microtopographies that exhibited contact angle anisotropy between contact angles measured parallel and perpendicular to the features [90, 91]. This work demonstrates the importance of anisotropy in the design and study of antifouling surfaces. It has been suggested that

microtopographies might also influence near-surface fluid dynamics and thus hydrodynamically prevent settlement [52]. While these studies demonstrated the antifouling potential of microtopographical surfaces in the marine environment, the underlying mechanisms responsible for reduced fouling (i.e., settlement and attachment) remain unclear. Nevertheless, the most developed concept assumes that adhesion strength is related to the number of attachment points of the marine organism on the surface [92, 93]. Genzer and others suggested that a topographical pattern having a single length scale will not likely perform as a generic antifouling surface, since biofouling includes marine organisms with sizes of several orders of magnitude (e.g., bacteira, diatoms, barnacle cyprids) [90]. Since biofouling marine organisms can vary in size over several orders of magnitude (e.g., spores, cells, larvae), hierarchical micro-topographies based on nano- to micro-scale surface topographies are currently being extensively studies [28, 94].

Amphiphilic nanostructured surfaces

Another recent approach in designing experimental coatings for biofouling management has been to create surfaces with chemical heterogeneity at the nanoscale through the thermodynamically driven, self-assembly of polymers, followed by *in situ* crosslinking. Such coatings may be designed using mixtures of block copolymers with contrasting chemistries [95, 96]. The first published example of an amphiphilic coating for use in marine antifouling, reported by Gudipati *et al.* [97], was based on

hyperbranched fluoropolymers and linear poly(ethylene glycols) (PEG), which self-assemble on crosslinking to form complex surface topographies and chemical domains of both nanoscopic and microscopic dimensions. The surface patterns were strongly influenced by immersion and by the relative proportions of the two polymers. The coating design anticipated that this surface complexity would either have a deterrent effect on the settling stages of fouling organisms or would be unfavourable for adsorption and unfolding of adhesive proteins.

Krishnan *et al*. used two types of polystyrene block copolymers, one with poly(ethylene glycol) side-chains and the other with liquid crystalline, fluorinated side-chains, to prepare amphiphilic copolymers with hydrophilic and hydrophobic properties, respectively [96]. Similar to this, Martinelli *et al.* developed amphiphilic fluorinated block copolymers [98] and styrene/PEGylated-fluoroalkyl styrene block copolymer [99]. In both cases, these surface-active block copolymers were deposited as a thin film over a thick layer of an elastomeric thermoplastic material to provide a suitable low modulus. These coatings have been tested in bioassays to explore their intrinsic ability to resist the settlement and reduce the adhesion strength of two marine algae, namely, the macroalga (seaweed) *Ulva* (which has affinity for hydrophilic surfaces) and the unicellular diatom *Navicula* (which prefers hydrophobic surfaces). Both *Ulva* and *Navicula* showed weak adhesion to the amphiphilic surface-active block copolymers coatings compared with a standard fouling-release coating of PDMS.

Surface modification with fouling-resistant and stimuli-responsive polymers

Surface-tethered polymers with fouling-resistant properties have been extensively utilized in biomaterials and biomedical devices. Based on this concept, a variety of functional polymers have been developed for combating marine biofouling with much less environmental impact than traditional biocides. Fouling-resistant polymer coatings are usually prepared from hydrophilic polymers. The high degree of hydration increases the energetic penalty of removing water when biofoulants attach, resulting in resistance to protein adsorption and settlement of fouling organisms [100]. Several hydrophilic polymers such as poly(ethylene glycol) (PEG), hydrogels, and polyzwitterions have been studied for marine antifouling applications [101].

PEG-based polymers have been widely used as antifouling materials. Due to their large exclusion volume, high mobility of hydrated chains and steric hindrance effect, PEG units effectively resist protein and platelet adhesion, as well as cell attachment [102]. Their anti-biofouling efficacies in the marine environment have also been explored [22, 103]. In spite of good anti-adsorption efficacy, PEG is a polyether that oxidizes easily, especially in presence of transition metal ions, and is also susceptible to thermal degradation [104].

Another promising group of chemistries that deter the adsorption of proteins and cells are zwitterionic polymers, such as poly(sulphobetaine) (PSBMA) and poly(carboxybetaine) (PCBMA). In antifouling assays zwitterionic polymers grafted onto

glass surfaces through surface-initiated atom transfer radical polymerization almost completely inhibited the settlement of spores of the green alga *Ulva*; the attachment of diatom cells was also strongly reduced. In both cases, the few cells that did settle were only loosely attached [105]. They also resisted settlement of barnacle larvae [25]. The resistance of zwitterionic materials to the adsorption of proteins and attachment of cells is generally attributed to a strong electrostatically induced hydration layer that creates a superhydrophilic interface. In the case of marine organisms this means that the secreted proteoglycan bioadhesives are unable to achieve a strong bond to the synthetic material by excluding water molecules from the interface. Currently, the development of zwitterionic polymer coatings for marine antifouling application is focused towards incorporation zwitterionic polymers within the backbone of other types of polymers that are currently used for coatings.

Stimuli-responsive polymeric materials [54] are a class of polymers that respond to changes in temperature, pH, light, and ionic strength, and have been widely utilized in developing intelligent or smart materials with great promise in drug delivery systems [3, 7, 55], microfluidic devices [15], and bioadhesion mediators [53, 56, 57]. Previously, our group (Ista, Lopez *et al.*) have shown that thermo-responsive poly(N-isopropylacrylamide) (PNIPAAm) can exhibit fouling release properties [15, 106-108]. PNIPAAm is a well-studied thermally responsive polymer, which undergoes a sharp and reversible phase transition in water at its lower critical solution temperature (LCST

~ 32°C) [58]. The phase transition arises from the entropic gain as water molecules associated with the side-chain isopropyl moieties are released into the bulk aqueous phase as the temperature increases past binodal temperature [54]. By grafting PNIPAAm polymer brushes from standard substrates (e.g., glass and Au), it was shown that model cultured bacteria (e.g., *Staphylococcus epidermidis*, *Cobetia marina*) and their biofilms can be reversibly attached and released by changing the substrate temperature below and above the LCST of PNIPAAm [15, 106, 109].

While many of the above mentioned surface modification strategies seem promising for antifouling applications, there is a budding consensus that all these methods --including SAMs [110], 'sharklet' patterns [111-113], and PEG-based [114], zwitterionic, and super hydrophobic surfaces [115, 116]-- fail upon long term exposure to robust and complex natural marine environment.

2.4 Research Motivation

There are various interesting biological species that have unique surface topography or/and functions to keep their surfaces clean against fouling and infections. Examples include ─ settlement inhibiting micro- and nano-topographies, secreted bioactive molecules, sloughing surface layers, mucus secretions and ciliary cleaning for active fouling management [117, 118]. Though these biological innovations have significant potential as inspirations for anti-fouling technologies, they suffer some inherent disadvantages, such as necessitating complicated fabrication and not being

suitable for harsh fouling environments. In collaboration with Zhao and coworkers, we proposed an approach that can actively and effectively detach micro- and macro-fouling organisms from silicone surfaces through dynamic deformation of surfaces and their topology in response to external stimuli. These dynamic surfaces can be fabricated from materials that are already commonly used in marine coatings and medical devices and have promising practical applications. Secondly, we postulated that it is unlikely that non-biocidal approaches based on coating designs incorporating a single attribute will solve the fouling management problem. One way forward is to design 'multifunctional coatings', incorporating a range of attributes, for example, dynamic deformable surface topography combined with a suitable amphiphilic or zwitterionic surface chemistry that deter settlement of fouling species. Such multifunctional coatings, which synergistically combine fouling-resistance and fouling-release, may be useful for biofouling control in mitigation of marine fouling and various other applications as well, such as preventing the buildup of infectious biofilms in urinary catheters. This research presents a promising new set of studies on using dynamic surface deformation of elastomers for triggered fouling release and in combination with other approaches for biofouling management.

3. Chapter 3: Active deformation of elastomer surfaces for detachment of biofilms and barnacle

This chapter reflects part of the work for Specific Aim 1 and includes electro-actuation and pneumatic-action approaches for biofouling management in laboratory environment. Sections of the text and figures included in Chapter 3 were published in Advanced Materials. The full citation for the article is: P. Shivapooja, Q. Wang, B. Orihuela, D. Rittschof, G.P. López and X. Zhao. Bioinspired surfaces with dynamic topography for active control of biofouling. Advanced Materials, 03 JAN 2013; 25 (10), 1430-1434. Phanindhar Shivapooja was the lead author of this article and was given permission by the publisher, John Wiley and Sons, to reprint this manuscript in this dissertation.

3.1 Synopsis

Dynamic change of the surface area and topology of elastomers is used as a general, environmentally friendly approach for effectively detaching micro- and macro-fouling organisms adhered on the elastomer surfaces. Deformation of elastomer surfaces under electrical or pneumatic actuation can debond various biofilms and barnacles. The bio-inspired dynamic surfaces can be fabricated over large areas through simple and practical processes. This new mechanism is complementary with existing materials and methods for biofouling control.

3.2 Introduction

Biofouling, the accumulation of boiomolecules, cells, organisms and their deposits on submerged and implanted surfaces, is a ubiquitous problem across many human endeavors including maritime operations, medicine, food industries and biotechnology [54, 76, 119]. Examples include: (i) the high cost of mitigation of biofouling on maritime vessels [120], (ii) the growing significance of infectious biofilms (matrix-enclosed microbial adlayers) as a failure mode of implanted materials and devices [119], and (iii) the adaptation of antibiotic resistant bacterial strains within biofilms in medical and industrial settings [121]. Creating environmentally friendly and biocompatible surfaces that can effectively manage biofouling has been an extremely challenging "holy grail". In spite of substantial research efforts for several decades, cost effective control of biofouling is still an elusive goal in all areas that require long-term compatibility with biological systems [54]. Current commercial antifouling approaches and technologies include self-polishing surfaces that rely on controlled release of biocides [73, 108] and fouling-release surfaces [122]. The next generation of fouling management includes specialized surface chemistries [21] and topographic patterns [84, 123] that deter settlement of biofouling organisms. These approaches are generally limited to specific organisms or levels of fouling [21, 76, 119, 120, 124, 125] or have unacceptable impacts on the environment or human health with long-term usage [73].

Nature offers multipronged solutions to biofouling that have not been implemented by humans [126]. An enormous number of biological surfaces clean themselves through active deformation and motion [126-130]. For example, cilia on the surfaces of respiratory tracts constantly sweep out inhaled foreign particles that are sequestered in hydrated, protective mucus layers [127-129]. Ciliary cleaning is also widely used by mollusks, corals and many other marine organisms for active fouling management in marine environments [126, 130]. Engineering surfaces coated with pillars that mimic cilia have been fabricated and proposed for biofouling management [129, 131-134]. Despite their potential, surfaces coated with biomimetic cilia (i) generally require complicated fabrication processes and are thus limited to relatively small areas, (ii) still require development of practical actuation schemes, and (iii) are made of fragile structures not suitable for harsh biofouling environments.

Here, we report a general, bio-inspired approach for actively and effectively detaching micro- and macro-fouling organisms through dynamic change of surface area and topology of elastomers in response to external stimuli. These dynamic surfaces can be fabricated from materials that are already commonly used in marine coatings and medical devices and can be actuated by practical electrical and pneumatic stimuli. New antifouling strategies based on active surface deformation can also be used in combination with other existing and emerging management approaches for biofouling.

3.3 Experimental methods

3.3.1 Fabrication of electro-active surfaces

A rigid polymer substrate, Kapton, (DuPont, USA) with Young's modulus of 2.5 GPa and thickness of 125 μm was sputter-coated with a 10 nm gold layer underneath. A 50 μm polydimethyl siloxane (Sylgard 184 Dow Corning, USA) film was spin coated on top of the Kapton film and cured at 65°C for 12 hours. The cross-linker density of the Sylgard 184 was varied from 2% to 10% to obtain elastomer films with shear moduli ranging from 60 kPa to 365 kPa. The thickness and shear modulus of the films were measured by Dektak 150 Stylus Profiler (Bruker AXS, USA) and a uniaxial tensile tester (TA instruments, USA), respectively. Figure 6 illustrates the schematic of the electro-active surface.

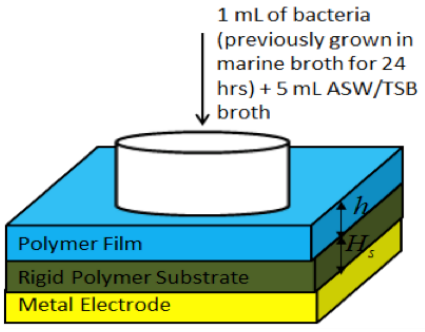

Figure 6: Schematic of the fabricated electro-active surface. Sputter-coated gold is a metal electrode in the bottom, *h* represents the thickness of Sylgard 184 and H_s represents the thickness of Kapton.

3.3.2 Formation of bacterial biofilms

Cobetia marina (*basonym, Halomonas marina*) (ATTC 4741) and *Escherichia coli* (ATTC 15222) in marine broth (MB) (2216, Difco, ATTC, USA) and trypsin soy broth (TSB), respectively, containing 20% glycerol was stored frozen in stock aliquots at -80°C. Artificial seawater was prepared as reported previously [108]. Experimental stock preparations were maintained on agar slants and were stored at 4°C for up to 2 weeks. A single colony from an agar slant was inoculated in MB (50 ml, for *Cobetia marina*) or TSB (50 ml, for *Escherichia coli*) and grown overnight with shaking at 25°C (*Cobetia marina*) or 37°C (*Escherichia coli*). The bacterial concentrations were 7 X 10^7 cells mL^{-1} and 11 X 10^7 cells mL^{-1} for *Cobetia marina* and *Escherichia coli*, respectively.

The surfaces used for growing biofilms were sterilized by rinsing several times with ethanol and then with copious amounts of sterilized DI water. *Cobetia marina* or *Escherichia coli* bacterial culture (1 mL) was placed on the sample surface along with sterilized artificial seawater (5 mL) or TSB broth (5 mL). The samples were stored for a desired period in an incubator maintained at 26 °C for *Cobetia marina* and 37 °C for *Escherichia coli*. The samples were carefully monitored and artificial seawater or TSB broth (about 1 to 2 mL) was added, as needed every day, to compensate for dehydration (Figure 6). The *Cobetia marina* was allowed to form biofilms on the elastomer surfaces for 4 days.

3.3.3 Biofilm thickness measurements

The thickness of the biofilm (see Figure 7) formed on the surface was measured using an inverted confocal microscope (Zeiss LSM 510) equipped with an argon ion laser operating at an excitation wavelength of 488 nm. For imaging, the biofilm was stained using SYTO 13 (see Methods). Using a 40X objective, a series of images were collected across the depth of the biofilm using the Z-stack software module provided by Zeiss. The start and end points for Z-stack imaging were determined by doing a fast XY scan while focusing on and out of the specimen surface; the images were automatically captured at each z-axis depth interval of 3 μm.

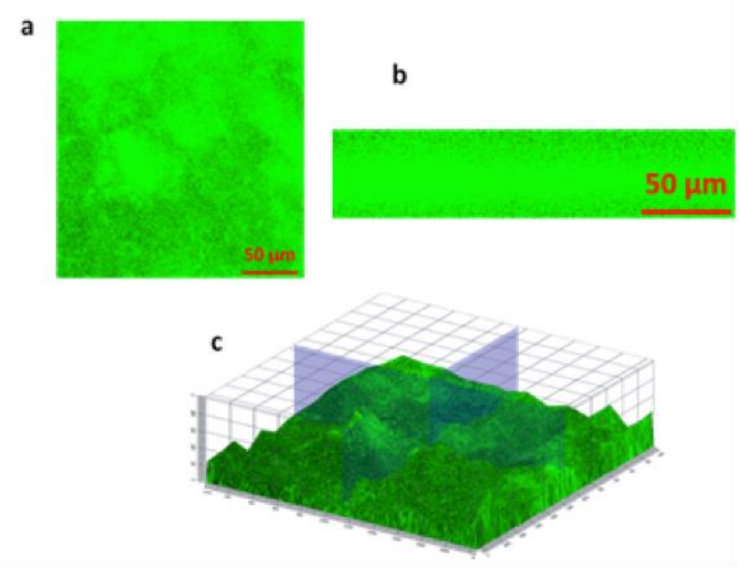

Figure 7: Confocal images of the *Cobetia marina* biofilm grown on Ecoflex for 4 days. (a) Z-stack image of *Cobetia marina* biofilm surface as seen from the top, (b) the cross-sectional view of the biofilm and (c) the 3-D reconstruction image of the biofilm

3.3.4 Effect of shear flow alone on the detachment of biofilms

Biofilms formed on Sylgard 184 surfaces were subjected to a continuous flow of artificial seawater at 0.5 mL/min for 10 minutes as shown in Figure 8a. Analysis of the biofilm surfaces before and after flow did not show any significant detachment of the adhered biofilms as shown in Figure 8b and 7c. The flow alone was only able to remove the detached biofilm without electro-actuation.

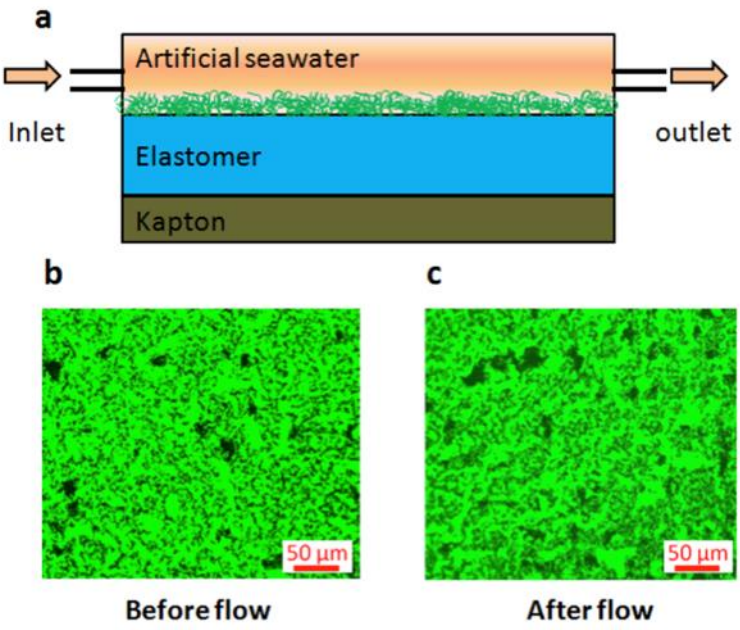

Figure 8 Effect of the shear flow on detachment of biofilms. (a) Schematic showing the flow on the *Cobetia marina* biofilm grown on Sylgard 184 for 6 days. Fluorescence images of the stained biofilm captured using 10X objective (b) before flow and (c) after flow.

3.3.5 Biofilm detachment from electro-active surfaces

A DC voltage was applied between artificial seawater and the bottom electrode by a controllable voltage supply (Mastsusada, Japan). The voltage was switched on and

off at a frequency of 0.33 Hz for 10 minutes on each sample with a continuous low-shear flow (0.5 mL/min) of artificial seawater to carry away the detached biofilms. The electric fields were calculated using $E = \Phi/\left(h + H_s\,\varepsilon/\varepsilon_s\right)$, where Φ is the applied voltage, h is the thickness of Sylgard 184 film, $H_s = 125\mu m$ is the thickness of the substrate, $\varepsilon = 2.65\varepsilon_0$ and $\varepsilon_s = 3.5\varepsilon_0$ are the dielectric constants of Sylgard 184 and Kapton respectively, where $\varepsilon_0 = 8.85\times10^{-12}Fm^{-1}$ is the permittivity of vacuum.

3.3.6 Analysis of biofilm detachment

The biofilms on control and electroactuated samples were stained using SYTO 13 (Invitrogen Inc.); the procedure is detailed elsewhere [135]. The stain-washed biofilm surface was air dried in the dark for about 30 minutes and analyzed using a fluorescent microscope (Ziess Axio Observer) using a 10X objective. At least five images at different regions were captured from each stained surface under same exposure time. The average percentages of biofilm detached from the surfaces were calculated by comparing the relative fluorescence intensities between the experimental and control samples.

3.3.7 Characterization of surface strain

The surface strain induced by electro-actuation was characterized using markers imprinted on the surface. The fabrication procedure for the surface with markers is shown in Figure 9a. In brief, the markers were fabricated by casting a 50 μm thick

Sylgard 184 film on a silicon mold with pillars arranged in a square lattice generated with photolithography. The feature size of the pillars on the mold is represented in Figure 8a. The distance between two adjacent pillars (5 μm) is much smaller than the thickness (50 μm) of the Sylgard 184 film. Therefore, the markers have negligible effect on the deformation of the Sylgard 184 film. Images (see Figure 8b) of the Sylgard 184 surface at flat and deformed states were captured using a microscope (Nikon, Japan). The initial (X_J) and deformed coordinates (x_i) were measured with an image processing software (ImageJ, NIH, USA) and the deformation gradient $F_{iJ} = \partial x_i / \partial X_J$ was computed using finite element analysis [136]. The Green strain was then calculated as $E = \left(F^T F - I\right)/2$, where I denotes the Kronecker delta tensor. The maximum principal Green strain was computed and plotted in Figure 9b.

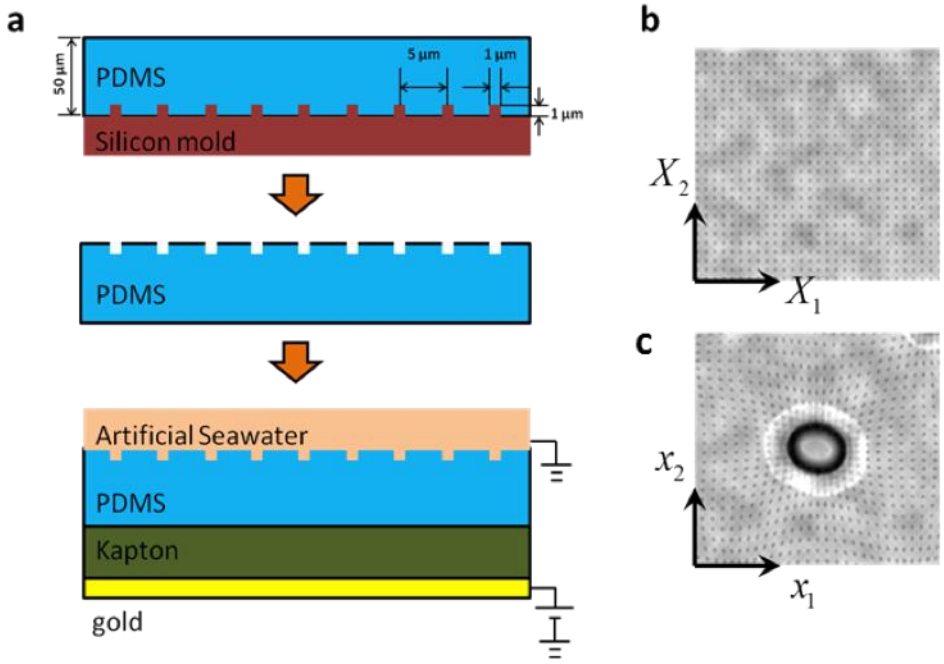

Figure 9: Surface deformation due to electroactuation, (a) Schematic illustration of process for fabrication of the Sylgard 184 surface with markers. Phase contrast optical microscopy images of the Sylgard 184 surface in (b) the undeformed flat state and (c) the deformed, "cratered" state.

3.3.8 Barnacle reattachment on surface and adhesion strength measurements

Reattachment of barnacles followed a previously published protocol[137]. Briefly, barnacles (*Amphibalanus (=Balanus) amphitrite*) were reared to cyprids, settled on T2® (a gift from North Dakota State University) and cultured to a basal diameter of 0.5 cm in about 7 weeks. Barnacles were pushed off the T2 surface and immediately placed on the test surfaces in air and incubated in 100% humidity for 24 hours. Thereafter, the surfaces were submerged in running sea water and fed with brine shrimp daily for 2 weeks and tested.

3.3.9 Biofilm and barnacle detachment from stretched surfaces

Films of the silicone elastomer, Ecoflex 00-10 (Smooth-On, USA) were used to detach biofilms or barnacles by mechanical stretching. The thickness and shear modulus of the Ecoflex films was 1 mm and 10.4 kPa, respectively. After biofilms and barnacles adhered to a film, the two ends of the film were clamped and stretched and relaxed in a periodic manner. The film was stretched to prescribed strains and relaxed for 30 cycles in 3 minutes, during which a continuous low-shear flow (0.5 mL/min) of artificial seawater was used to carry away the debonded organisms.

3.3.10 Biofilm morphology on deformed substrate

Biofilms of *Cobetia marina* were grown on rectangular Ecoflex surfaces for six days and stained using similar procedure as detailed above. The stained biofilm gave a uniform coverage over most area of the Ecoflex surface as shown in Figure 10a. The Ecoflex substrate with the stained biofilm was then clamped on two opposing edges and slowly stretched in a uniaxial direction to 20% strain. The substrate was held in the stretched state and observed under the microscope to examine the effect of surface deformation on biofilm morphology. As shown in Figure 9b, the biofilms on the deformed substrate maintained its integrity over a length scale much larger than the thickness of the biofilms (i.e. 30 μm- 80 μm). The detachment of the biofilm therefore, can be analyzed as a debonding process of a film from substrate.

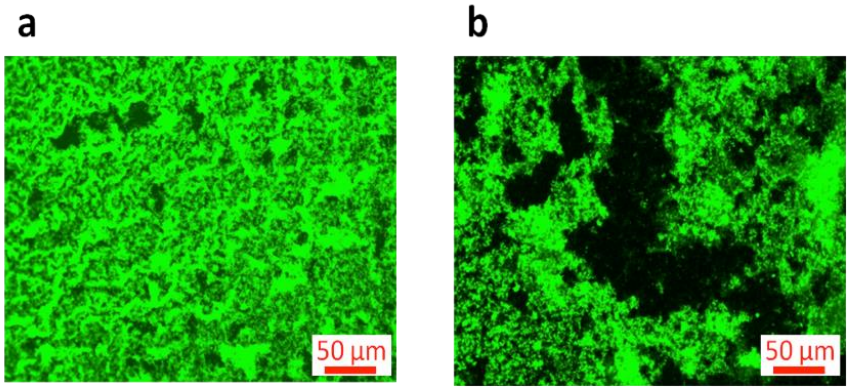

Figure 10: Fluorescence microscpy images of *Cobetia marina* biofilm surface (a) before stretching and (b) after stretching to 20% strain.

3.3.11 Energy release rate for debonding of barnacles

The system of a row of barnacles on an elastomer film was simplified as a 2D plane-strain model as shown in Figure 11a. The Ecoflex film was modeled as a Neo-Hookean material with shear modulus μ_s and was assumed to be infinitely thick. The barnacle was modeled as a rigid body. The bonding length between the barnacle and the polymer substrate is denoted as L. The energy release rate G was computed by a commercial finite element package ABAQUS 6.10.1 (SIMULIA, USA). As shown in Figure 11b, the normalized energy release rate $G/(\mu_s L)$ increases with the applied strain e and the normalized contact length L/S, wherein S is the width of the polymer film. If the applied strain is small (e< 10%), the energy release rate can be analytically expressed as [138]

$$G = \frac{1}{2}\mu_s L\left[e^2 \tan\left(\frac{\pi L}{2S}\right)\left(\frac{S}{L}\right)\right] \quad (1)$$

In addition, if S is much larger than L, Equation (1) further reduces to $G = \pi\mu_s L e^2 / 4$. From Figure 11**b**, it can be seen that the numerically calculated G at low values of e and L/S matches consistently with the analytical solution.

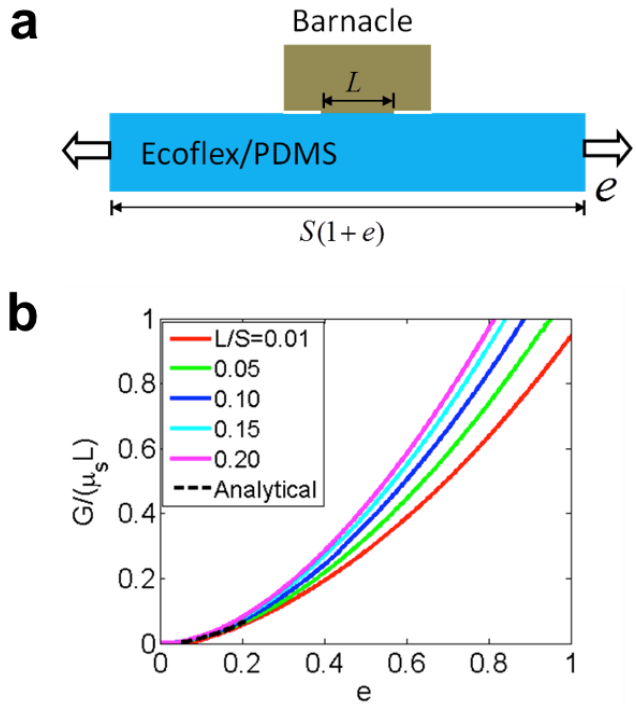

Figure 11: Normalized energy release rate for debonding of barnacles from the substrate. (a) Schematic for the elastomer-barnacle system under uniaxial stretching. (b) The relation between the normalized energy release rate with applied strain e and the ratio L/S.

3.3.12 Process for fabrication of pressure-actuation prototype

As shown in Figure 12a, a plastic prototype fabricated by a 3D printer (Stratasys, USA) was used as a mold to cast a patterned Ecoflex network. The network (Figure 12b) was then placed over an uncured Ecoflex film (~200 μm) spin-coated on a glass slide.

After curing, the patterned Ecoflex network was firmly bonded to the glass slide to form enclosed air channels. Each air channel was covered by a long Ecoflex strips with thickness of ~1mm. Small holes were punched on two opposite walls of the network: one connected to a rubber tubing for air inlet and the other to a digital pressure transducer (Tachikara, Inc.). As air pressure in the channels increases, the thin Ecoflex strip above the air channel buckles upward generating surface deformation.

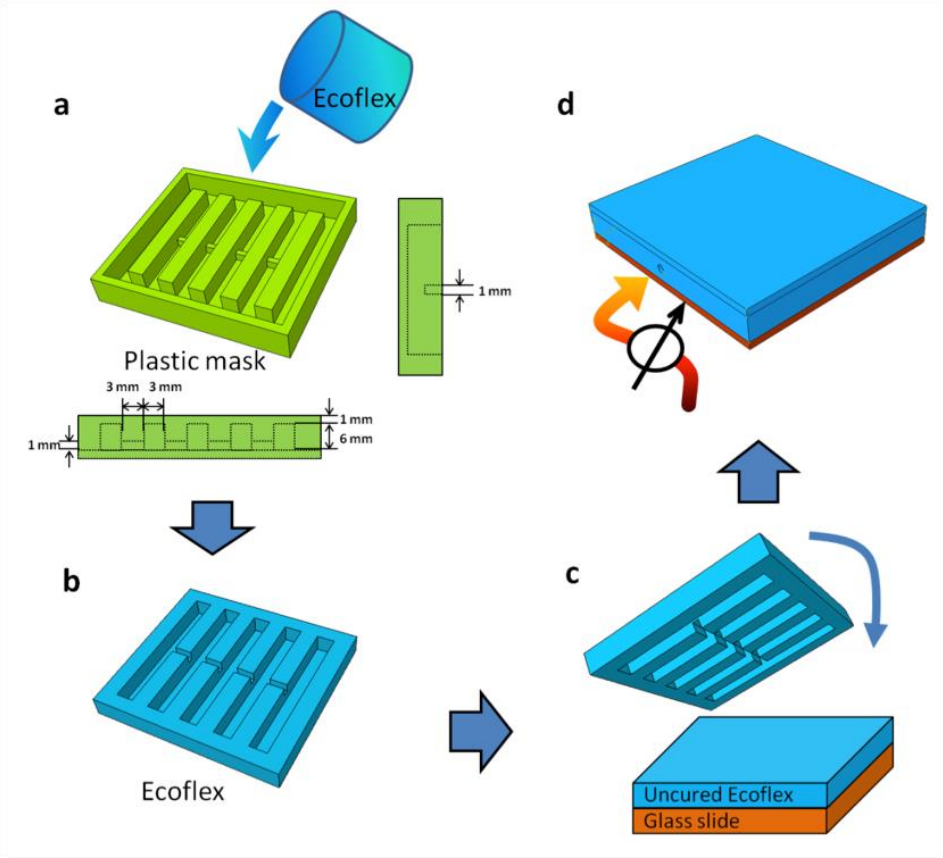

Figure 12: Fabrication of dynamic surfaces actuated by pressurized air. (a) A plastic prototype fabricated by a 3D printer was used as a mold to cast a patterned Ecoflex network. (b) Patterned Ecoflex with air-pass channels inside. (c) The patterned

Ecoflex with air-pass channels inside was adhered on a glass slide with uncured Ecoflex. (d) After curing, the patterned Ecoflex with embedded air channels was firmly bonded to a glass slide.

3.3.13 Pressure versus strain for dynamic surface actuated by pressurized air

The pressure-controlled buckling of the Ecoflex strip above the air channel network was modeled as shown in Figure 13a [139]. A 2D plane-strain model was constructed to account for the deformation of the long Ecoflex strip. The Ecoflex strip clamped at two ends was subjected to a uniform pressure P, buckling out as an arc with radius R. We denote the initial and blistered length as $2L$ and $2l$, and initial and blistered thickness of the film as H and h.

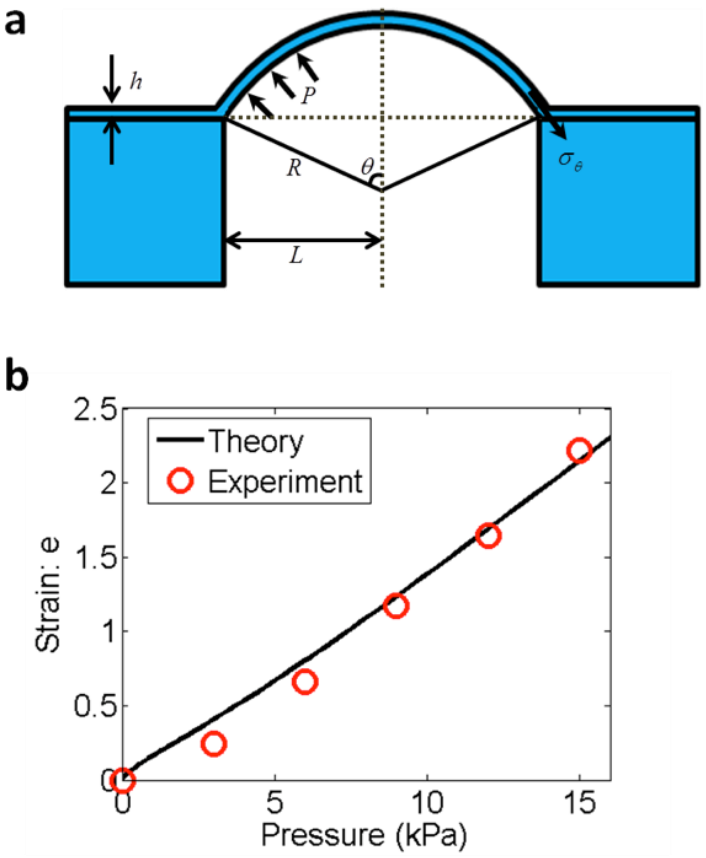

Figure 13: Pressure versus strain for dynamic surfaces actuated by air pressure. (a) 2D schematic for blistering of the Ecoflex surface due to air pressure. (b) Relation between the surface strain and the air pressure.

As illustrated in Figure 14a, force balance gives

$$PR = \sigma_\theta h \tag{2}$$

where σ_θ is the membrane stress. The two principal stretches in the film are

$$\lambda_\theta = \frac{l}{L} = \frac{\theta}{\sin\theta}, \quad \lambda_r = \frac{h}{H} = \frac{1}{\lambda_\theta} \tag{3}$$

where 2θ is the angle of the arc as show in Figure 14a. The Ecoflex film obeys the Neo-Hookean model, i.e.

$$\sigma_\theta = \mu\lambda_\theta^2 - P_0\,,\ \ \sigma_r = \mu\lambda_r^2 - P_0 \tag{4}$$

where P_0 is the hydrostatic pressure to ensure the incompressibility of the elastomer. Given that the radial stress $\sigma_r \approx 0$, Equation (4) gives

$$\sigma_\theta = \mu\left(\lambda_\theta^2 - \lambda_r^2\right) \tag{5}$$

Combining equations (2, 3, and 4), we can calculate the relation between the applied pressure P and the surface strain of the Ecoflex film $e = \lambda_\theta - 1$. The theoretical results consistently match with the experimental data (see Figure 13b).

3.4 Results and discussion

Figure 14a illustrates the structure of an electro-active antifouling coating (See Methods for details of fabrication). Films of a silicone elastomer, a rigid insulating substrate, and a metal foil were bonded together to form a tri-layer laminate [13, 140]. The laminate can be readily fabricated to cover large areas. The elastomer surfaces were exposed to artificial-seawater suspensions of a model marine bacterium, *Cobetia marina* (7×10^7 cells/mL), which is known to colonize many materials rapidly and to mediate the attachment of other fouling organisms in seawater [141-143]. The *Cobetia marina* was allowed to form biofilms on the elastomer surfaces for 4 days (Figure 14a). The elastomer surfaces were electrically grounded by placing a ground electrode into the artificial seawater, which flowed gently over the surface of the attached biofilm. Control studies showed that the flow alone does not detach biofilms (see Figure 7). As a DC

voltage was applied to the metal foil under the laminate, an electric field developed in the elastomer. When the electric field exceeds a critical value, the surface of the elastomer becomes unstable, deforming into a pattern of "craters" (Figure 14a-b). The critical electric field for the electro-cratering instability can be expressed as [13, 140]

$$E_c \approx 1.5\sqrt{\mu/\varepsilon} \tag{6}$$

where μ and ε are the shear modulus and dielectric constant of the elastomer. When the electric field is removed, the elastomer returns to its initial, flat topography. We characterized the surface strain of the elastomer under electric fields by imprinting markers on its surface (Figure 14b). The size of the markers is much smaller than that of the craters and the markers form a regular square lattice on the undeformed surface. The surface strain is calculated by tracking the relative displacements of the markers (see Figure 8). Figure 14**b** gives the distribution of the maximum principal strain on the deformed surface. It can be seen that the maximum principal strain is over 20% on most of the surface. After 200 on-off cycles of the applied voltage in 10 min, over 95% of the biofilm on the elastomer surface is detached (Figure 14c). To our knowledge, this is the first observation that voltage-induced deformation of polymer surfaces can actively and effectively detach adherent biofilms.

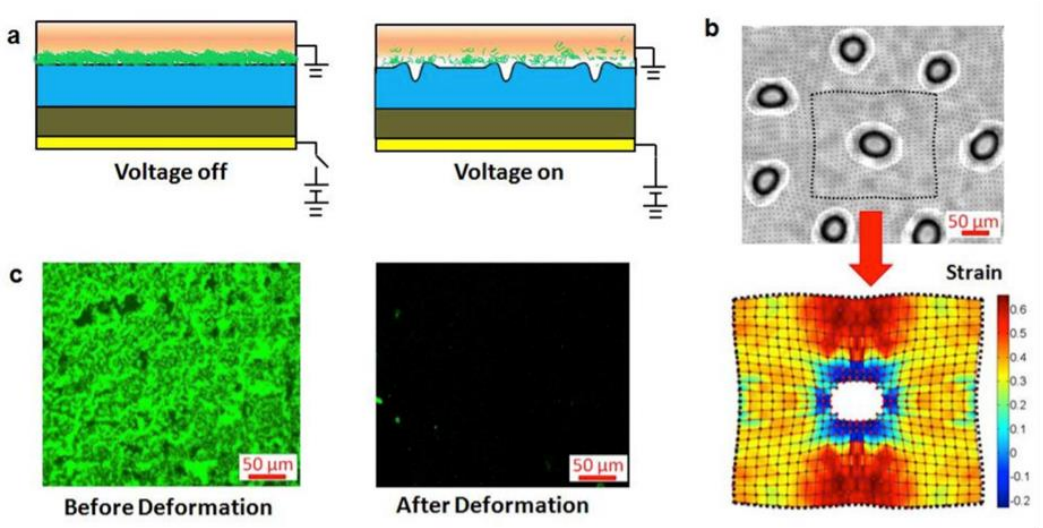

Figure 14: Detachment of bacterial biofilms from dielectric elastomers under applied voltages. (a) Schematic illustration of the laminate structure, actuation mechanism, and the detachment of a bacterial biofilm. (b) The applied electric field can induce significant deformation of the elastomer surface as given by the contours of the maximum principal strain. (c) The deformation detaches over 95% of a biofilm (*Cobetia marina*) adhered to the elastomer surface, which is periodically actuated for 200 cycles within 10 minutes.

We hypothesized that the deformation of the elastomer surface, but not the presence of the electric voltage, causes biofilm detachment. To test this hypothesis, we decoupled the effects of the voltage and surface deformation on biofilm detachment using a set of silicone elastomer layers with moduli ranging from 60 kPa to 365 kPa. Biofilms of *Cobetia marina* were grown on the elastomer surfaces as described above. The applied electric fields in the elastomers were controlled according to Equation (1), such that the same electric field E can induce significant deformation for those elastomers where $E > E_c$ but not for those where $E < E_c$. In Table 1, the deformed surfaces are indicated by white background and the undeformed by grey background; significant

detachment of biofilms (*i.e.* >85%) occurs only on those surfaces that undergo deformation. Although they were subjected to the same electric fields, the undeformed surfaces exhibited minimal detachment (*i.e.* <15%) of biofilms. These results suggest that surface deformation is the dominant mechanism for detachment of biofilms from the elastomer surfaces actuated by electric fields.

Table 1: The percentage of *Cobetia marina* biofilm detached (%) from elastomer films (Sylgard 184) with various moduli and under a range of applied electric fields. The cross-linker density of the Sylgard 184 was varied to obtain elastomer films with shear moduli ranging from ~60 kPa to 365 kPa. The electric field was periodically varied between zero and a maximum value (as shown in the table) for 200 cycles in 10 minutes. Imposition of electric fields below E_c caused no surface deformation (indicated by grey background) and had minimal percentage (~15%) of biofilm detached. Imposition of electric fields below E_c resulted in formation of craters such that the surface switched reversibly from a flat state to the deformed state (indicated by white background), resulting in high percentage (~95%) of biofilm detachment.

Shear Modulus (MPa) / Electric Field (MV/m)	0.060	0.155	0.365
2.3	12 ± 2.3	10 ± 2.5	11 ± 2
4.2	87 ± 7.1	15 ± 1.7	16 ± 5.5
7.0	88 ± 6	95 ± 2.7	11 ± 1.3
11.7	90 ± 3.6	96 ± 2.8	97 ± 1.6

Next we studied the effect of surface deformation on the detachment of various forms of biofouling by mechanically stretching elastomers without imposition of electric voltages. Biofilms of different thicknesses on the elastomers were formed from *Cobetia*

marina and *Escherichia coli* by varying their time in culture [144]. Thereafter, each elastomer with biofilm was stretched uniaxially to a prescribed strain for 30 cycles within 3 minutes, while artificial seawater was gently flushed across the surface of the elastomer to carry away detached biofilm. After stretching, the percentage of biofilm detachment was measured as a function of the applied strain. Figure 15c and Figure 15d show that surface deformation induces significant detachment of *Cobetia marina* and *Escherichia coli* biofilms (i.e. >80%) when the applied strain exceeds critical values ranging from 2% to 14%. The critical value of the applied strain depends on the thickness of the biofilm (Figure 15c). Interestingly, a thicker biofilm requires a lower critical strain for significant detachment.

We interpret the detachment of biofilms as a debonding process from the substrate[145]. Prior to debonding, the mechanical strain in the polymer layer and the biofilm is the same. If the biofilm is considered to be linear elastic at the deformation rates used in the current study[146], the elastic energy per unit area in the biofilm can be expressed as $HYe^2/2$, where e is the applied strain, Y is the plane-strain Young's modulus of the biofilm, and H the thickness of the biofilm. Given that the biofilm maintains integrity over a length scale much larger than its thickness (See Figure 9), debonding occurs when the elastic energy of the biofilm exceeds the adhesion energy between biofilm and the polymer. Therefore, the critical applied strain for the detachment of biofilm can be expressed as

$$e_c = \sqrt{\frac{2\Gamma}{HY}} \tag{7}$$

where Γ is the biofilm-polymer adhesion energy per unit area. Equation (7) predicts that the critical strain is a monotonically decreasing function of the biofilm thickness. The prediction is consistent with the experimental results in Figure 15c, where a thinner biofilm requires a higher critical strain for the detachment.

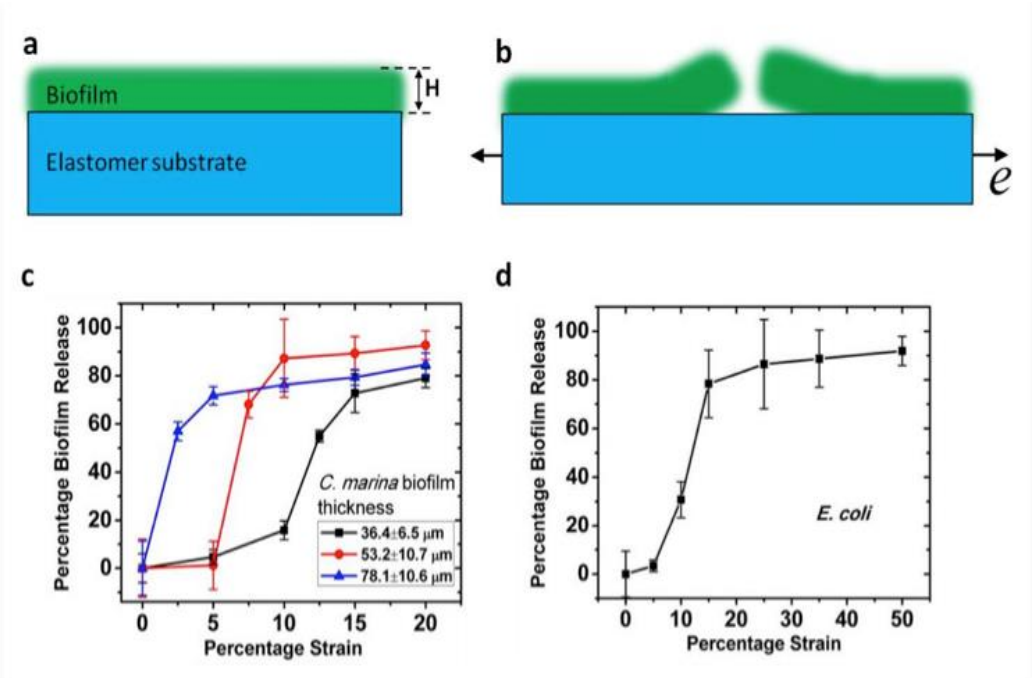

Figure 15: Debonding of biofilms from stretched elastomer films. (a-b) Schematic illustration of the debonding mechanism. (c) Percentage of detachment of *Cobetia marina* biofilm as a function of the applied strain. (d) Percentage of detachment of *Escherichia coli* biofilm as a function of the applied strain. The elastomers are periodically stretched uniaxially to a prescribed strain for 30 cycles within 3 minutes.

To examine the effect of surface deformation on macrofouling organisms, we reattached adult barnacles, *Amphibalanus (= Balanus) Amphitrite* [137], to the surfaces of two types of silicone elastomers, Sylgard 184 and Ecoflex (Figure 16a). After the barnacles were firmly reattached, the elastomer layers were stretched to various prescribed strains periodically and then the shear forces for detaching the barnacles were determined [137]. The shear force for barnacle detachment was plotted as a function of the applied strain on the elastomer layer (Figure 16d). Deformation of the polymer significantly reduced the shear force required for barnacle detachment. For instance, an applied strain of 25% on the Sylgard 184 substrate (μ_s = 155 kPa) reduced the detachment force by 63%, and an applied strain of 100% fully detached the barnacles.

The debonding process of a barnacle due to substrate deformation can be understood as the symmetric propagation of two cracks at the barnacle-polymer interface (Figure 16b**)**. The cracks will propagate if the decrease of the elastic energy of barnacle-polymer system exceeds the adhesion energy between barnacle and polymer substrate [147]. The base plate of the barnacle is much more rigid than the polymer substrate [148]. The substrate under a row of barnacles (Figure 16c) is assumed to deform under a plane-strain condition (Figure 16a and Figure 16b**)**. The energy release rate due to crack propagation (i.e., the decrease of the system's elastic energy when the crack propagates a unit area) can be expressed as

$$G = \mu_s L f\left(e, L/S\right) \tag{8}$$

where μ_s is the shear modulus of the polymer substrate, L the length of the adhered region between barnacle and substrate, S the width of the substrate, and f a non-dimensional function given in Figure 11 by finite-element calculation. From Figure 11, it can be seen that G is a monotonically increasing function of μ_s, e and L. By equating the energy release rate G with the adhesion energy between barnacle and substrate Γ, we can calculate the adhesion length L between barnacle and substrate at any applied strain e. From Figure 16d, it can be seen that the adhesion strengths for barnacle-Sylgard 184 and barnacle-Ecoflex systems are approximately the same. However, the Sylgard 184 (μ_s = 155kPa) has a much higher shear modulus than the Ecoflex (μ_s = 10.4 kPa), and so, when subjected to the same applied strain, the Sylgard 184 substrate should detach barnacles more effectively (i.e. yield smaller *L*) than the Ecoflex substrate. This prediction is consistent with the experimental results (Figure 16d). Debonding of rigid islands from deformed substrates has been intensively studied theoretically [147, 149] and experimentally [150, 151] as a failure mode of electronic devices. Here, we demonstrated the debonding mechanism can be harnessed for active detachment of barnacles by deforming the substrates.

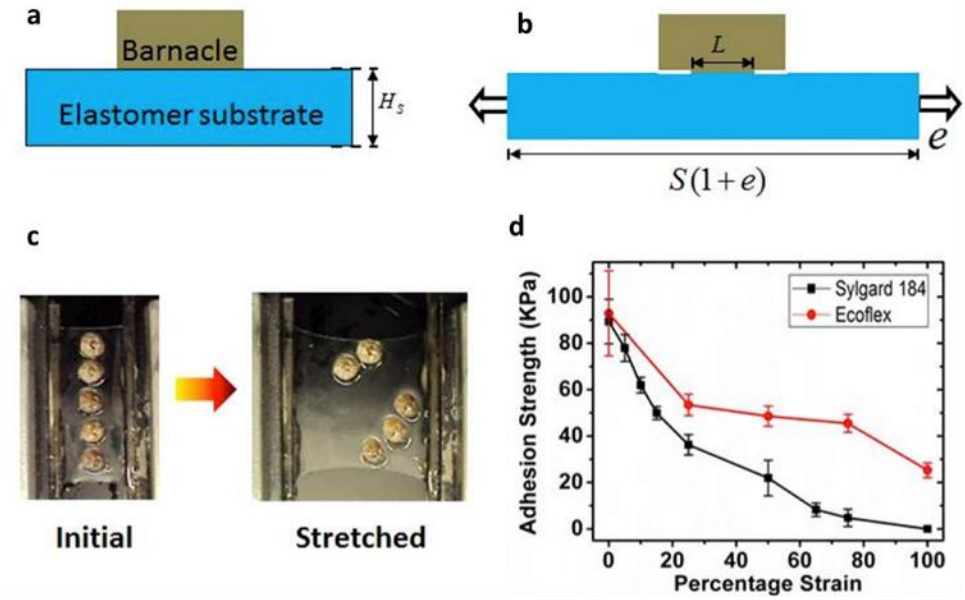

Figure 16: Debonding of barnacles from stretched elastomer films. (a) Schematic illustration of the debonding mechanism. (b) A photo showing the detachment of barnacles from a stretched elastomer film. (c) The shear stress necessary to detach barnacles from the elastomer film decreases with the applied strain on the film. The elastomers are periodically stretched uniaxially to a prescribed strain for 30 cycles within 3 minutes.

As an alternative means for achieving surface deformation, we examined the use of pneumatic networks [152] for active detachment of micro- and macro-biofouling models. As illustrated in Figure 17a, air channels were fabricated beneath an elastomer layer, while the bottom surface of the network was bonded to a rigid plate (see Figure 12 for details). When air is pumped into the channels, the top surface of the network buckles out and induces controlled surface deformation (Figure 17a). The relation between the air pressure and the strain of the surface is given in Figure 13. Biofilms of *Cobetia marina* were grown on the surface of the elastomers for 7 days after adult barnacles were reattached to the surfaces and grown. The pressure in the air channels

was gradually increased, and the coverage of biofilms and the shear stress for detaching barnacles were measured.

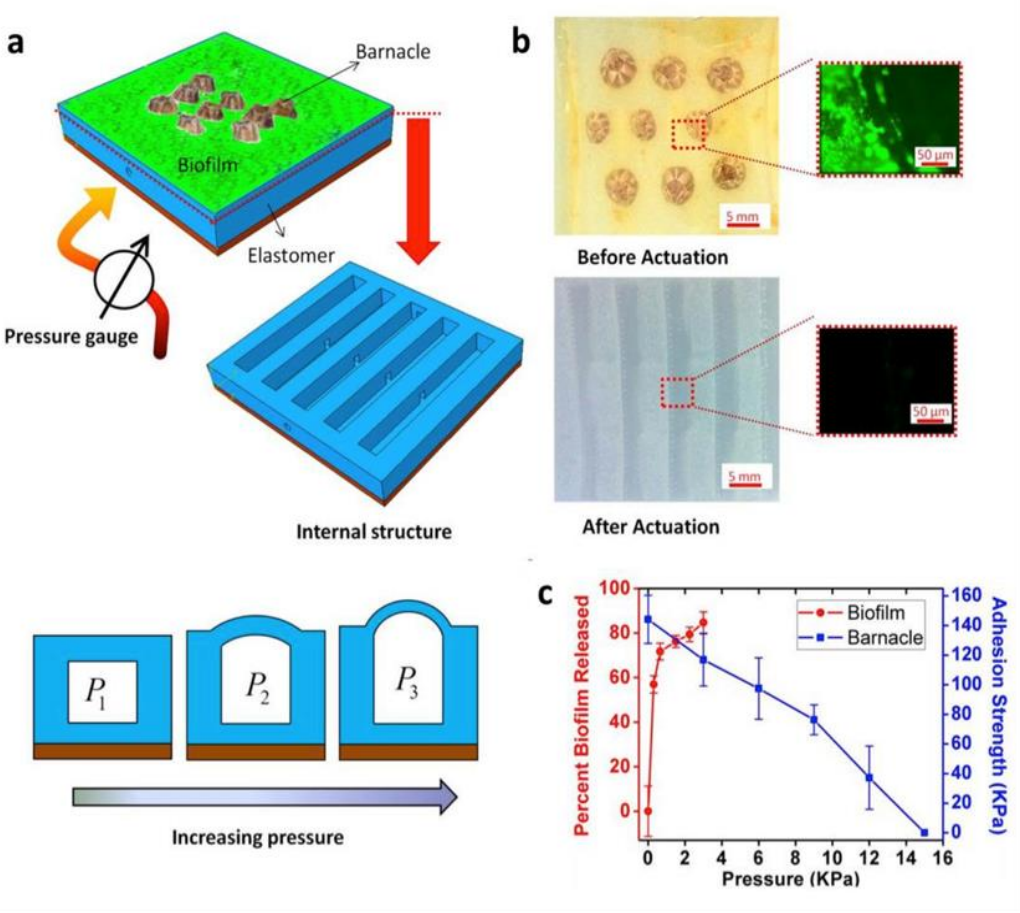

Figure 17: Detachment of bacterial biofilms from dynamic surfaces actuated by pressurized air. (a) Schematic of the structure of the dynamic surface colonized by both a biofilm of *Cobetia marina* and barnacles, (b) photos and fluorescent microscope images of the surface before and after actuation, and (c) the percentage of biofilm detachment and the detachment shear stress for barnacles as functions of applied pressure. The dynamic surfaces are actuated for 30 cycles within 3 minutes.

As shown on Figure 17b and Figure 17c, the dynamic elastomer surfaces of the pneumatic network can actively and effectively detach both biofilms and barnacles. For

example, an air pressure of 3kPa induced 23% surface strain and almost 100% detachment of the biofilm. To fully detach the barnacles, a higher pressure (~ 15kPa) was required. Soft robots [152] and snapping surfaces [153] driven by pressured air have been recently studied and proposed for a variety of applications. Here, we give the first demonstration of antifouling capabilities of dynamic surfaces actuated by pneumatic networks. We expect that hydraulic networks for deformation of elastomers [154] will perform similarly.

3.5 Conclusions

In summary, we discovered that the deformation of polymer surfaces can effectively detach microbial biofilms and macro-fouling organisms. Inspired by active biological surfaces, we created simple elastomer surfaces capable of dynamic deformation in response to external stimuli including electrical voltage, mechanical stretching and air pressure. The use of dynamic surface deformation is complementary and can enhance other means for biofouling management such as surface modification, controlled release and micro- and nanotopography.

3.6 Chapter Acknowledgements

The work presented in this chapter was supported by the National Science Foundation's Research Triangle Material Research Science and Engineering Center (DMR-1121107) and the Office of Naval Research (N00014-10-1-0907). This work was

also supported by the NSF (CMMI-1200515), NIH (UH2 TR000505) grants to Xuanhe Zhao and the ONR (N00014-10-1-0850 and N00014-11-1-0180) grant to Daniel Rittschof.

4. Chapter 4: Biofouling management in natural marine environment using dynamic surface deformation of elastomers

This chapter is part of the work for Specific Aim 1. It includes experimental results of biofouling control in natural marine environment and emphasis on the practical applications of dynamic surface deformation approach. Sections of the text and figures included in Chapter 4 were published in Biofouling. The full citation for the article is: P. Shivapooja, Q. Wang, L.M. Szott, B. Orihuela, D. Rittschof, X. Zhao and G.P. López. Dynamic surface deformation of silicone elastomers for management of marine biofouling: laboratory and field studies using pneumatic actuation. Biofouling, 28 APR 2015, 31 (3), 265-274. The publisher (Taylor & Francis Group) granted permission to the authors to reuse this article as a chapter in this dissertation.

4.1 Synopsis

Many strategies have been developed to improve the fouling release (FR) performance of silicone coatings. However, biofilms inevitably build on these surfaces over time. Previous studies have shown that intentional deformation of silicone elastomers can be employed to detach biofouling species. In this study, inspired by the methods used in soft-robotic systems, controlled deformation of silicone elastomers via pneumatic actuation was employed to detach adherent biofilms. Using programmed surface deformation, it was possible to release > 90% of biofilm from surfaces in both laboratory and field environments. A higher substratum strain was required to remove

biofilms accumulated in the field environment as compared with laboratory-grown biofilms. Further, the study indicated that substratum modulus influences the strain needed to de-bond biofilms. Surface deformation-based approaches have potential for use in the management of biofouling in a number of technological areas, including in niche applications where pneumatic actuation of surface deformation is feasible.

4.2 Introduction

Biofouling occurs on synthetic surfaces exposed to natural aqueous environments and is a significant economic problem in the marine industry [55, 155-158]. Biofouling on ship hulls results in increased hydrodynamic drag, fuel consumption, as well as an increase in maintenance and environmental compliance costs [59, 159, 160]. The performance of other kinds of marine equipment such as oceanographic sensors, seawater piping, heat exchange systems and ultrafiltration membranes is also negatively impacted by biofouling, the management of which can cost over $15 billion each year [161-163].

Current measures to control biofouling typically involve expensive manual cleaning and the use of biocides [73, 164]. Increased ecological awareness and the high cost of registration of antifouling paints containing toxic ingredients (e.g., copper oxide and organic biocides) has led to substantial interest in the development of non-toxic coatings to reduce biofouling [165, 166]. Silicone based, fouling release (FR) coatings that offer an alternative approach to biocide-containing paints are widely being investigated

by various researchers. FR coatings function by minimizing the adhesion strength of attached fouling species, which can be removed (i.e., "shed off") relatively easily due to shear during cleaning procedures, such as application of water pressure or light scrubbing. The lower adhesion strength of fouling organisms to silicone surfaces has been attributed to its critical surface energy (between 20 and 30 mN/m), smoothness, and reduced opportunities for hydrogen-bonding and polar interaction at the material-liquid interface [78, 79, 167, 168]. Further, it was previous shown through theoretical and experimental studies that the modulus and thickness of the silicones films are also important for their efficacy and durability as FR coatings [169-171]. Surface active silicone compounds are also known to disrupt the curing process of adhesive glues produced by macro-fouling species (e.g., barnacles), thereby reducing their adhesion strength [18, 172].

FR silicone coatings, however, have some disadvantages, and represent only a small proportion of the current total marine coatings market. . They are relatively less durable than other types of coatings (e.g., commercial acrylate self-polishing coatings) and are known to frequently foul with brown slimes (which are dominated by diatoms) that attach strongly to hydrophobic surfaces [16]. Surface energy characteristics of silicone polymers are also known to be altered upon prolonged exposure to sea water, thus affecting their ability to control biofouling [77]. Therefore, efforts are being made to further improve the performance of silicone coatings. For instance, several commercial

silicone coatings incorporate silicone oils to further diminish the adhesion strength of different fouling species without significantly affecting silicone's critical surface energy [173, 174]. In addition, the anti-fouling and FR performance of silicone coatings have been shown to be enhanced through the use of bioinspired, textured surfaces (e.g., Sharklet® surfaces) [53, 175-179], incorporation of amphiphilic polymers (e.g. Intersleek® 900) [98], and tethering of anti-fouling moieties, such as quaternary ammonium salts [180] and zwitterionic polymers [82, 105].

As an alternative and complementary method to the above mentioned, existing surface modification approaches, this article builds upon two recent reports, which demonstrated that dynamic deformation of silicone elastomer surfaces can be highly effective in the release of both soft (e.g., bacterial biofilms) and hard (e.g., barnacles) foulers. [12, 181]. The approach is based on the fundamental hypothesis that biofouling on a soft, elastomeric substrate (e.g., polydimethylsiloxane (PDMS)) can be de-bonded if sufficient strain is applied to the substrate. Using silicone elastomers that allow manual, electric, or pneumatic actuation for controlled surface deformation, it was demonstrated that a critical substrate strain is needed to de-bond bacterial biofilms from a silicone substrate. However, those studies were conducted using model, single-species bacterial biofilms grown in laboratory environment over short time periods (e.g., 48 h). It is generally accepted that biofilms formed in actual marine environments can be of highly complex composition and thus can exhibit robust adhesion properties [182].

This study includes two main objectives: (i) to test the above hypothesis (i.e., that surface deformation can result in biofilm detachment) in the laboratory and in the field environment, and (ii) to examine whether shear modulus of the substrate affects the strain needed for biofilm detachment. Controlled, reversible surface deformation was applied through a pneumatic actuation method that has been developed for soft robotics applications (Vogel 2012). Two similar silicones (Ecoflex-10 and Ecoflex-50) that have different shear modulus were used in this study. The field studies were conducted at the Duke University Marine Lab in Beaufort, NC, while the laboratory studies were conducted using *Cobetia marina* and *Escherichia coli* biofilms.

4.3 Materials and Methods

4.3.1 Fabrication of elastomer pneumatic networks

Ecoflex® Supersoft 0010 and Ecoflex® Supersoft 0050 platinum catalyst-based silicone formulations (Smooth-On Inc., USA) (from here on, referred in the text as Ecoflex-10 and Ecoflex-50) were used to fabricate elastomeric pneumatic networks by molding of 3D printed plastic (acrylonitrile butadiene polystyrene, ABS) templates. The plastic template (Figure 18a) is comprised of multiple long parallel stripes and shorter perpendicular stripes, designed in such a way so that the prepared elastomer pneumatic network can be subjected to controlled surface deformation. Thoroughly mixed Ecoflex silicone precursors (part A: part B = 1:1 v/v) were poured into the plastic mold and cured at room temperature for 12 hours. The cured Ecoflex was removed from the mold and

carefully placed with bottom side up (i.e. smooth-side facing upwards) on a glass slide (75 x 50 mm) that was spin-coated with a 2mm thick layer of uncured Ecoflex. The layer was allowed to cure over night to form a sealed pneumatic network comprising of 2mm thick silicone layer on top of the air-channels (40 mm long) that are interconnected (Figure 18b). One side of enclosed elastomeric pneumatic network was connected to a polyurethane tube (5 mm in diameter) using a 16-gauge syringe needle. The other end of the tube is connected to a pneumatic pump, which was used to vary the pressure in the air channels. The pressure inside the air channel was measured using a pressure gauge (Cole-Parmer, USA).

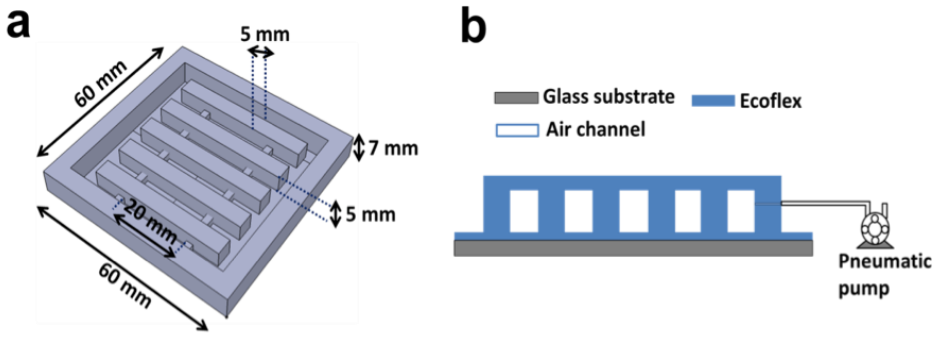

Figure 18: Fabrication and calibration of elastomer pneumatic networks. Schematic and dimensions of the plastic 3-D-printed template used for making the prototype elastomer pneumatic networks (a), cross-section schematic of an Ecoflex elastomer pneumatic network connected to a pneumatic pump for actuation (b).

4.3.2 Shear moduli of Ecoflex silicone elastomer

Using the Arruda-Boyce model [183], the nominal stress (s) for plane-strain uniaxial tension is given by,

$$s = \mu[(\varepsilon + 1) - (\varepsilon + 1)^{-3}]\left[1 + \frac{I_1}{5N} + \frac{11I_1}{175N^2}\right] \quad (9)$$

where, μ is shear modulus of the Ecoflex film, ε is the uniaxial strain, $I_1 = (\varepsilon + 1)^2 + (\varepsilon + 1)^{-2} + 1$, and N is a parameter that accounts for the stiffening effect. This equation was fitted to the experimental data obtained from uniaxial tension tests (see Figure 19) using parameters μ = 10.5 kPa and *N* = 7.28 for Ecoflex-10, and μ = 50.2kPa and N = 7.17 for Ecoflex-50.

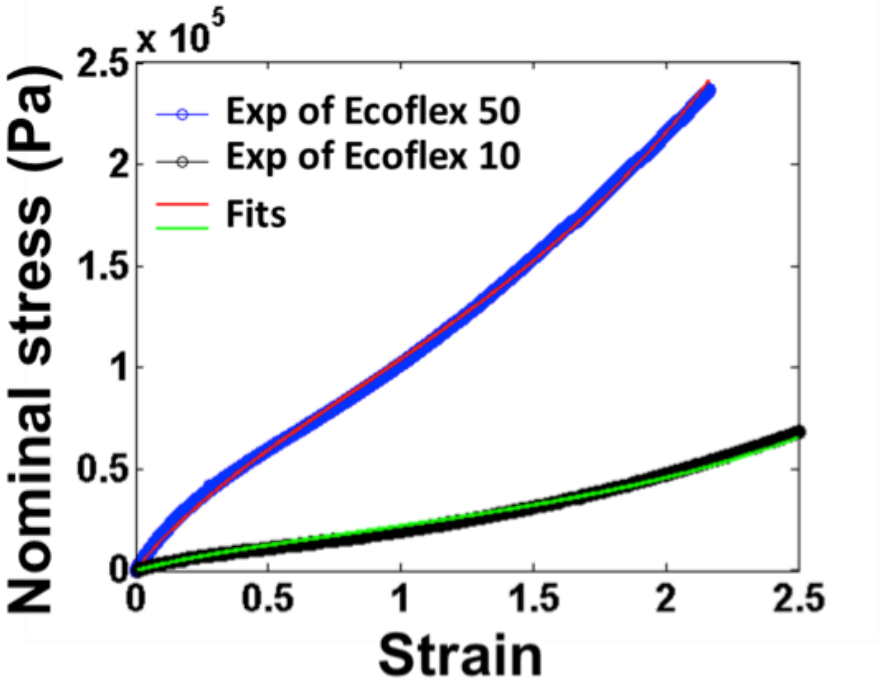

Figure 19: Effect of applied nominal stress on generated surface strain (ε)

4.3.3 Two-dimensional plane strain model for theoretical prediction of surface strain

A 2D plane-strain model was used by considering the deformation of a long strip of thin Ecoflex membrane on the top of a pneumatic channel. Under an applied uniform

pressure P (> atmospheric pressure), the Ecoflex film on top of the pneumatic network will deform outwards as an arc with radius R; the force balance is given by,

$$PR = \sigma_\theta h \tag{10}$$

where σ_θ is the membrane stress. By denoting the initial and inflated lengths as 2L and 2l, and the initial and deformed thicknesses of the film as *H* and *h* respectively, the two principal stretches in the film are given by,

$$\lambda_\theta = \frac{l}{L} = \frac{\theta}{sin\theta},\ \lambda_r = \frac{h}{H} = \frac{1}{\lambda_\theta} \tag{11}$$

where 2θ is the angle of the arc. The Ecoflex film obeys the Arruda-Boyce model i.e.,

$$\sigma_\theta = -p_0 + \mu\lambda_\theta^2\left(1 + \frac{I_1}{5N} + \frac{11I_1^2}{175N^2}\right) \tag{12}$$

$$\sigma_r = -p_0 + \mu\lambda_r^2\left(1 + \frac{I_1}{5N} + \frac{11I_1^2}{175N^2}\right) \tag{13}$$

where p_0 is the hydrostatic stress in the elastomer, μ is the shear modulus of the Ecoflex film, and $I_1 = \lambda_\theta^2 + \lambda_r^2 + 1$. Given that the radial stress $\sigma_r = 0$, the membrane stress can be expressed as

$$\sigma_\theta = \mu\left(\lambda_\theta^2 - \lambda_r^2\right)\left(1 + \frac{I_1}{5N} + \frac{11I_1^2}{175N^2}\right) \tag{14}$$

Based on Equations (10) – (14), the relationship between the applied pressure and applied surface linear strain is calculated using the resulting equation $\varepsilon = (\lambda_\theta - 1)$.

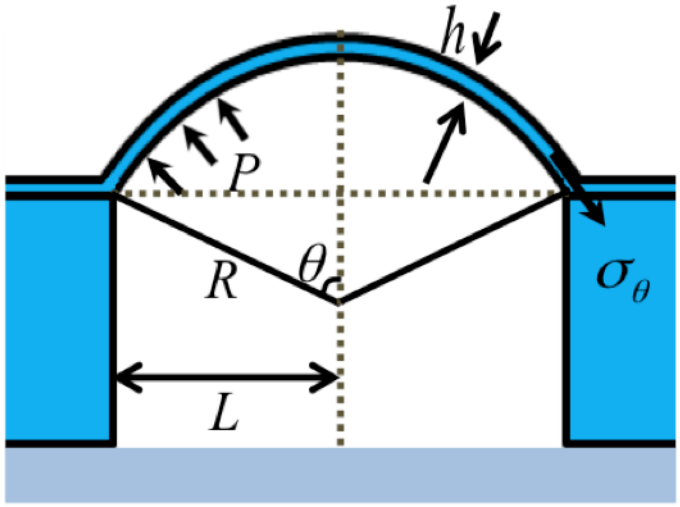

Figure 20: Schematic shows the 2D cross-section view of deformation of a thin elastomer membrane, caused by increase in air pressure (P > atmospheric pressure).

4.3.4 Analysis of substrate shear modulus and strain

To measure the shear modulus of Ecoflex-10 and Ecoflex-50, flat rectangular films of 2 mm in thickness were prepared and subjected to uniaxial tension tests (to collect stress versus strain data) on a micro-strain analyzer (TA Instruments, USA) at a loading rate of 1×10^{-4} s^{-1}. 2 mm thickness was chosen because the silicone layer above the air channels of the pneumatic network samples was also 2 mm in thickness. The stress-strain data of the Ecoflex film were fitted to the Arruda-Boyce model [183] to evaluate the shear modulus. The measured shear modulus for Ecoflex-10 and Ecoflex-50 was 10.5 kPa and 50.2 kPa, respectively. The strain generated on the surface of pneumatic network was determined by measuring the contour length of the deformed surface using d digital photographs taken before and after actuation. The measured surface strain for various pressures applied was in agreement with a theoretical 2D plane strain-model.

4.3.5 Formation of model bacterial biofilms in the laboratory

A chamber was created by fabricating Ecoflex sidewalls along the edges of the pneumatic network using 3D printed plastic supports. *Cobetia marina* (basonym, *Halomonas marina*, ATTC 4741) and *Escherichia coli* (ATTC 15333) bacteria were chosen for laboratory studies, because their biofilms can be easily grown in commonly used media are very commonly found in natural estuarine and sea water environments [143, 184]. Model bacterial biofilms of *C. marina* and *E. coli* were grown on test surfaces in static media under laboratory conditions using a procedure reported previously [181]. In brief, *C. marina* in marine broth and *E. coli* in tryptic soy broth (TSB) were cultured in separate 50 mL conical flasks. The Ecoflex sample surface was sterilized by multiple rinses with 70% ethanol and then rinsed using sterilized DI water. Next, 1 mL of bacterial culture was added on the sterilized Ecoflex surface along with 5 mL of sterilized artificial seawater (for *C. marina*) or TSB broth (for *E. coli*). The samples were stored in an incubator for 7 days at 26 °C (for *C. marina*) or 37 °C (for *E. coli*). Sterilized artificial seawater or TSB media was added as needed to compensate for dehydration of the media over time.

4.3.6 Analysis of *C. marina* and *E. coli* biofilm detachment

After the 7 days of biofilm growth, the test surfaces were stained with SYTO13 (Invitrogen Inc.) using a procedure reported previously [181]. The stained and washed biofilm surfaces were air dried in the dark for 15 minutes and analyzed under a

fluorescent microscope (Zeiss Axio Observer, Germany) using a 10X objective. At least five images at different regions across the surface of each sample were taken using the same exposure time. The percentage of biofilm detached from the surface was calculated by comparing the relative fluorescence intensities between the actuated and control (non-actuated) samples.

4.3.7 Field studies

Multiple replicates of Ecoflex-10 and Ecoflex-50 pneumatic network samples were prepared using the procedure mentioned above and attached to a plastic mesh that was secured to a rectangular frame of dimension 5 feet x 4 feet. The rectangular frame with samples was then attached to a wooden panel on the floating research dock that was previously established for biofouling studies at Duke University Marine Laboratory (May 2013, Beaufort, NC). The test samples attached to a rectangular frame were immersed perpendicular to the water surface, with the test surfaces oriented to the east (compass direction). The samples were immersed to a depth of 1 meter to enable biofilm formation and growth for a period of 14 days. After 14 days, each of the test surfaces was individually and repeatedly actuated in place to a pre-determined pressure using a pneumatic pump (Cole Parmer, USA) fitted with 5 mm flexible polyurethane tubing. One end of the tube was connected to the side inlet of the elastomer pneumatic network. By operating the pneumatic pump, the pressure in the air channels of pneumatic network was increased, which causes a deformation of the Ecoflex surface. The

deformed surface was then reverted to its initial flat state by reversing the direction of airflow through the pneumatic pump.

4.3.8 Analysis of marine biofilm released using crystal violet assay

An aqueous stock solution of crystal violet (tris (4-(dimethylamino) phenyl) methylium chloride) (Sigma-Aldrich, USA) with a concentration of 0.1% by volume was prepared and stored at room temperature. The samples removed from the field were stained using crystal violet for 15 min and gently rinsed three times with DI water. The samples were then allowed to dry in the dark for 15 min at room temperature and at least 10 images were taken across each sample at 4X magnification using an optical microscope (Olympus SZX7, Japan). Control studies indicated that crystal violet effectively stained the biofilms accumulated over the surfaces. The surface area of biofilm coverage was measured by converting the images to binary scale using ImageJ software and adjusting the threshold to precisely differentiate between areas with and without biofilm. The percentage of biofilm released due to pneumatic actuation was calculated by taking the ratio of the surface area of biofilm on actuated versus control samples.

4.4 Results and Discussion

4.4.1 On-demand controlled surface deformation using pneumatic actuation

To remove adherent biofilms, this study employs pneumatic actuation for dynamic surface deformation, inspired by the recent advances in field of hybrid soft

robotic systems [152, 185]. Model silicones (e.g., based on PDMS) commonly used in biofouling studies are also extensively used in the field of soft robotics research. A typical soft robotic system may be fabricated from easily deformable elastomers, molded using 3-D printed templates, and can be powered by an external source, such as pneumatic air pumps [186]. For example, Whitesides and coworkers recently reported that such "pneumatic networks" can be used to form a simple 'starfish-like' robotic structure comprised of three layers of silicones with varying moduli [187]. Using a similar approach, pneumatic networks prepared from Ecoflex silicone elastomer were used in this study to investigate the effect of controlled surface deformation on biofilm release.

Pneumatic networks were made of Ecoflex-10 and Ecoflex-50 using the procedure detailed above. A pneumatic pump was used to increase the pressure in the air channels of the network to levels above atmospheric pressures, exerting a stress on the thin (2 mm) Ecoflex layer above the channels, causing it to stretch and generate strain along its surface (Figure 21a). The amount of deformation is proportional to the pressure in the air-channels and can be controlled. Since the air channels are well connected, the air pressure distributes uniformly inside the pneumatic network. The direction of airflow through the pneumatic pump can be reversed such that the elastomer surface can be controllably reverted to its original flat state.

The surface strain generated by pneumatic actuation was determined by measuring the contour length as described above. The strains measured for varied applied pressures (0 - 20 kPa) were compared with a theoretical prediction of a 2D plane-strain model (Figure 19). The theoretical predicted surface strain matches well with the measured experimental data for both Ecoflex-10 and Ecoflex-50, as shown in Figure 21b, and provides the relationship between applied pressure and generated strain.

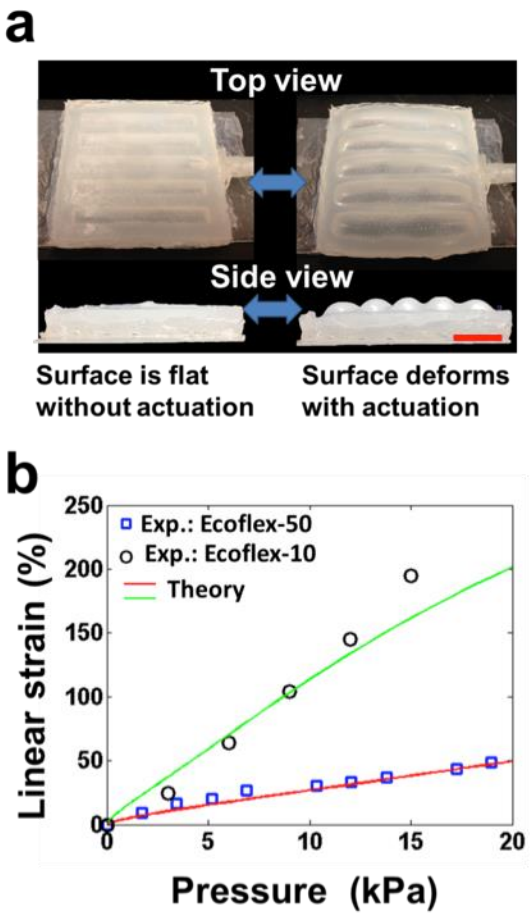

Figure 21: Optical photographs of a pneumatic networks (Ecoflex-10) that shows the surface to be flat without actuation and undergoes deformation when pneumatic pressure is applied (a). The scale bar (red) represents 12 mm. Relationship of applied internal pressure by pneumatic actuation on strain generated on the surface of Ecoflex-10 and Ecoflex-50 (b); the experimental data matches with the theoretical predicted strain.

4.4.2 Detachment of model bacterial biofilms

It was recently reported that deformation of a surface caused by application of controlled dynamic stresses can be used as an effective approach to control biofouling [12, 181]. The objective of laboratory studies is to investigate the effect of substrate strain

and substrate modulus on the detachment of model bacterial biofilms. The procedure used for growing bacterial biofilms in the laboratory is detailed above.

Biofilms were allowed to grow on the surface of elastomer pneumatic network for 7 days and then slowly rinsed using ASW (for *C. marina* biofilm) or TSB (for *E. coli* biofilm) to detach loosely adhered biofilm. The surfaces were then actuated repeatedly to a prescribed strain using pneumatic actuation. The actuation was conducted for 20 cycles at a constant strain rate (50 mm/min). The actuated and control (non-actuated) samples were gently rinsed with sterilized DI water and stained with a fluorescent dye to analyze the surface biofilm coverage. Representative optical microscopy images of a fluorescently stained *C. marina* biofilm on Ecoflex-10 pneumatic before and after pneumatic actuation at a strain of 45% are presented in Figure 22a. The images clearly show that more than 90% of the surface adhered biofilm (green fluorescence) present on the surface before actuation was detached after pneumatic actuation followed by a gentle rinse with DI water.

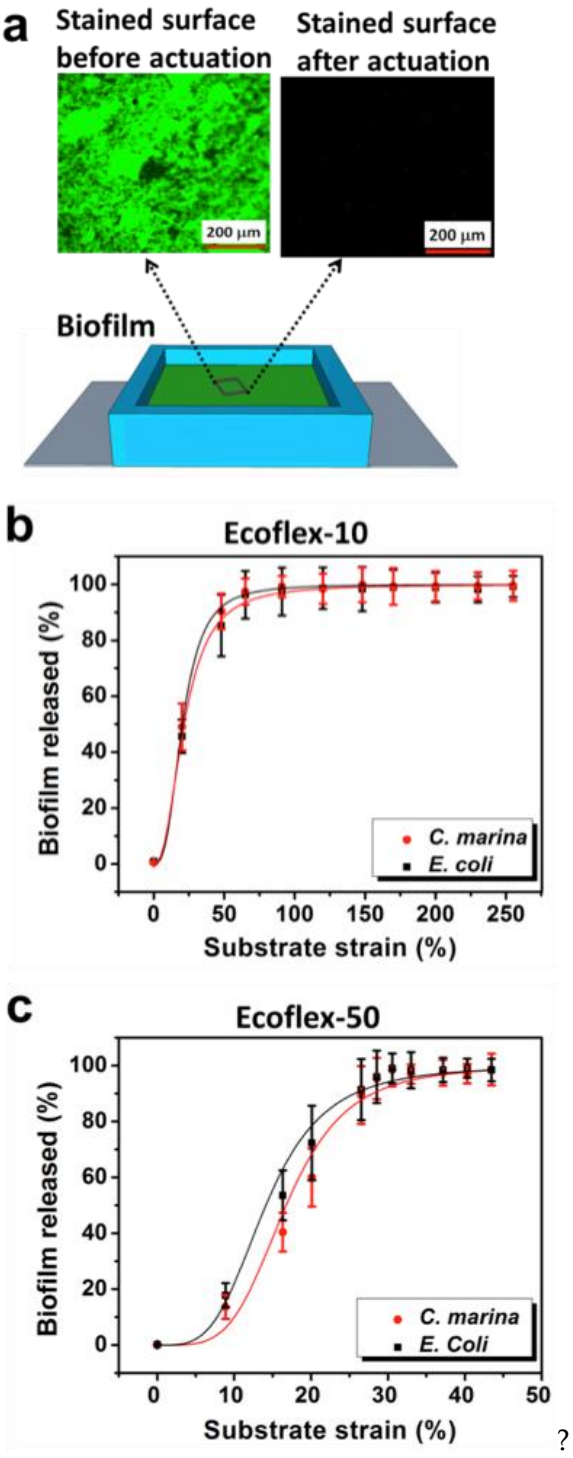

?

Figure 22: Detachment of model bacterial biofilms (*C. marina* and *E. coli*) from Ecoflex elastomer surfaces upon pneumatic actuation. Microscopic images of

fluorescently stained *C. marina* biofilm show evidence that surface adherent biofilm (green fluorescence) present on the surface before actuation was detached significantly (by > 90%) due to pneumatic actuation followed by gentle rinsing (~ 5 mL min -1) with DI water (a). Percentage of biofilm released from the surface of Ecoflex-10 (b) and Ecoflex-50 (c) elastomers for different amounts of applied strain via pneumatic actuation; each error bar represent the standard deviation of the mean (n = 5). The curves were fitted using Equation (2) and the R^2 values of all the individual curves were ≥ 0.98.

The detachment of biofilm due to deformation of a surface can be described as a de-bonding process. When a deformable silicone surface with an adherent uniform biofilm is stretched, the biofilm generates elastic energy due to its viscoelastic nature. It is hypothesized that when this generated elastic energy per unit area exceeds the biofilm's adhesion energy to the substrate, the biofilm de-bonds from the substrate. The de-bonded biofilm can then be easily removed by applying low surface shear forces through, for example, gentle rinsing. Biofilm detachment of more than 90%, such as that illustrated in Figure 22a, indicates that the applied strain (45%) was greater than or equal to that needed to de-bond the biofilm. For a given strain rate, considering the biofilm to be linearly elastic, the critical strain needed to detach the biofilm from the substrate is hypothesized to be given by:

$$\varepsilon_c = \sqrt{\frac{2\Gamma}{YH}} \tag{7}$$

where Y, H and Γ represent the biofilm Young's modulus, biofilm thickness and biofilm-polymer adhesion energy per unit area, respectively.

To validate this relationship, *C. marina* and *E. coli* biofilms were grown separately on multiple replicates of Ecoflex-10 and Ecoflex-50 pneumatic networks and subjected to varying amount of strains. Figure 22b shows that approximately 50% of both types of biofilms (*C. marina* and *E. coli*) were released from Ecoflex-10 at low surface strain (25%), suggesting that only a small strain (< 20%) is necessary for the biofilm to de-bond from the surface. Upon applying higher strains (> 50%) more than 90% of the biofilm was released from the surface. Similar biofilm detachment profiles were observed on Ecoflex-50 (Figure 22**c**). The experimental data were fitted using the following equation:

$$P = 1 - \left(\frac{1}{1 + \left(\varepsilon_{50} / \varepsilon \right)^{k}} \right) \tag{15}$$

where P represents the fraction of biofilm released from the surface, ε_{50} represents the strain required to detach 50% of the biofilm and *k* is an empirical constant. Using the fitted data, the average strain required to release 50% of the *C. marina* biofilm (i.e., ε_{50}) from Ecoflex-10 and Ecoflex-50 was determined to be 21 ± 0.5 and 16 ± 0.5 %, respectively (the R^2 value for all the fitted curves was > 0.98). Similar trends were observed in the detachment of the *E. coli* biofilms (Figure 22b and Figure 22c). More than 90% of *E. coli* biofilms were released above critical strain and the ε_{50} values were different for Ecoflex-50 (ε_{50} = 15%) and Ecoflex-10 (ε_{50} = 20%) test surfaces. Figure 23 summarizes the average strains necessary to detach 20, 50 and 80% of each type of biofilm.

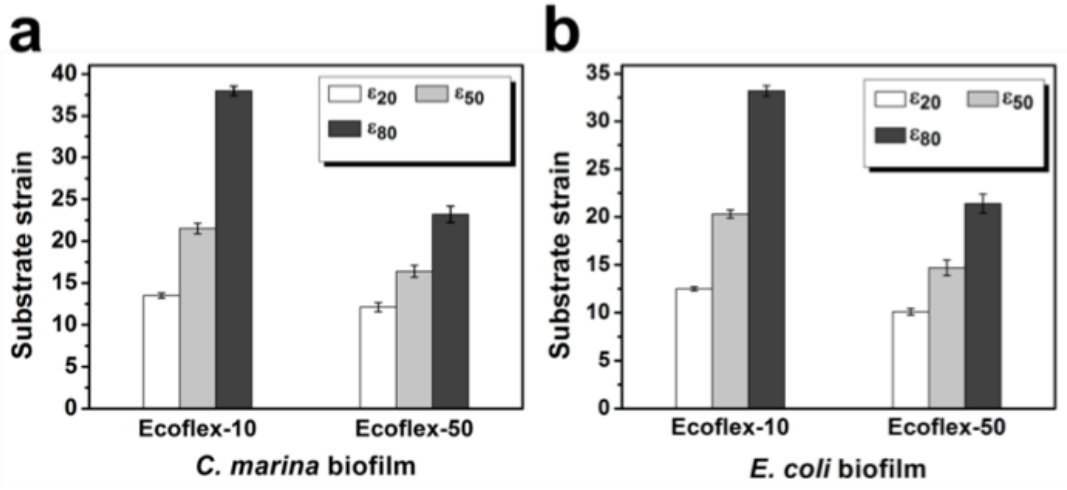

Figure 23: Effect of substrate strain on bacterial biofilm release. The percentage of substrate strain needed to detach 20% (ε_{20}), 50% (ε_{50}) and 80% (ε_{80}) of *C. marina* and *E. coli* biofilms from Ecoflex-10 and Ecoflex-50 was measured by fitting the experimental data to Equation (14).

Ecoflex-10 and Ecoflex-50 have similar chemical formulation (i.e., are platinum-cured silicone elastomers), but different substrate moduli. This suggests that substrate modulus might be responsible for the observed difference in ◎50 between Ecoflex-10 and Ecoflex-50 elastomer pneumatic networks. The substrate modulus, which was measured to be different for Ecoflex-10 (μ = 10.5 kPa) and Ecoflex-50 (μ = 50.2 kPa), might influence each of the biofilm specific properties in Equation 1 (i.e., the thickness (H), Young's modulus (Y) and surface adhesion strength (Γ) of the biofilm), which in turn affect the critical strain needed for biofilm detachment (Equation 7). The relative contributions of these variables were not investigated in the current study and further studies are needed to systematically investigate the role of surface modulus on the strain needed for biofilm detachment. It was previously reported that modulus and thickness of PDMS coatings

significantly influenced the adhesion strength of certain foulers such as green algae *Ulva* [169] and pseudobarnacles [188]. In summary, the laboratory studies support the hypothesis that controlled substrate deformation (e.g., via pneumatic actuation) can effectively detach model bacterial biofilms. Also, the effect of substrate modulus on the strain required to detach biofilm (which has been not considered in the previous analysis of Equation (7) [181]) is reported for the first time.

4.4.3 Detachment of natural biofilms in the marine environment

In contrast to most laboratory cultures, microorganisms in nature exist in mixed populations and are under constant environmental selection to adhere to surfaces and form biofilms [182]. As a result, field experimentation offers the most rigorous and realistic conditions for the testing of materials that attract, repel or release biofilms in marine applications [189]. It should also be noted, however, that field studies generally require a longer immersion time, which can negatively impact the rate at which new coatings are developed. Hence, correlation and statistical comparison between lab assays and field tests is desirable to assess the performance of new biofouling management approaches [190].

As a first step towards addressing suitability of elastomer surface deformation for FR in relevant field environments, experiments were conducted to investigate the effect of substrate strain on detachment of surface adhered biofilms that formed naturally in a marine environment. The objective was to test the laboratory-validated

hypotheses in an actual marine environment, i.e., that controlled surface deformation can be used to release biofilms and there exists a critical strain above which biofilms de-bond from the surface easily. A secondary objective was to compare the ε_{50} of our model marine biofilm (*C. marina*) with that of biofilms formed in an actual marine environment. The infrastructure used and procedures followed in the field studies are detailed in the Materials and Methods section.

Multiple replicates of Ecoflex-10 and Ecoflex-50 elastomer pneumatic networks were assembled on a panel and immersed in marine water at Pivers Island near Beaufort NC (Figure 24a and Figure 24b) for a period of 14 days to allow for biofilm formation and growth. Digital photographs (Figure 24c and Figure 24d) of the elastomer surface before and after 14 days of immersion clearly show the accumulation of biofilm on the elastomer surfaces. To quantify the surface coverage of biofilm, a standard crystal violet staining assay was used [191]. Crystal violet stains cells and other biological materials adherent on the surface, including biofilm matrix components. Control experiments (Figure 24e) showed that the crystal violet staining protocol used here resulted in only minimal staining of silicone surfaces not subjected to field immersion. By contrast, retention of crystal violet dye on the experimental samples provides a clear evidence of biofilm accumulation on the entire surface (Figure 24f).

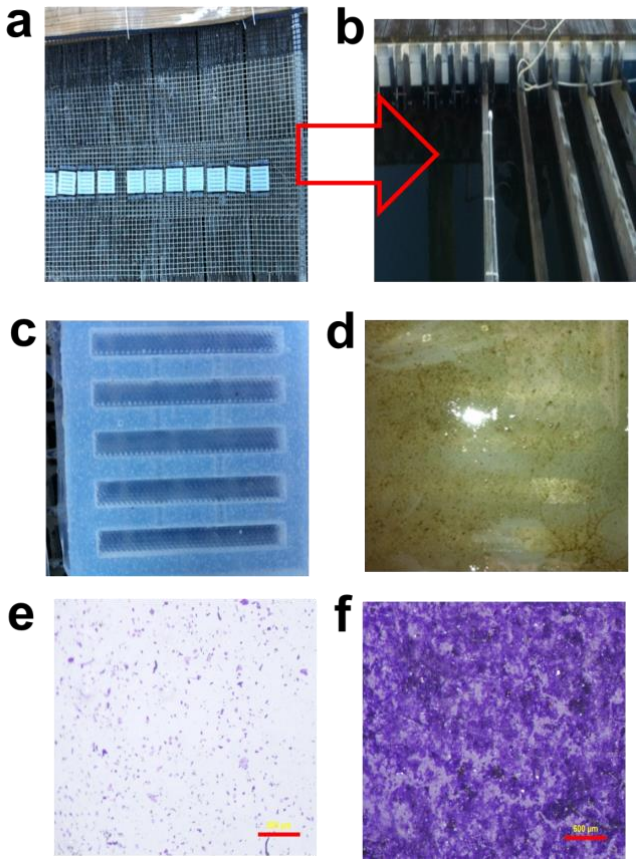

Figure 24: Field studies conduction at the research dock of the Duke University Marine Laboratory (Beaufort NC). Multiple replicates of test surfaces (elastomeric pneumatic networks) made from Ecoflex-10 and Ecoflex-50 immobilized on a mesh-panel were immersed in the marine water to a depth of 1 meter below water level, and subjected to biofilm formation for a period of 14 days (a-b). Representative digital photographs of an Ecoflex-10 elastomer surfaces before (c) and after 14 days (d) of immersion shows the formation of a biofilm. Microscope images of sample surface stained using crystal violet dye before (e) and after 14 days (f). Scale bars on (e) and (f) represents 500 μm.

After 14 days of biofilm accumulation, the elastomer pneumatic networks were individually actuated while still submerged using a protocol similar to that of the laboratory studies. Actuated and control (i.e., non-actuated) samples were carefully

removed from the field site and analyzed in the laboratory using the crystal violet staining assay explained above. Optical microscopy images of the stained surfaces were collected, and the surface biofilm coverage was quantified using the procedure detailed above. On the Ecoflex-10 surface (Figure 25a), it was observed that only low amount (< 15%) of adherent biofilm was detached for substrate strains up to 50%. However, when the strain was increased above 50%, a dramatic increase in the amount of biofilm release was observed. These results suggest that, as for laboratory grown biofilms, a critical substrate strain is needed to detach natural biofilms formed in field environments. As substrate strain reaches a certain critical value, adherent biofilm de-bonds from the surface and is subsequently released by the shear forces from water flow. Similarly, a sudden increase in biofilm detachment from Ecoflex-50 surfaces (Figure 25b) was observed when the applied strain was above 30%. These results demonstrate that controlled dynamic deformation of elastomeric substrates *in situ* can effectively detach (> 90%) natural biofilms formed in the marine field environment.

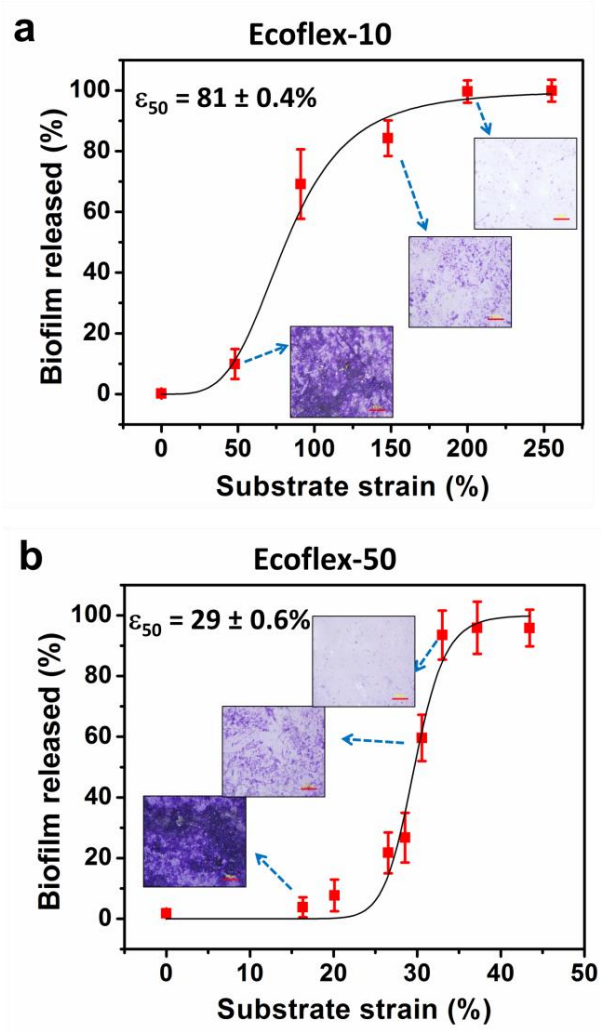

Figure 25: Effect of maximum applied substrate strain on biofilm release in a marine field environment. Multiple replicates of test surfaces (elastomer pneumatic networks) made of Ecoflex-10 (a) and Ecoflex-50 (b) were kept in the field for 14 days to allow biofilm formation. The test surfaces were then pneumatically actuated for 20 cycles to substrate strains in the range of 0 – 250% (for Ecoflex-10) and 0 – 50% (for Ecoflex–50). Each error bar represents the standard deviation of the mean (n = 5). Representative microscopy images of the amount of surface biofilm coverage after actuation are included as insets; the scale bars represent 500 μm. The data were curve fitted using equation (2) and the R^2 values for the curves in (a) and (b) are 0.98 and 0.94, respectively.

As with the FR experimental data on laboratory grown biofilms, Equation (14) was used to determine the strain needed to detach 50% of the marine environment grown biofilm (i.e.,ε_{50}) on each substrate. A strain of 81% was needed to detach 50% of the biofilm on Ecoflex-10, while a strain of 30% achieved the same result on Ecoflex-50. The significant difference in ε_{50} between Ecoflex-10 and Ecoflex-50 in field studies may be due to the factors such as biofilm adhesion strength and thickness as mentioned above. Furthermore, the ε_{50} values for Ecoflex-10 and Ecoflex-50 obtained in the field studies were much higher than those obtained for model bacterial biofilms (*C. marina* and *E. coli*) studied in the laboratory. This difference could be due to the difference in biofilm composition between laboratory and field studies. For example, field accumulated biofilm might include diatoms, which will increase the biofilm adhesion strength [179, 192]. While the experimental conditions used in the laboratory were not chosen in a deliberate attempt to mimic those in the field, the above results illustrate both the value of laboratory and field studies, and the limitations of laboratory studies. While a similar dependence of ε_{50} on substrate modulus was observed in both types of experiments, different magnitudes of ε_{50} were observed between laboratory and field experiments. The results demonstrate that the type of biofilm that forms on a surface, and the mechanical properties of the substrate, both significantly affect the substrate strain needed to release biofilm. In this present study a constant rate of substrate strain was used in order to have consistent experimental conditions between laboratory and

field studies; however, it should be noted that the rate of substrate strain can also influence the detachment of biofilms. A quantitative relationship between applied strain rate, biofilm detachment, and de-bonded biofilm segment length is reported previously [12].

It is important to emphasize that the methods to achieve FR presented here are, in principle, complementary to other established methods. The FR performance of pneumatically actuated silicones (i.e., the reduction in amount of critical strain needed to de-bond biofilms) may be enhanced, for example, by modifying the silicone polymer by known approaches. For example as mentioned earlier, addition of silicone oils (1 – 10% by weight) increases the fouling release performance of silicone coatings without significantly compromising their durability [173, 174]. The non-reactive silicone oils are not covalently bound in the elastomeric network and migrate to the surface forming a weak boundary layer (at the aqueous interface) that decreases the adhesion energy of the biofilm/fouling species. Such phenomena may in turn reduce the substrate strain needed to de-bond the biofilm (Equation 7). Also, anti-fouling compounds such as triclosan and sparfloxacin [193-195] can be impregnated in deformable silicone elastomers and subjected to controlled and triggered release via dynamic actuation methods to improve surface anti-fouling properties. In summary, as on-demand controlled surface deformation can be easily achieved using pneumatic methods, this soft robotics-inspired approach can have potential applications for biofouling

management on certain suitable maritime equipment, such as seawater cooling pipes, oceanographic sensors and power transmitters/receivers.

4.5 Conclusions

Silicone-based FR coatings are a potential alternative to traditional biocidal-coatings in biofouling management. It was recently reported that silicone substrate deformation reduces barnacle adhesion strength and allows facile removal of model biofilms. Inspired by the recent development of silicone soft robotic devices, an approach to achieve dynamic surface deformation via pneumatic actuation was used in this study to investigate the effect of substrate deformation on the detachment of model microbial biofilms under laboratory conditions and naturally grown biofilms in field studies. Both laboratory and field studies showed that effective triggered detachment of biofilms occurs above a critical substrate strain. It was also found that the substrate modulus affected the strain needed to detach biofilm with higher modulus silicone substrates requiring less maximal strain for efficient detachment. Since silicone coatings are widely used in efforts to manage biofouling, it may be possible in certain applications to enhance these efforts by implementing the approach of dynamic silicone surface deformation via pneumatic (or other) actuation to control biofouling on maritime equipment. Though biofouling control via pneumatic actuation may not be practically feasible for ship hulls, it can have potential applications for underwater autonomous environment monitoring devices such as acoustic sensors, optical sensors,

and gliders. Further, pneumatic actuation can also be employed in industrial water pipelines and biomedical urinary catheter devices where clogging due to biofilms is a major problem.

4.6 Chapter Acknowledgements

The work presented in this chapter was supported by the Office of Naval Research [Grant N000141310828] and the NSF's Research Triangle Materials Research Science and Engineering Center [Grant DMR-1121107].

5. Chapter 5: Chemical modification of dynamic elastomer surfaces to develop multi-functional biofouling management systems

This chapter reflects the work for Specific Aim 2 and presents a new type of multi-functional surface for biofouling management. Sections of the text and figures included in Chapter 5 were published in ACS applied materials & interfaces. The full citation for the article is: P. Shivapooja, Q. Yu, B. Orihuela, R. Mays, D. Rittschof, J. Genzer and G.P. López, Modification of silicone elastomer surfaces with zwitterionic polymers: Short term fouling resistance and triggered biofouling release. ACS applied materials & interfaces, 10 NOV 2015, 7 (46), p. 25586-25591. Phanindhar Shivapooja was the lead author of this published article and was granted permission by ACS Publications for reuse in this dissertation.

5.1 Synopsis

This work presents a method for dual-mode-management of biofouling by modifying surface of silicone elastomers with zwitterionic polymeric grafts. Poly(sulfobetaine methacrylate) was grafted from poly(vinylmethylsiloxane) elastomer substrates using thiol−ene click chemistry and surface-initiated, controlled radical polymerization. These surfaces exhibited both fouling resistance and triggered fouling-release functionality. The zwitterionic polymers exhibited fouling resistance over short-term (~hours) exposure to bacteria and barnacle cyprids. The biofilms that eventually accumulated over prolonged-exposure (~days) were easily detached by applying

mechanical strain to the elastomer substrate. Such dual-functional surfaces may be useful in developing environmentally and biologically friendly coatings for biofouling management on marine, industrial, and biomedical equipment because they can obviate the use of toxic compounds.

5.2 Introduction

Biofouling, i.e., the accumulation of biomolecules, cells, and organisms on wetted surfaces, is a ubiquitous problem in maritime operations, medicine, food industries, and biotechnology [119, 196]. Many of the current commercial coatings for marine equipment (*e.g.*, ship hulls) rely on anti-fouling paints that leach out broad-spectrum biocides (*e.g.*, copper oxide, copper thiocyanate) to resist the surface accumulation of fouling species [197]. Due to the deleterious effects of such biocides in aquatic environments, there is a pressing need for alternative, effective and eco-friendly coatings [76, 197]. Silicone-based surfaces have been of great interest in marine, biotechnological and medical contexts, mainly because they are non-toxic and exhibit low surface adhesion strength to bio-foulants, which can be easily removed using surface cleaning methods (e.g., water jets, grooming). While the exact mechanism of silicone fouling-release behavior is still incompletely understood, it has been attributed to a combination of surface properties, including low surface energy [76, 198], low modulus [199], and surface-enrichment of silicone oils (oligomers), which can have a number of effects, both physical[17] and biological (e.g., inhibition of enzymatic activity[200]).

Biomimetic surface topologies [201], polymer brushes [15, 101, 202, 203], amphiphilic block copolymers [76] and oil infused surfaces [17, 204] can be effective against short-term biofouling (and are referred to herein as fouling-resistant surfaces). While promising, there is growing consensus that all of the fouling-resistant surfaces developed thus far eventually succumb to surface-colonizing species in complex marine and biomedical aqueous milieus [110, 119, 204, 205]. Hence, there is need to develop multifunctional coatings that can synergistically exhibit both fouling-resistance and fouling-release properties, and thus enable multipronged, proactive approaches to biofouling management [76, 101]. We recently showed that dynamic change of surface area of elastomers (i.e., cyclic deformation beyond a critical strain) effectively detaches biofilms and barnacles [206-208]. Electro-, pneumatic-, and direct mechanical-actuation were used as external stimuli to generate controlled and on-demand surface deformation of silicone elastomers.

The objective of this study was to develop a method to tailor the surface properties of silicone elastomers using polymers that have fouling-resistant properties. We hypothesized that biofouling-resistant polymers grafted from such elastomers can be used as a bifunctional surfaces, which (i) prevent short-term fouling and (ii) can undergo mechanical strain to detach biofilms that accumulate over prolonged exposure to a fouling environment.

5.3 Materials and Methods

5.3.1 Materials

N-(3-Sulfopropyl)-*N*-(methacryloxyethyl)-*N,N*-dimethylammoniumbetaine or sulfobetaine methacrylate (SBMA, 97%), *N*-isopropylacrylamide (NIPAAm), $Cu^{II}Br_2$ (98% pure), 1,1,4,7,7- pentamethyldiethylenetriamine (PMDETA; 99% pure), ascorbic acid (reagent grade), tin 2-ethylhexanoate, tetrahydrofuran and (tris(4-(dimethylamino)phenyl)methyliumchloride) (crystal violet, 10% aqueous) were purchased from Sigma-Aldrich (USA) and stored under dry conditions until use. Fluorescein-conjugated streptavidin was purchased from Life Technologies (USA). Sylgard 184 silicone elastomer kit and glass microscope slides were purchased from Dow Corning (USA) and VWR, respectively. Poly(vinylmethoxysiloxane) was ordered from Gelest, Inc. (USA). Poly(vinylmethylsiloxane). (PVMS) (M_n~35 kDa) was synthesized by ring-opening polymerization as previously reported.[14] The ω-mercaptoundecyl bromoisobutyrate (ATRP-initiator) was synthesized according to a previously reported procedure [209].

5.3.2 Spin-coated PVMS on glass substrate

PVMS oligomer, poly(vinylmethoxysiloxane) cross-linker, tin2-ethylhexanoate (in tetrahydrofuran 1:10 v/v) catalyst and fumed-silica filler particles in the weight ratio of 10:0.48:0.1:0.2 were thoroughly mixture and degassed using an electric mixer (ThinkyMixer, USA). The mixture was then immediately spin-coated on a clean glass

substrate (2.5 cm x 2.5 cm) at 250 rpm for 1 min to form uniform layer (≈500 μm in thickness). The samples were carefully place in an oven and cured at 65 °C for 2 - 4hrs.

5.3.3 Preparation of Sylgard® ring

A silicone rubber ring of 2 cm diameter was prepared by curing thoroughly mixed Sylgard 184 silicone precursors in a 3D-printed plastic mold in shape of a hollow cylinder.

5.3.4 ARGET-ATRP procedure for modification of PVMS with PSBMA

PSBMA polymer was grafted from the initiator-immobilized on PVMS (PVMS-Br) using activators regenerated by electron transfer-atom transfer radical polymerization (ARGET-ATRP). A 50 mL glass beaker containing PVMS-Br surface and a small magnetic stir bar was place on a stir plate and charged with 0.6 M SBMA monomer, 0.4 mM $CuBr_2$ and 0.7 mM PMDETA dissolved in 30 mL of DI water/methanol (1:1 by vol). 8 mM of ascorbic acid was added to the above solution at room temperature to initiate the ARGET-ATRP reaction, which was allowed to continue for 30 min. The sample surface was then removed from the solution, and rinsed successively with copious amounts of ultrapure water and methanol to remove any monomer, and then dried under a nitrogen gas flow. The mechanism and kinetics of ARGET-ATRP reaction have been reported previously [15, 210].

5.3.5 X-ray photoelectron spectroscopy (XPS)

The elemental composition of the surfaces was determined with a Kratos Analytical Axis Ultra X-ray photoelectron spectrometer equipped with a monochromatic Al Kα source. High-resolution scans were acquired at a pass energy of 20 eV and a resolution of 0.1 eV. Survey scans were acquired with pass energy of 160 eV and a resolution of 1.0 eV. All XPS data were analyzed using CASA XPS software. All binding energies were referenced to the main hydrocarbon peak designated as 284.5 eV.

5.3.6 Fourier transform infrared spectroscopy (FTIR)

The attenuated total reflection-infrared absorption spectra of the surfaces were obtained using a Thermo Electron Nicolet 8700 (Thermo Scientific, USA) spectrometer equipped with germanium crystal. The sample surface to be analyzed was placed against the germanium crystal and absorption data for 32 spectral scans were recorded from 4000 – 900 cm^{-1}, averaged and analyzed using the OMNIC (Thermo Scientific) software program. Before collecting the spectral data, the FTIR sample chamber along with sample surface were purged with nitrogen gas for 5 min to reduce the air humidity inside the chamber. (Note: the humidity level was not precisely monitored.)

5.3.7 Ellipsometry

The thickness of PSBMA polymer grafted from Au-coated glass substrates was measured using an M-88 spectroscopic ellipsometer (J.A. Woollam Co., Inc.). The thickness values reported represent the average of three replicates. Ellipsometric data

were fitted to obtain thicknesses of the polymer films using a Cauchy layer model with fixed A_n (1.47) and B_n (0.01) values.

5.3.8 Contact angle goniometry

Static water contact angle measurements at 22 °C were obtained by the sessile drop method using a contact angle goniometer (Rame-Hart Model 100-00). Each of the average contact angle measurements reported were obtained from five sample replicates.

5.3.9 Scanning electron microscopy (SEM)

To observe the morphology of attached bacteria, the sample surfaces were gently rinsed in ultrapure water at 22 °C to remove unattached cells, fixed with a 2.5% glutaraldehyde solution for 2 hrs, dehydrated in a series of ethanol solutions (30 - 100%), and air-dried [211]. Before characterization, the samples were sputter-coated with a 5 nm layer of gold. The surfaces were then examined using an FEI XL30 scanning electron microscope at an accelerating voltage of 7 kV.

5.3.10 Bacterial strains

Cobetia marina (basonym, *Halomonas marina*) (ATCC 15222) was obtained from the American Type Culture Collection (ATTC, Bethesda, MD) and stored as frozen stock aliquots in marine broth (MB) (2216, Difco, ATTC, USA) containing 20% glycerol at −80 °C. Experimental stock cultures were maintained on MB slants and were stored at 4 °C for up to 2 weeks. A single colony from the slants was incubated in 50 mL of MB and

grown overnight with shaking at 37 °C. After growth, the bacterial culture was centrifuged at a relative centrifugal force of 11,952g for 10 min at 4 °C. The pellet was then suspended in 0.85% NaCl. This washing procedure was repeated twice. The final concentration of bacteria was ≈1 × 10^7 cells/mL, as measured in a C-chip (Cytogen Corp., Sunnyvale, CA) using phase-contrast microscopy (Axioimager, Carl Zeiss Microimaging, Inc., Jena) through a 40X objective lens.

5.3.11 Attachment and detachment of bacteria

Attachment of bacteria on the sample surfaces was assessed using 50 mL *C. marina* suspension (1 × 10^7cells/mL in 0.85% NaCl).[109] Prior to introduction of the sample surfaces, the cell suspensions were pre-equilibrated to 22 °C in glass Petri dishes. The sample surfaces were placed on the bottom of another glass Petri dish, test surface up, and incubated with bacterial suspensions at 22 °C for 2 hrs. The surfaces were then gently rinsed with ultrapure water pre-equilibrated at 22 °C to remove loosely attached cells and salts and dried under a low-pressure stream of dry nitrogen. The attached bacteria were examined using a phase-contrast optical microscope (Axioimager, Carl Zeiss, Inc.) through a 40X objective, and images of 10 randomly chosen fields of view were captured. For each sample, three replicates were performed and the density of attached bacteria was analyzed by ImageJ (National Institutes of Health) to obtain averages and standard deviations.

5.3.12 Cyprid settlement assay

Amphibalanus (=*Balanus*)[212, 213] barnacle nauplii obtained from field-collected adults were reared in mass culture to the cyprid or settlement stage on *Skeletonema costatum* [214]. Cyprids were collected by a sieve cascade from cultures after 4 days, cleaned of debris and held at 6 °C for 3 days and then settled on glass microscope slides, PVMS and PVMS-PSBMA. The settlement assay was performed by placing a large drop of seawater with 5 – 10 cyprids on the test substrata. The substrata were then put in a plastic container (approximately 38 x 25 x 8 cm) lined with moist paper towels, and covered with plastic wrap, and a lid. The moist towel maintained the humidity within the plastic container, preventing the evaporation of the drop of water containing the larvae. The container was kept at 27 ± °C for cycles of 12 hrs in light followed by12 hrs. in darkness. Settlement on each surface was recorded, and pictures were taken every 12 hrs. for 2.5 days.

5.3.13 Protein adsorption assay

Fluorescein- (a green fluorophore) conjugated streptavidin was dissolved in PBS (137mM sodium chloride, 27 mm potassium chloride, 10 mM phosphate buffer) (pH 7.4) at a concentration of 0.1 mg/mL. Multiple test replicates of glass, PVMS and PVMS-PSBMA were kept in 6-well plates and 1 mL of the above protein solution was slowly added on each of the test surfaces and incubated in the dark for 2 hrs. at ~22 °C. Following protein adsorption, the surfaces were immersed in fresh protein-free PBS for

10 min (three times) to remove loosely held protein. The surfaces were then rinsed briefly with ultrapure water to remove salts and dried under a nitrogen stream. The adsorption of proteins was assessed using fluorescence microscopy (Zeiss Axio Imager2) with a 40X objective and a 650/673 nm filter. All images used for comparison of fluorescence intensities were obtained using identical exposure times, image contrast and brightness settings. Fluorescence intensity of images was analyzed using Zeiss Axio Vision software. For each sample, 5 images from random areas across the sample surface were captured and analyzed to obtain the average fluorescence intensity.

5.3.14 Formation of *C. marina* biofilms

The detailed procedure for growing *C. marina* biofilms on test surfaces was previously reported [215]. In brief, the surfaces used for growing biofilms were sterilized by rinsing several times with ethanol and then with copious amounts of sterilized DI water. The test surface was placed in a small glass Petri dish and *C. marina* culture in MB (1 mL) was added on the sample surface along with sterilized artificial seawater (ASW, 5 mL). The samples were stored for a desired period in an incubator maintained at 22 °C. The samples were carefully monitored, and small amounts of ASW were added, as needed every day, to compensate for dehydration.

5.3.15 Analysis of biofilm surface coverage

A standard crystal violet assay was used for analyzing the surface biofilm coverage [216]. In brief, the biofilms on sample surfaces were gently rinsed with ASW to

remove any loosely adhered bacteria and then stained using 5 mL of 0.1% crystal violet aqueous solution for 20 min. The stained biofilm was rinsed twice with ultrapure water and air dried for 15 min before taking digital photographs using an iPhone5 (Apple Inc.). At least five images at different regions were captured from each stained surface under consistent magnification and exposure times. The biofilm coverage on each image was measured by converting the image to binary scale using ImageJ software and adjusting the threshold to precisely differentiate between areas with and without biofilm.

5.4 Results and Discussion

Poly(dimethylsiloxane) (PDMS) based-elastomers are often used as model silicone fouling-release surfaces for biofouling studies. Previous reports on surface modification of PDMS with fouling-resistant polymers have involved physical methods for surface oxidation (e.g., oxygen plasma or ultraviolet/ozone treatment) as an intermediate step prior to reaction with silane coupling agents [217, 218]. Use of such methods can dramatically increase the surface modulus by forming a stiff silica-like layer [219], which may reduce fouling-release properties [76, 199]. It was previously reported that brief ultraviolet (UV) irradiation of poly(vinylmethylsiloxane) (PVMS) based elastomers in the presence of alkylthiol molecules does not significantly alter the modulus, and can be used to produce high-surface-density self-assembled monolayers (SAMs) via thiol-ene click chemistry [220]. We used this approach to graft initiators on

PVMS, which were used to grow zwitterionic polymers from silicone surfaces using activators regenerated by electron transfer for atom transfer radical polymerization (ARGET-ATRP) [15, 210].

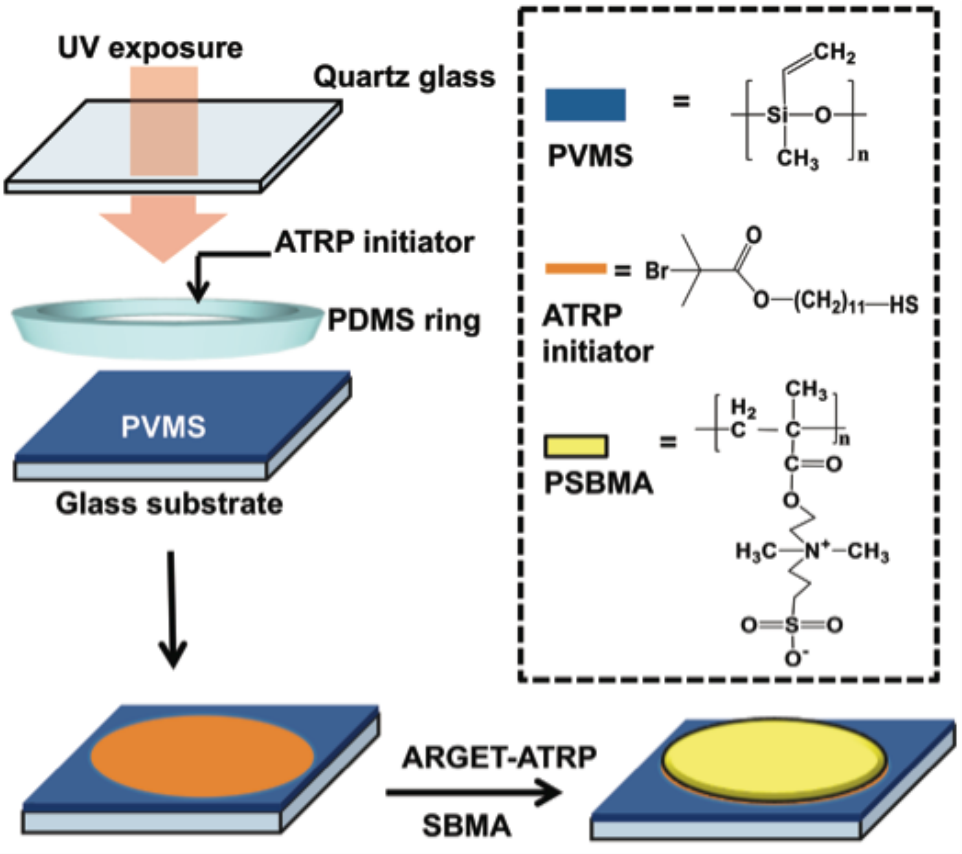

Figure 26: A PVMS elastomer coating (thickness ~ 500 μm) cured on a glass substrate was covered with 2 mM ATRP initiator contained in a PDMS ring. The top surface was then briefly exposed to UV light (λ = 254 nm) to immobilize ATRP-initiator and followed by ARGET-ATRP to graft PSBMA.

The method we used to modify PVMS surfaces is illustrated in Figure 26. The elastomer surfaces were prepared using a previously established method: a precursor

mixture was spin-coated on clean glass slides (25 mm x 25 mm) and cured at 65 °C for 2 hrs. The PVMS precursor mixture comprised an oligomer, a cross-linker, a catalyst and filler particles (see methods section). We fabricated a ring of silicone rubber (Sylgard 184®, Dow Corning) and placed it on the cured PVMS to contain an ethanolic solution of 2 mM of ω-mercaptoundecyl bromoisobutyrate (the ATRP-initiator). This solution on the PVMS was exposed to UV light (λ = 254 nm, 8 W/cm^2, Spectrolinker™ XL-1500, Spectroline Inc. USA) for 5 min through a thin quartz glass. Under UV exposure, the thiol-terminated initiator molecules reacted with the vinyl groups on the surface of PVMS via a thiol-ene reaction (the reaction product is denoted herein as PVMS-Br). After thorough rinsing of the PVMS-Br surface, a surface-initiated ARGET-ATRP reaction developed by Matyjaszewski et al.[210] was conducted for 30 min to grow poly(sulfobetaine methacrylate) (PSBMA). The ARGET-ATRP reaction procedure is described in the methods sections. ARGET-ATRP was used because it offers a simple method to graft uniform polymers without requiring the necessity for oxygen-free reaction conditions. In this application, given that silicone elastomers are porous and readily absorb air, the ARGET-ATRP approach may be especially advantageous over conventional ATRP. Zwitterionic PSBMA was considered in this study because it has been shown to offer fouling-resistance towards a variety of biofouling agents [202].

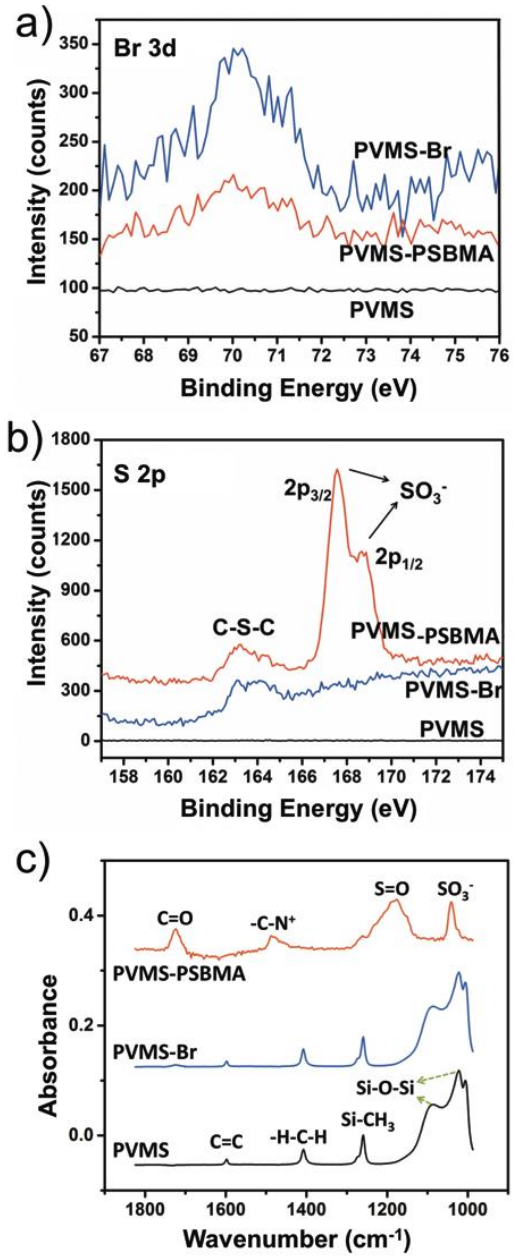

Figure 27: XPS high-resolution spectra of ((a) Br-3d and (b) S-2p) and (c) FTIR absorption spectra of PVMS, PVMS-Br and PVMS-PSBMA.

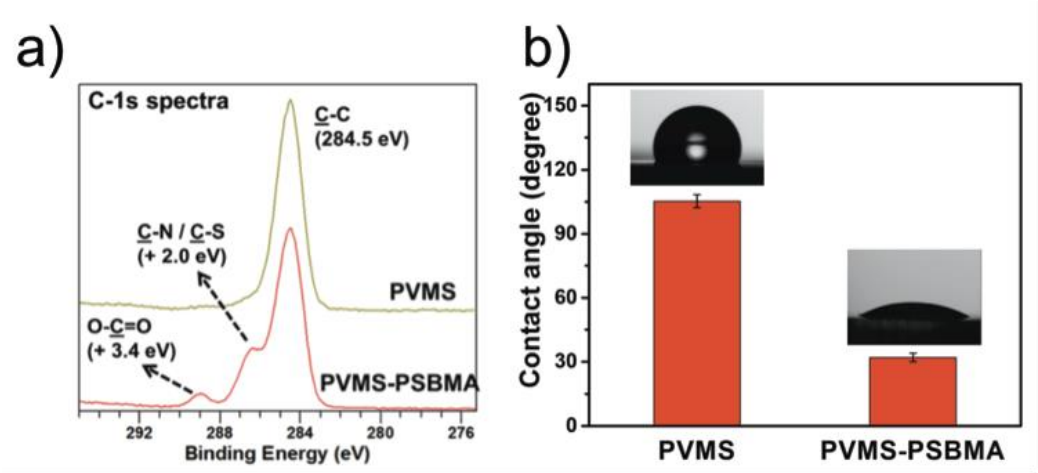

Figure 28: XPS carbon-1s high-resolution spectra of PVMS and PVMS-PSBMA surfaces. The additional carbon peaks observed on PVMS-PSBMA surface at the binding energies of 286.5 and 287.4 eV correspond to the carbon bonded to nitrogen/sulfur (C-N/C-S) and oxygen (O-C=O), respectively and verify the presence of PSBMA after the ARGET-ATRP reaction. (b) Static water contact angles on PVMS and PVMS-PSBMA at 22 °C.

The PVMS-Br and PSBMA-modified PVMS (denoted herein as PVMS-PSBMA) surfaces were characterized using X-ray photoelectron spectroscopy (XPS), Fourier transform infrared spectroscopy (FTIR), and static water contact angle (CA) measurements. On PVMS-Br, the bromine XPS peak (Figure 27a) at 69.8 eV suggests the presence of ATRP-initiator and the sulfur peak (Figure 27b) at ~164 eV represents the bonds formed between sulfhydryl groups of ATRP-initiator and vinyl groups on PVMS (C-S-C). This confirms the successful covalent attachment of the initiator to the PVMS surface. For PVMS-PSBMA samples, the XPS sulfur peak (SO_3^- peak at ~168 eV) and carbon peaks (C-N/C-S and O-C=O at 286.6 and 287.4 eV, respectively) (Figure 27**b** and Figure 28a) confirm the presence of PSBMA. FTIR spectra (Figure 27**c**) show absorption

peaks corresponding to C=C (1590 cm^{-1}) on both PVMS and PVMS-Br, which suggest that the thiol-ene coupling is restricted to the surface of PVMS and does not occur appreciably within the bulk of the elastomer. The absorption spectrum of PVMS-PSBMA (Figure 27c) shows distinct peaks when compared against PVMS and PVMS-Br. The absorption peaks corresponding to C=O (1725 cm^{-1}), C-N (1490 cm^{-1}) and asymmetric stretching of S=O (1180 cm^{-1}) are characteristic of PSBMA and confirm successful grafting of the zwitterionic polymer from the PVMS-Br surface. The CAs (Figure 28b) measured show a significant difference between PVMS (105 ± 3°) and PVMS-PSBMA (32 ± 2°). The relatively low CA on PVMS-PSBMA reflects the high degree of solvation due to strong interactions of PSBMA with water [105]. To summarize, the results from XPS, FTIR and CA measurements confirm that the surface of PVMS was modified with PSBMA polymer using thiol-ene coupling and ARGET-ATRP. It was not feasible to measure the thickness of the grafted PSBMA using ellipsometry directly because the PVMS elastomer is optically clear, so we grafted PSBMA from ATRP-initiator immobilized on gold surfaces under similar reaction conditions and measured the dry thickness of PSBMA on gold surfaces (Au-PSBMA) using ellipsometry. The measured thickness of polymer on Au-PSBMA was 28 ± 3 nm, which is our best estimate of the dry thickness of PSMA on PVMS-PSBMA.

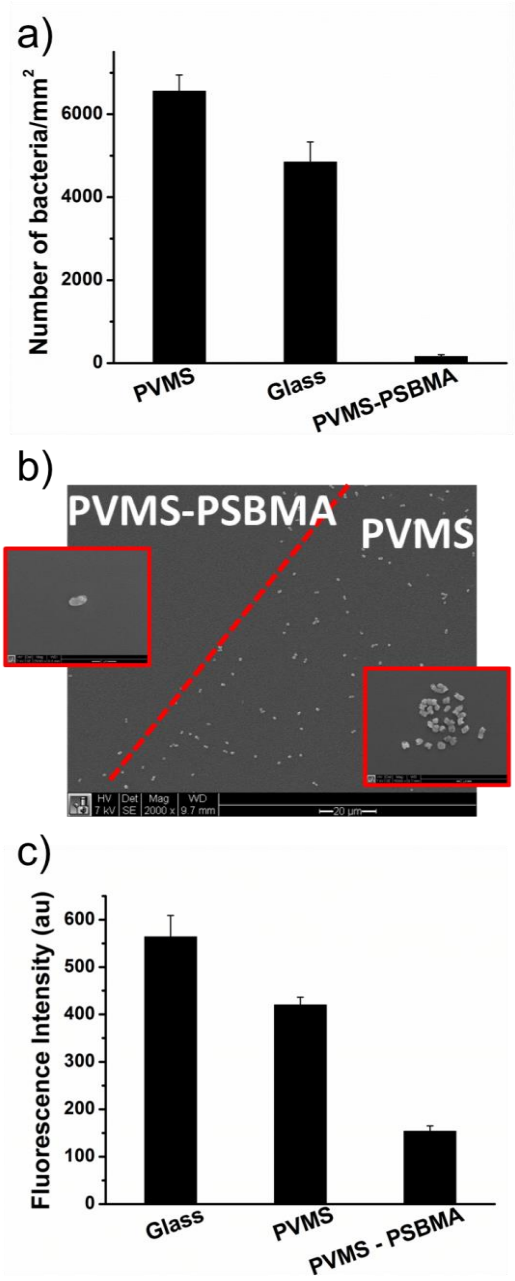

Figure 29: (a) Attachment density of *C. marina* on glass, PVMS and PVMS-PSBMA after exposure to 1 × 107 cells/mL for 2 hrs. at 22 °C. (b) (a) Scanning electron microscope images of *C. marina* on test surface at the boundary (dashed red line) between PVMS and PVMS-PSBMA. (c) The adsorption of fluorescently labeled streptavidin on glass, PVMS and PVMS-PSBMA for 3 hrs. The error bars in (a) and (c) correspond to the standard deviation of the mean (n = 5).

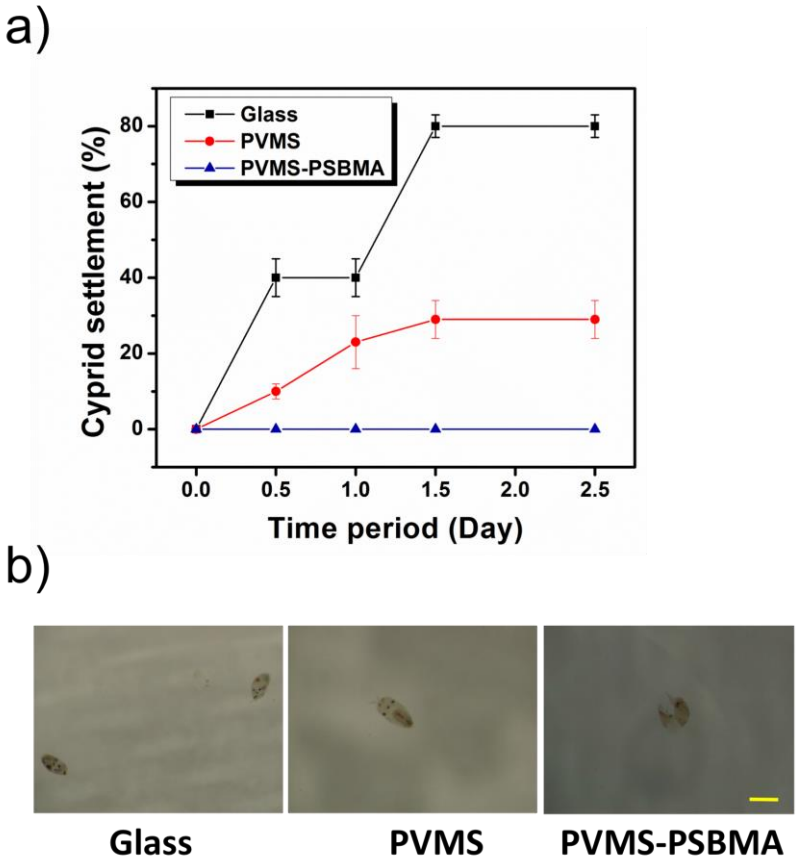

Figure 30: Percentage of barnacle cyprids settled over a period of 2.5 days on glass, PVMS and PVMS-PSBMA. The error bars correspond to the standard deviation of the mean (n = 5). (b) Representative optical microscopy images of settled barnacle cyprids on glass, PVMS, and PVMS-PSBMA surface after 36 hours. The average size of each cyprid was 1.3 mm (length) x 0.7 mm (width). On glass and PVMS surfaces, the cyprids settled and were alive. In contrast, the cyprids exposed to PVMS-PSBMA died after 24 hrs. The scale bar (yellow) on corresponds to 1 mm.

To test the hypothesis that zwitterionic polymer-modified silicones exhibit fouling-resistance, multiple replicates of PVMS-PSBMA, PVMS and clean glass substrates were subjected to suspensions of a model, Gram-negative, marine bacterium,

Cobetia marina (1×10^7 cells/mL in 0.85% NaCl) for 2 hrs at 22 °C. The surfaces were then very gently rinsed with ultrapure water, dried in air, imaged using phase contrast microscopy and analyzed to determine surface density of cells. Figure 29a summarizes the results of surface density of attached cells. Glass and PVMS surfaces exhibited high densities of cell attachment (> 4,500 cells/mm^2), while PVMS-PSBMA exhibited low cell density (< 200 cells/mm^2). This corresponds to > 95% reduction of cell attachment on PVMS-PSBMA. Zwitterionic polymers, owing to their strong electrostatically induced hydration, form a tightly bound water layer in the vicinity of polymer chains, which can prevent the attachment of microbes and other fouling species [101, 202, 221]. The cell morphology of the attached *C. marina*, imaged using scanning electron microscopy, was similar on both PVMS (control) and PVMS-PSBMA (Figure 29b), suggesting that PSBMA does not influence cell structure. PVMS-PSBMA also showed resistance to non-specific protein adsorption in comparison to PVMS (Figure 29**c**) as well. These results suggest that PVMS-PSBMA exhibits short-term fouling resistance.

Figure 30a presents the results of settlement of barnacle cyprids, *Amphibalanus* (= *Balanus*) *Amphitrite* [222], on glass, PVMS and PVMS-PSBMA test surfaces. Barnacles are common non-motile macro-fouling species that attach to surfaces in the last larval, cyprid, stage after which they metamorphose into juvenile barnacles [223]. Large drops of seawater containing 5 to 10 cyprids were carefully placed on each test substrate and allowed to settle for a period of 2.5 days (see methods section for detailed procedure).

PVMS-PSBMA test surfaces inhibited the settlement of cyprids for the entire duration of the study, whereas glass and PVMS experienced increasing amounts of cyprid settlement with time (Figure 30a). On PVMS-PSBMA, it was observed cyprids became trapped in the aqueous seawater layer and later died after 24 hours (Figure 30b). It has been reported that entrapping of cyprids delays their metamorphosis, which, in turn, often influences their growth and survival [223]. These results are in agreement with previous assays of settlement on zwitterionic polymer brushes grafted from glass and Au-coated substrates [202, 224]. In summary, the results in Figure 29 and Figure 30 support the hypothesis that PVMS modified with zwitterionic polymers can inhibit biofouling over short-time intervals.

To examine the fouling of PVMS-PSBMA over longer-terms, multiple replicates of PVMS-PSBMA, PVMS and glass surfaces were exposed to suspensions of *C. marina* for 1-5 days (see methods section for procedure), after which each test surface was gently rinsed with sterilized artificial sea water (ASW), stained with 0.1% crystal violet (aqueous), dried in air and photographed. The surface biofilm coverage was estimated by converting the color images to binary scale using ImageJ software and adjusting the threshold to precisely differentiate between areas with, and without, visible biofilm [207]. The rate of biofilm formation on PVMS-PSBMA was slower than on glass or PVMS. PVMS and glass surfaces had >80% biofilm surface coverage within 3 days, whereas PVMS-PSBMA had ≈45% biofilm coverage in 5 days, as shown in Figure 31.

When the fouling time period was extended to 2 weeks, >97% of PVMS-PSBMA surface was covered with biofilm, indicating that fouling resistance of PVMS-PSBMA diminishes upon longer-term exposure to biofouling conditions. This could be due to various factors, for example, to instability of hydrated polymer chains in aqueous solution over longer time-intervals, or to a steady overcoming of the hydration layer resistance of the PVMS-PSBMA by *C. marina* to result in the accumulation of microbes on the surface over time [110, 225].

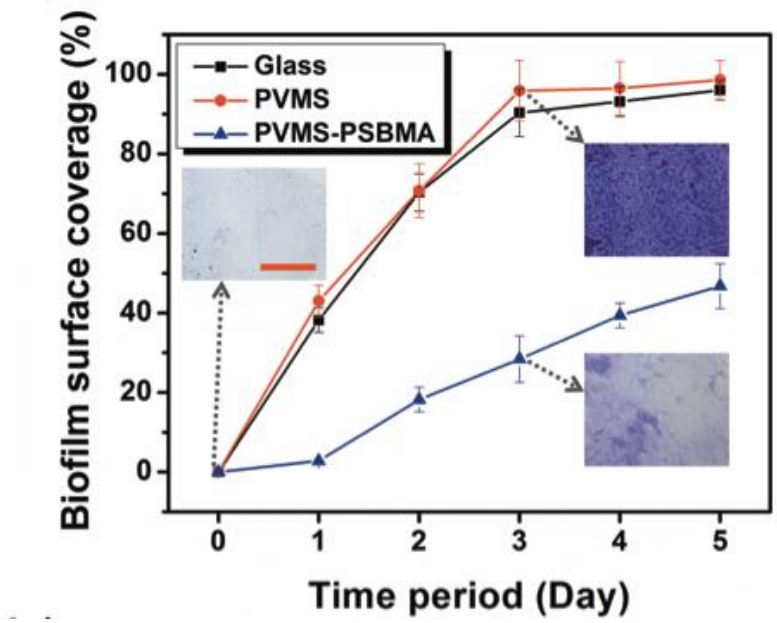

Figure 31: Surface coverage of *C. marina* biofilms on glass, PVMS and PVMS-PSBMA surfaces over a time period of 5 days. The insets are photographs of crystal violet stained biofilm on PVMS and PVMS-PSBMA after 0 and 3 days; the scale bar corresponds to 2.5 mm. The error bars correspond to the standard deviation of the mean (n = 5).

Lopez, Zhao and coworkers recently reported that biofilms accumulated on silicone elastomers can be efficiently released by active deformation of the surface.[206-208] Surface deformation can be achieved by various means, for example, by directly stretching the elastomer or by using more indirect methods, such as electro- and pneumatic-actuation. In this study, we examined the hypothesis that biofilms accumulated on PSBMA-modified silicones can be released using surface deformation. PVMS elastomer coupons (25 mm × 10 mm) of 3 mm thickness were prepared by curing the precursor mixture in a 3-D printed plastic mold. The cured elastomer was removed from the mold and PSBMA was grafted on one side of the film surface (see Scheme 1) using surface-initiated ARGET-ATRP. To examine the mechanical stability of the grafted polymer under substrate deformation, PVMS-PSBMA films were subjected to uniaxial strain of 50% for at least 20 cycles using a tensile tester (Test Resources, USA). The films were then sonicated in DI water, dried in nitrogen gas and analyzed by XPS. The elemental composition of PVMS-PSBMA surface before and after stretching was almost identical (Table 2) suggesting that the polymer layer on the PVMS was stable after repeated substrate deformation

Table 2: XPS elemental composition of PVMS-PSBMA before and after cyclic stretching. The stretching was performed by applying a linear strain of 50% and then relaxing it back to 0% strain for 20 cycles at a strain rate of 50 mm/min. The films were then sonicated in DI water, dried in nitrogen gas and analyzed by XPS. There were no significant changes (P > 0.05) in the XPS elemental composition of the PVMS-PSBMA surface before and after stretching, indicating that the grafted PSBMA on the PVMS is stable against applied mechanical substrate deformation.

Element	Binding Energy (eV)	PVMS-PSBMA	
		Before stretching	After stretching
C %	284.5	61.9 ± 0.4	62.0 ± 0.5
N %	396.3	2.1 ± 0.2	1.8 ± 0.3
S %	167.3	2.4 ± 0.3	2.4 ± 0.1
O %	531.2	23.5 ± 0.8	23.7 ± 0.6
Br %	69.3	0.2 ± 0.1	0.2 ± 0.1
Si %	101.4	9.9 ± 0.1	9.9 ± 0.3

To examine whether surface deformation can detach biofilms accumulated on polymer-modified silicones, multiple replicates of PVMS-PSBMA and PVMS (control) films were subjected to *C. marina* biofilm formation for 14 days. Each test surface with biofilm was carefully subjected to 15 cycles of fixed (5%, 10%, 15% or 20%) uniaxial strain, at a constant strain rate (50 mm/min). The films were then gently rinsed (5 mL/min for ≈ 2 min) with sterilized ASW and analyzed for surface biofilm coverage using the procedure detailed above. The percentage of biofilm released was estimated by taking the ratio of surface coverage of biofilm before and after the deformation [207].

Figure 32 illustrates the percentage of biofilm released from PVMS and PVMS-PSBMA surfaces under various amounts of applied strain (Figure 33 shows images). For low substrate strains (ε) of 0 or 5%, no significant biofilm release was observed, but at higher strains, substantial release of biofilm occurred (e.g., for $\varepsilon > 10\%$ for PVMS; $\varepsilon > 15\%$ of PVMS-PSBMA more than 85% of the biofilm was released). Zhao et al. postulated that elastic energy per unit area in the biofilm increases with substrate strain and when this energy exceeds the biofilm-substrate adhesion energy, the biofilm de-bonds from the substrate [206]. The de-bonded biofilm can then be easily removed upon gentle rinsing. Figure 32 and Figure 33 show that the value of ε required for release of the *C. marina* biofilms was lower for PVMS (≈ 10%) than that for PVMS-PSBMA (≈ 15%). This observed difference could be due to a number of factors [207, 208]. For instance, the biofilm thickness and/or the Young's modulus (both of which have been postulated to effect the critical strain necessary for biofilm debonding [206, 208] may also depend on the substrate upon which it forms. In this study, the slower rate of biofilm accumulation on PVMS-PSBMA observed (Figure 31) suggests that the biofilm formed on PVMS-PSBMA may be thinner than on PVMS at the 14 day time point when they were subjected to strain treatment.

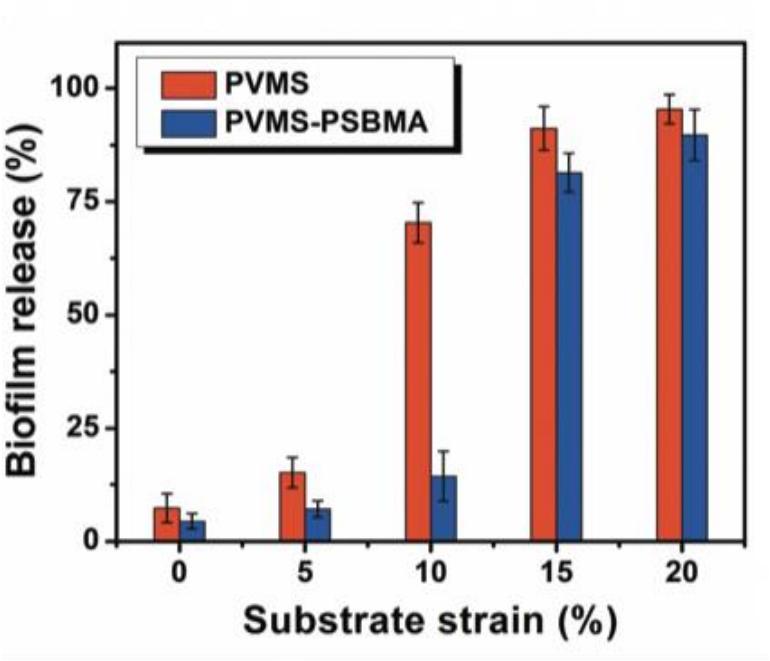

Figure 32: The percentage of *C. marina* biofilms (grown for 14 days) released from PVMS and PVMS-PSBMA surfaces under a range (0 - 20%) of applied strain. The error bars correspond to the standard deviation of the mean (n = 5).

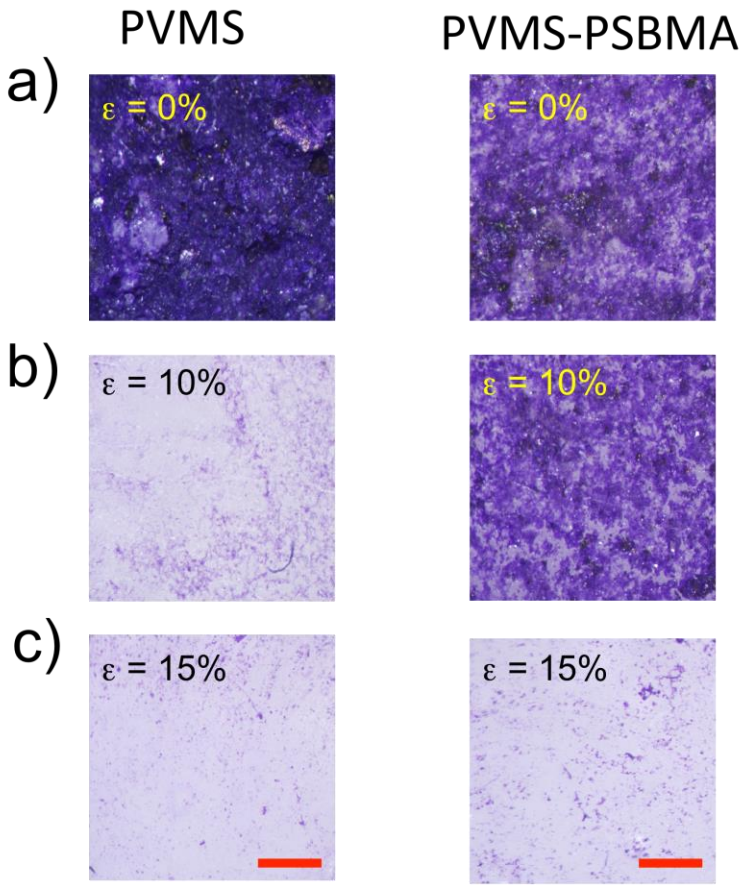

Figure 33: Digital photography images of crystal violet-stained *C. marina* biofilms (grown for 14 days) on PVMS and PVMS-PSBMA before strain (a) and after 10% cyclic strain (b) and after 15% cyclic strain (c), in each case followed by gentle rinsing. The purple regions on the surfaces correspond to the stained *C. marina*. The surfaces with 0% strain represent the control surfaces (i.e., no deformation). The 10% (b) and 15% (c) strain were applied using a tensile tester for 15 cycles at a constant strain rate of 50 mm/min, slowly rinsed with DI water, and stained with crystal violet dye. The scale bar on the images represent 1 mm.

Finally, we examined whether the PVMS-PSBMA film after biofilm detachment could exhibit and retain fouling resistance when re-immersed in a fouling environment. PVMS-PSBMA exhibited fouling resistance (Figure 34), but to a lesser extent (e.g., 37 ± 2% biofilm coverage in 3 days) as compared to a pristine PVMS-PSBMA surface (Figure

31). This suggests that the fouling resistance of PVMS-PSBMA may reduce over repeated cycles of biofilm formation; such reduction may be alleviated by improvements in the performance and stability of zwitterionic polymers [225].

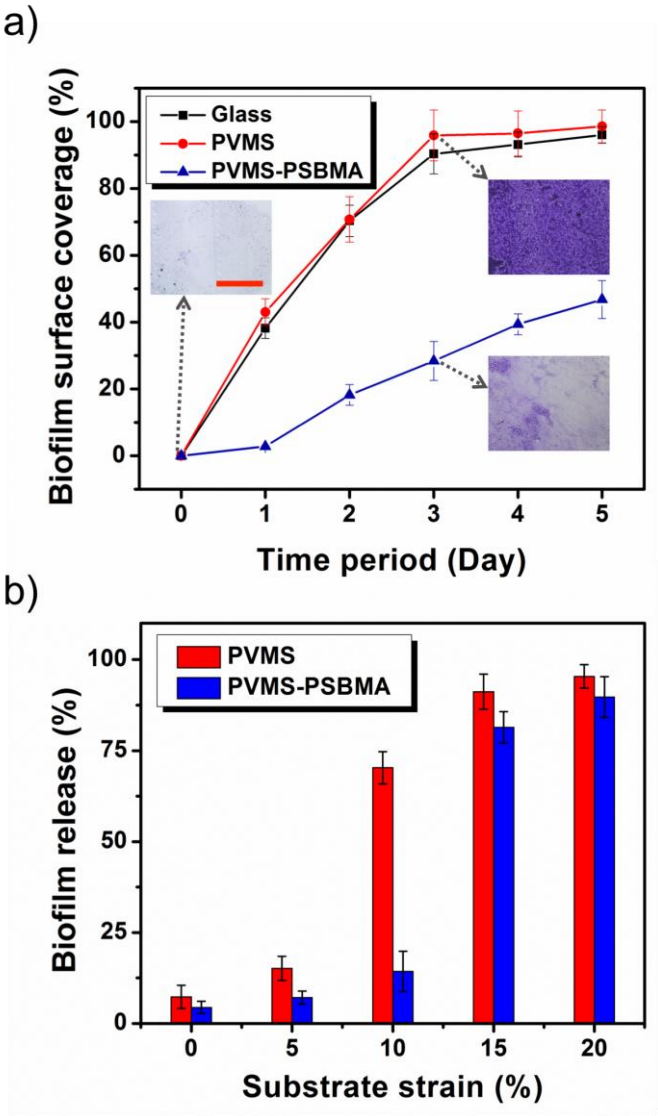

Figure 34: PVMS and PVMS-PSBMA films after biofilm detachment via surface deformation were again exposed to *C. marina* to result in biofilm formation. (a) Rate of surface biofilm coverage over a period of 0 to 7 days. The inset images in

(a) are representative digital photographs of crystal violet stained C. marina biofilm on PVMS and PVMS-PSBMA after 3 days exposure to C. marina. b) After 9 days of biofilm re-growth, PVMS-PSBMA was subjected to uniaxial stretching to a varied amout of strain (0 - 20%). The surfaces were then gently rinsed with ASW and surface biofilm coverage was analyzed and compared against control surface (i.e. 0% strain). While, no significant biofilm was released at ε = 10%, >85 ± 5 % of the biofilm was release at ε = 15%. The inset images in (b) are representative digital photographs of the crystal violet stained C. marina biofilm after 10% and 15% strain. The scale bar on the digial photographs on (a) and (b) correspond to 1 mm.

5.5 Conclusions

This study presents a chemical approach to easily modify the surface properties of PVMS-based elastomers with fouling resistant zwitterionic polymers. This chemical modification approach is applicable to grafting other types of biofunctional polymers as well (*e.g.*, thermo-responsive poly(*N*-isopropyl acrylamide) which provides another mechanism for triggered-fouling release). Biofilms accumulated on zwitterionic PSBMA polymers over long-term fouling exposure are effectively released by applying mechanical strain to the PVMS substrate. These types of bifunctional surfaces may be applicable for pro-active biofouling management on marine equipment (*e.g.*, ship hulls, sensors), industrial equipment [196] and biomedical devices (*e.g.* urinary catheters [207]) and can be implemented with electro- or pneumatic-actuation systems [206], for example.

The design of long-term, fouling-resistant surfaces provides extraordinary challenges, since biofouling environments can consist of myriad, and often cooperatively interacting, surface-active species. To our knowledge, so far, none of the fouling-

resistant surface modification strategies developed resist biofouling in the long term. The substrate deformation approach presented in this study for zwitterionic fouling resistant surfaces should also be applicable to other existing and emerging [226] types of fouling-resistant strategies as well.

5.6 Chapter Acknowledgements

The work presented in this chapter was supported by the ONR (Grant N00014-13-1-0828) and the NSF's Research Triangle MRSEC (DMR-1121107). This work was also supported by the ONR grants to Genzer (N00014-12-10642) and to Rittschof (N00014-14-1-0336, N00014-12-1-0365 and N00014-11-1-0180).

6. Chapter 6: Incorporation of silicone-oil additives in stretchable silicone elastomers to improve fouling-release performance

The study presented in this chapter describes the experimental results for Specific Aim 3 and demonstrates the advantage of incorporating silicone-oil additives in stretchable elastomer for easier detachment of barnacles using dynamic surface deformation. This chapter represents the preliminary manuscript version of the full article that we intend to submit to Biofouling journal for publication. Phanindhar Shivapooja is the lead author for this manuscript.

6.1 Synopsis

Barnacles are a major concern in management of biofouling on surfaces submerged in seawater (e.g., ship hulls). Silicone-oil additives (0 – 10 wt%) are often used in fouling-release silicone coatings to improve their performance. Silicone-oil additives are known to segregate to the surfaces of coatings' and exhibit surface-properties (e.g., slipperiness and inhibition of bioadhesive curing) that enable easier detachment of barnacles. The coauthors of this report recently reported that surface strain generated using deliberate deformation of stretchable silicone elastomers effectively result in detachment of barnacles and other fouling organisms. This study presents a dual-mode-approach for barnacle detachment by incorporating silicone-oils in stretchable silicone elastomers. We hypothesized that silicone-oil additives reduce the amount of substrate strain needed to detach barnacles. We employed Ecoflex-based

silicone elastomer and two silicone-oil additives to investigate this hypothesis. Furthermore, we examined the effect of change in substrate modulus (due to silicone-oil additives) on barnacle adhesion strength. This study de-coupled the two effects of silicone-oils (i.e., surface-action and alteration in bulk modulus) and examined their contribution on barnacle adhesion strength. It was observed that surface-action of silicone-oil reduces the substrate strain required for barnacle detachment, whereas decrease in substrate modulus increases the strain required to detach barnacles. A finite element model based on fracture mechanics was employed to elucidate the effects of surface strain and substrate modulus on barnacle adhesion strength. This study demonstrates that dynamic substrate deformation combined with silicone-oils can provide a bifunctional approach for management of biofouling by barnacles.

6.2 Introduction

Any surface submerged in seawater is exposed to the settlement of various non-crustacean (e.g., bacteria, algae) and crustacean (barnacle and mollusks) fouling organisms. Biological fouling (or biofouling) on surfaces has various deleterious effects, in particular for naval industry, because it leads to economic and environmental penalties [227-230]. Surface coatings used to prevent biofouling are broadly categorized into two types: anti-fouling (AF) and fouling-release (FR) coatings. AF coatings (e.g., self-polishing paints) function by releasing chemically-active biocide compounds which can kill the organisms or inhibit the settlement of organisms [231]. In contrast, FR

coatings mainly work to minimize the adhesion strength of the fouling organisms on its surface so that the organisms can be easily removed by hydrodynamic stress during navigation or by gentle mechanical cleaning [232]. Due to the increased environmental concerns and regulations on the use of biocide- (e.g., CuO) releasing paints, non-toxic FR coatings have become desired environment-friendly alternatives for biofouling management in marine environment.

Many researchers have attempted to develop new approaches to control biofouling using a wide range of different strategies. Examples include incorporation of silicone-oil additives [80, 233-235], engineered biomimetic surface topographies [93, 236], modification with amphiphilic copolymers [96, 98], and tethering of bioactive polymeric moieties [105, 237-240]. Among non-toxic FR approaches, poly(dimethylsiloxane) (PDMS) based silicone elastomers have received much attention due to their non-toxic and 'non-sticky' properties. The FR properties of silicones are mainly attributed to its low surface energy [241], smoothness, reduced polar interaction at the interfacial surface [242] and inhibition of the curing of biological adhesives [243].

Lopez, Zhao, Rittschof and co-workers previously reported a bioinspired approach for biofouling management, which was based on the concept of active surface deformation of stretchable elastomers [181, 244]. In this method, stretchable silicone elastomers that were fouled with a variety of organisms were dynamically strained using external stimuli (e.g., mechanical force, electrical field or pneumatic pressure) to

achieve detachment of both bacterial biofilms and barnacles. The amount of strain required for FR was dependent on the mechanical properties of the substrate and the biofouling layer. It was observed that substrate strain required for the detachment of barnacles was many times higher than bacterial biofilms. For instance, detachment of adult barnacle from PDMS required a substrate strain of ~100%, whereas bacterial-biofilms (~75 ◎m thickness) were effectively detached using a critical strain as low as ~15% [117]. The higher substrate strain required for barnacle detachment is likely due to a combination of their different attachment geometry and the greater adhesion strength of the barnacles' glue as compared to that of slimy bacterial biofilms [228].

Barnacle and other crustacean fouling species discharge a variety of biological adhesives, which affix onto surfaces and can cure in water [242, 245, 246]. Barnacles are a major target in biofouling management and a primary invertebrate model for biofouling studies in both, laboratory and field environments because of their common occurrence as problematic marine foulers and their tenacious adhesion [247, 248]. Silicone-oil additives are often used in FR coatings because the oil-additives passively elute to the surface through the porous silicone elastomer and enhance surface slipperiness, which decreases the coefficient of friction and favors easier release of fouling organisms [249, 250]. The mobile ('free') silicone-oil compounds on the elastomer surfaces are also known to alter the enzymatic curing process of the bioadhesives secreted by foulants, and lower their adhesion strength. In case of barnacles, Rittschof et al. [18] previously

reported that silicone-oils that elute to the surface significantly alter the enzymatic (transglutaminase) activity and alters the cross-linking of glue proteins. Both the above surface-actions (i.e., enhancement of surface slipperiness and inhibition of enzymatic cross-linking) are advantageous in mitigation of biofouling. Though potential deleterious effects of oils leaching from coatings on marine and benthic organisms have been pointed out, there is no statistical evidence to support these concerns [251, 252]. For example, Truby et al. reported that the oil leached from silicone coating was < 1.1 wt % over a period of one year in the laboratory environment [16].

While the incorporation of silicone-oil additives reduces the adhesive strength of fouling-species [253, 254], it is still a challenge to reduce the barnacle adhesion strength to a level such that a small amount of external force (e.g., hydrodynamic dragging force) can easily detach ('shear-off') the barnacles [255]. It is also impractical to impregnate a large amount of silicone-oil into the coating because it would compromise the durability of the coating, and also might increase ill-effects of the silicone-oils in the ocean environment. Thus, it is desirable to develop more efficient and eco-friendly approaches for easier detachment of barnacles and other fouling species.

This study aims to use a combination of active surface strain and silicone-oil additives to reduce the barnacle adhesion strength, while also reducing the amount of oil required. This study includes three specific objectives: (i) to investigate the hypothesis that incorporation of silicone-oil additives into elastomers reduces the

amount of substrate strain required for barnacle detachment, (ii) to decouple the effect of surface-action and change in elastomer modulus due to silicone-oil on barnacle detachment using substrate deformation, and (iii) to qualitatively elucidate the effect of substrate strain and modulus on barnacle detachment process using fracture mechanics. Ecoflex silicone-based elastomers and two types of silicone oils are used in this study. Ecoflex was chosen because it is a non-toxic, stretchable silicone and its use for fouling release via active substrate strain was previously demonstrated in laboratory and field environments [208]. The adult barnacles (*Amphibalanus* (= *Balanus*) *amphitrite*) used in this study were cultured, grown and reattached on Ecoflex elastomer test surfaces at the Duke University Marine Laboratory (Beaufort, NC). The experimental results support the above hypothesis and demonstrate the effectiveness of this dual-mode approach in the easier detachment of barnacles. The experiment and computation results on the effect of substrate modulus (with and without silicone-oil) prove that surface-elution of silicone-oil plays a major role in facilitating detachment of barnacles using surface strain.

6.3 Materials and Methods

6.3.1 Materials

Ecoflex® 0050 and Silicone Thinner® were purchased from Smooth-On Inc. (PA, USA). Ecoflex® 0050 is a platinum catalyst based silicone kit used in the preparation of silicone elastomers, while Silicone Thinner® is a silicone compound additive used for altering the modulus of the silicone elastomers. The chemical formula of Silicone

Thinner® is proprietary information of Smooth-On Inc. The silicone oils used in this study, DMS-TI5 (viscosity: 50 cSt, molecular weight: 3,780 g/mol) and DMS-T05 (viscosity: 5 ct, molecular weight: 770 g/mol) were purchased from Gelest Inc. (PA, USA). As shown in Table 3, both these oils have identical repeating units of dimethylsiloxane and, structurally, differ only in their molecular weight. In the following text, Ecoflex 0050, Silicone-Thinner®, DMS-T15 and DMS-T05 are respectively referred in short as Ecoflex, Silicone Thinner®, oil-T15 and oil-T05 for convenience.

Table 3: Structural formula, viscosity and molecular weight of oil-T15 and oil-T05.

Structural formula of DMS-T15 and -T05 silicone oil	Silicone oil	Viscosity (cSt)	Molecular weight (g/mol)
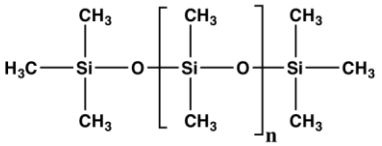	Oil-T15	50	3780
	Oil-T05	5	770

6.3.2 Sample Preparation

Ecoflex elastomer substrates without silicone-oil additive were prepared using 1:1 (weight) mixture of the two components (Part-A and Part-B) that comprise the Ecoflex® 0050 kit. This mixture was thoroughly mixed and degased using a planetary mixer (Thinky-Mixer, USA) and then gently poured into polystyrene Petri dish (90 mm dia.) to obtain a uniform 3 mm thick layer. The sample was then allowed to cure at room temperature for at least 8 hours to form a cross-linked elastomer. The cured elastomer

was peeled-off from the Petri dish, cut into a rectangular shape (70 mm x 40 mm) for use as a test surface. In the preparation of test surfaces with silicone-oil additive precisely weighed amounts (5 or 10 wt%) of oil-T15 or oil-T05 was added to the Ecoflex precursor mixture before mixing, degassing and curing. Figure 35**,** summarizes the step-wise procedure used in making the elastomers substrates infused with silicone-oil additives. In case of Ecoflex with Silicone Thinner®, the silicone-oil additive was substituted with Silicone Thinner®.

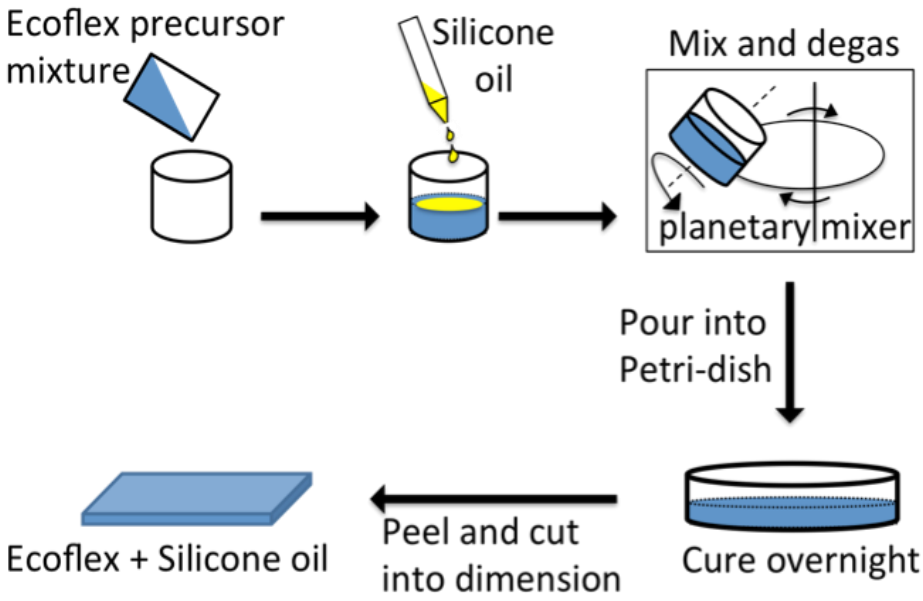

Figure 35: Procedure for fabrication of Ecoflex samples with silicone oil-additives. The mixture of Ecoflex precursors (part-A:part-B = 1:1 by weight) and a silicone-oil additive (5 or 10 wt%) are thoroughly mixed and degassed using a planetary mixer. The resultant mixture was carefully cast into a Petri-dish to a thickness of 3mm and cured overnight at room temperature. The cured samples were then peeled off and cut into rectangular shapes (70 mm x 40 mm).

6.3.3 Barnacle reattachment on elastomer surfaces

Reattachment of barnacles (*Amphibalanus* (= *Balanus*) *amphitrite*) on the test surfaces was performed using a procedure that is reported elsewhere [256]. In brief, barnacle cyprids were allowed to settle on SilasticT2® coated glass substrates (a gift from North Dakota State University*)* and cultured for 7 weeks to attain adult barnacles with a basal diameter of ≥ 0.5 cm. These adults were used for reattachment on Ecoflex test surfaces. For reattachment, the adult barnacles were carefully pushed off the SilasticT2® surface and immediately placed on the Ecoflex elastomer test surfaces and incubated in air under 100% humidity for a period of 24 hours. The test surfaces were then submerged in running seawater and fed with brine shrimp daily for 2 week, after which they were used in barnacle adhesion strength analysis assays.

6.3.4 Barnacle adhesion strength measurement

The adhesion strength between a barnacle and an elastomer substrate was measured following the procedure outlined in ASTM D-5618-94 (ASTM, 2011). According to this procedure, a handheld force gauge is used to apply a force parallel to the attachment plane of the barnacle at a rate of approximately 4.5 Ns^{-1} until the barnacle is completely detached from the surface of elastomer. As the elastomer surface, as cast, was flat, barnacle adhesive was assumed to be in contact with the substratum over the entire basal plate surface and hence, the size of the basal plate was used to determine the attachment area (A) of the barnacle. For this, the baseplate diameter of the detached

barnacle was measured in four different orientations using a caliper and then the average diameter (d) was determined for an individual barnacle. The attachment area was then calculated as $A = \pi d^2/4$. The adhesive strength (kPa) of individual barnacle was finally calculated by dividing the shear force (F) required to detach the barnacle by its attachment surface area (A).

6.3.5 Cyclic deformation of the elastomer substrate

The elastomer substrates with reattached barnacles were subjected to varying amounts of uniaxial strain (0–50%) using a universal test machine (Test Resources, USA) equipped with a loading frame, modular actuator and computerized controller. The Ecoflex elastomers with reattached barnacles were clamped onto the grips of the equipment and fixed amount (12.5, 25, 37.5 or 50%) of cyclic strain was applied for 15 cycles (see Figure 37) at constant strain rate of 50 mm/min (±0.5%).

6.3.6 Measurement of elastomer shear modulus

The shear moduli of silicone elastomer samples prepared with different compositions were measured using a Micro-Strain Analyzer (MSA, TA Instruments RSA III) under uniaxial tension. The elastomers were cut into thin strips (20 mm x 5 mm x 3 mm) and gripped firmly between the clamps of the instrument. Controlled uniaxial tension was applied on the elastomer strips using a preload of 0.01 N and a strain ramp of 0.05% min^{-1}. The displacement or stretch rate was set to 1 mm s^{-1}. The stress vs. stretch data recorded by the instrument was then fit to the neo-Hookean model to obtain the shear

modulus of each sample. The average shear modulus for each sample-type was calculated using five identical replicates (n = 5).

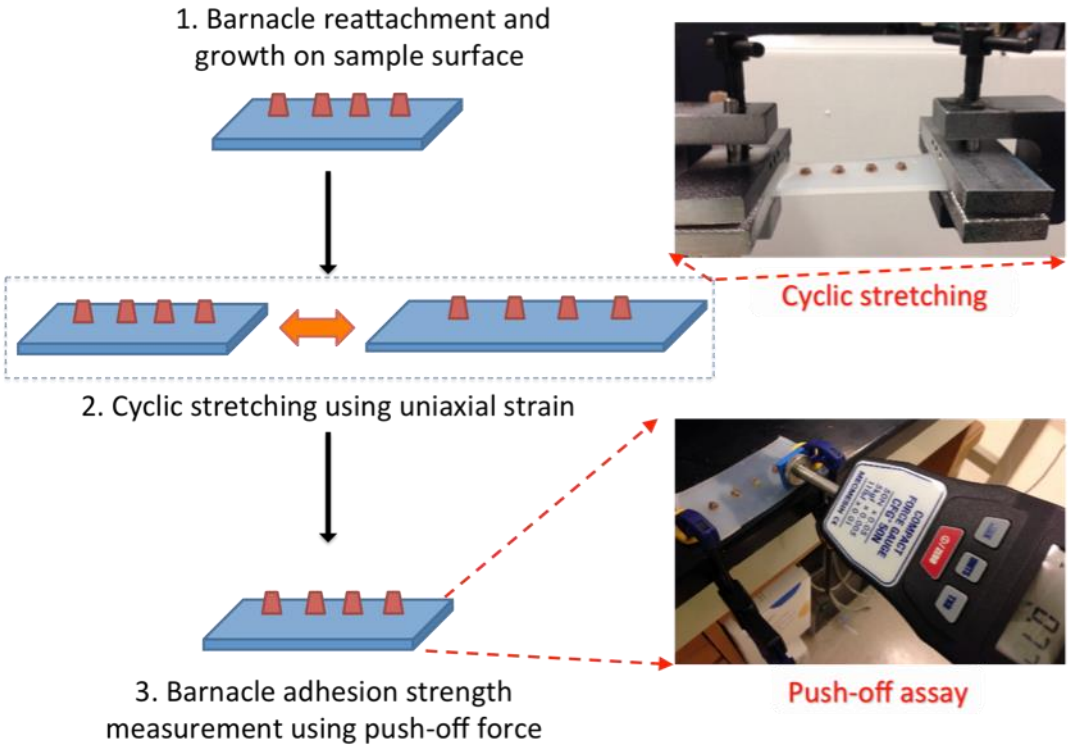

Figure 36: Dynamic surface deformation of an elastomer substrate and measurement of barnacle adhesion strength. (1) Barnacles were reattached on an elastomer test surface and allowed to grow for a period of 2 weeks in seawater. The conditions used for barnacle reattachment and growth are detailed in the Methods section. (2) The test surfaces with attached barnacles were subjected to 15 cycles of fixed amount substrate strain (12.5%, 25%, 37.5% or 50%) using a mechanical device. (3) After cyclic substrate strain, each barnacle was individually detached using push-off force applied parallel to the base of the barnacle. The barnacle adhesion strength for an individual barnacle is estimated by dividing the measured push-off force by the surface area of barnacle baseplate. The images are representative digital photographs of the cyclic stretching and the push-off assay.

6.3.7 Finite element modeling

The barnacle-elastomer substrate system was modeled using a FEM software package, ABAQUS 6.14. The barnacle was assumed to be a rigid material and the substrate was modeled as an incompressible Neo-Hookean material. The shear modulus of the substrate was based on the values measured from the uniaxial tensile tests, and discretized with hybrid quadratic elements (CPE8MH) under 2-D plane-strain deformation. Mesh convergence was carried out to verify the accuracy of the model. Due to symmetry, only one-half of the barnacle was modeled. The thickness of the substrate was treated as infinite compared to the barnacle adhesive layers. The displacement-control loading conditions were used to apply the uniaxial strains in the substrate. Periodic boundary conditions were prescribed along the vertical sides of the model, whereas the vertical displacement and the shear traction were prescribed to be zero on the bottom surface of the substrate. The energy release rate was calculated as $G = \lim_{a->0} \partial U / \partial a$, where U is the strain energy of the model, and a is the crack length.

6.4 Results and Discussion

6.4.1 Effect of silicone-oil and cyclic substrate strain on the barnacle adhesion strength

The preparation of elastomer substrates and the reattachment of barnacles are detailed in the methods section. The elastomers were conditioned in flowing seawater for a period of 2 weeks and then barnacles were reattached and grown on one side of the elastomer substrates for 2 weeks. As shown in Figure 36, the elastomer substrates with

reattached barnacles were stretched for 15 cycles to a fixed level of uniaxial strain (12.5%, 25%, 37.5% or 50%) at a constant strain rate of 50 mm min^{-1} using a universal testing machine. After cyclic stretching, the elastomer substrates were unloaded from the grips and the adhesion strength was measured and analyzed following the standard push-off assay according to ASTM D-5618-94 (ASTM, 2011).

Figure 37a shows optical images of a barnacle baseplate on Ecoflex elastomer before and after applying 50% uniaxial strain. Prior to straining, the adsorbed organic matter (i.e., adsorbed biofilm or secreted barnacle glue) area around the attached baseplate was stained by exposure to crystal violet dye (2% aqueous). As seen in Figure 37a, when the elastomer is stretched to 50% strain, the crystal violet boundary on the substrate (indicated by red dash-line) was displaced from the barnacle baseplate. This indicates the partial debonding of the barnacle baseplate when the substrate is strained. By considering the barnacle to be a rigid solid on a soft substrate, the de-bonding can be assumed as the inward propagation of the cracks at the edge of the barnacle-elastomer interface when the substrate is stretched [257].

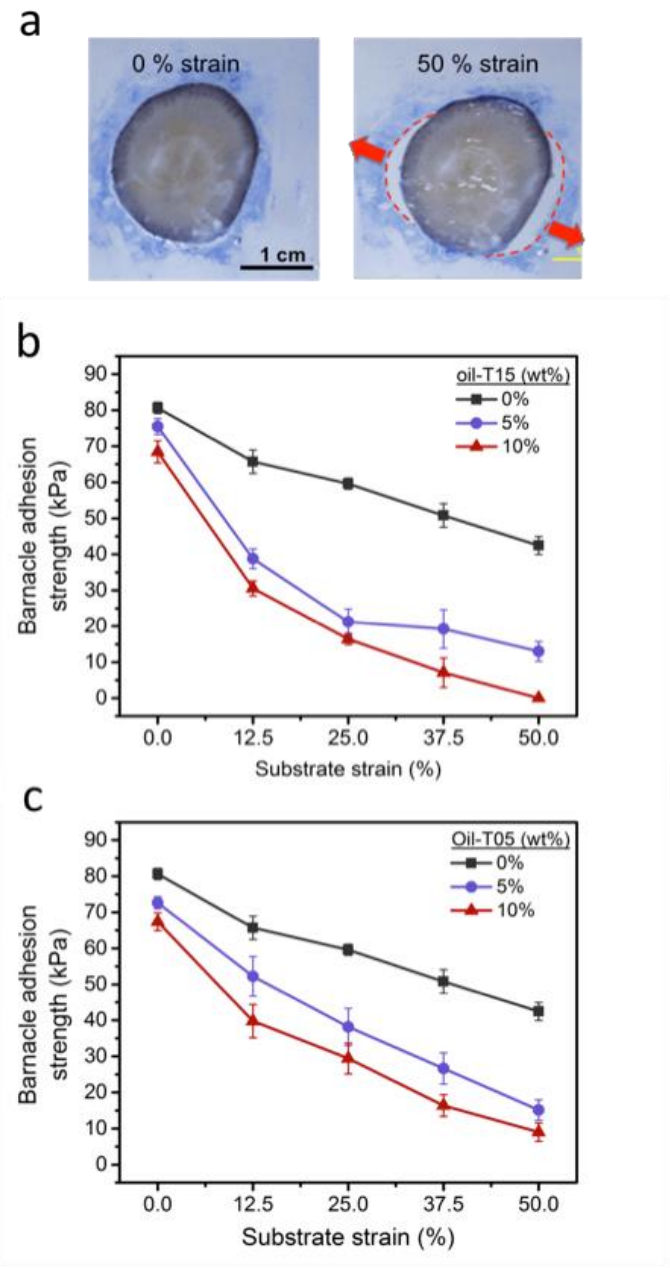

Figure 37: Effect of surface deformation and silicone-oil additives on barnacle adhesion strength (a) Optical images of the barnacle base-plate on an Ecoflex substrate before and under 50% uniaxial strain (image taken after 4.5 cycles of strain to 50%). The purple color on the substrate around the barnacle baseplate is due to crystal-violet stain. (b) Barnacle adhesion strength on Ecoflex incorporated with oil-T15 as a function of applied cyclic strain. (c) Barnacle adhesion strength on Ecoflex

infused with oil-T05 as a function of applied cyclic strains. The errors bar in (b) and (c) represent standard deviation of the mean (n = 15).

Figure 37b and 37c summarize the results of barnacle adhesion strength measurements as a function of the level of applied strain on Ecoflex with and without infused silicone-oils. When no substrate strain was applied, the adhesion strength of barnacle on the control surfaces (i.e., Ecoflex without silicone-oil) was ≈80.5 kPa, whereas on elastomers with 5 wt% silicone-oil, the adhesion strength decreased to ≈75 kPa (for oil-T15) and 72 kPa (for oil-T05). On Ecoflex with 10 wt% silicone-oil, the adhesion strength was further reduced to ≈68.5 KPa (oil-T15) and ≈67.5 kPa (oil-T05). These results indicate that incorporation of silicone-oil additives can reduce the barnacle adhesion strength on elastomers, and that the amount of reduction is dependent on the silicone-oil concentration. The largest decrease in barnacle adhesion strength (under no substrate strain) was observed to be ≈16%, for 10 wt% oil-T05.

When substrate strain was employed (i.e., strain > 0%), the barnacle adhesion strength for all elastomer substrate formulations studied significantly decreased with increase in applied strain (Figure 37b and 37c). Also, for any given specific strain, the barnacle adhesion strength on Ecoflex with silicone-oil additives was substantially lower than on Ecoflex without silicone-oil. For instance, after 50% cyclic strain the adhesion strength on Ecoflex without oil additive was ≈45 kPa, whereas on Ecoflex with 5 wt% oil-T15 the barnacle adhesion strength was ≈15 kPa (Figure 37b). Moreover, for any given strain, barnacle adhesion strength reduced with increase in silicone-oil additive

concentration (e.g., from Figure 37b, after 50% cyclic strain, the barnacle adhesion strength on Ecoflex with 10 wt% oil-T15 was reduced to 0 kPa). These results support the hypothesis that incorporation of silicone oils reduces the strains required to detach barnacles. Also, by comparing Figure 37b and 37c, the barnacle adhesion strength (at strain > 0) is slightly lower ($p < 0.05$ for any given strain) on Ecoflex with oil-T15 (Figure 37b) than that on Ecoflex with oil-T05 (Figure 37c). This suggests that barnacle detachment under deformation is influenced by multiple factors, including the concentration and the type of silicone-oil additive [80]. In the further experiments presented below, we limited our investigation to oil-T15 as a silicone-oil additive.

6.4.2 Effect of elastomer modulus vs. silicone-oil on substrate strain needed to detach barnacles

Incorporated silicone-oil additives are known to affect the mechanical properties of elastomers, and thereby can reduce the durability of coatings [16]. This is one of the major reasons coating companies restrict the concentration of silicone-oil additives in commercial FR coatings to < 20 wt% [251]. Several researchers have reported that the modulus of the silicone influences the adhesion strength [242, 258], base-plate geometry (Sun et al. 2004) and glue morphology of attached barnacles [259]. To our knowledge, however, there has been no quantitative study on the effect of change in substrate modulus due to incorporated silicone-oils on barnacle adhesion strength. Hence, in this study the effect of silicone-oils on the modulus of elastomer (Ecoflex in this case) was determined, and then Ecoflex elastomers without silicone-oil but matching modulus

were prepared by using Silicone Thinner® additive (Smooth-On, USA) (see Figure 37a). According to the manufacturer, Silicone Thinner® covalently bonds within the Ecoflex precursor mixture and modifies the modulus of Ecoflex. The change in modulus depends on the amount of Silicone Thinner® added. Unlike the silicone-oil additives (e.g., oil-T15 or oil-T05), Silicone Thinner® becomes part of the cross-linked Ecoflex elastomer matrix and thus should not leach from the surface; indicating that Silicon Thinner® can be expected to exhibit relatively much lower effect of surface action as compared to oil-T15 and oil-T05.

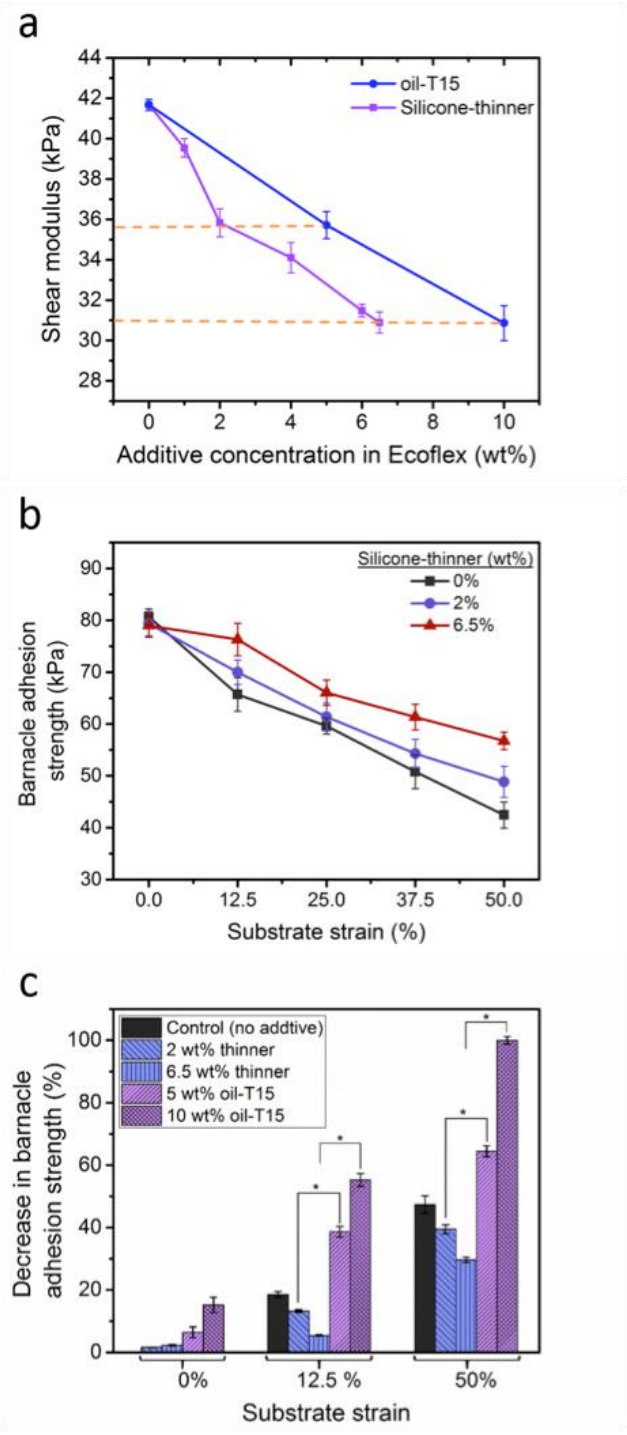

Figure 38: Effect of substrate modulus and substrate deformation on barnacle adhesion strength. (a) Variation of shear modulus of Ecoflex with addition of

different wt% of Silicone Thinner® and oil-T15 additives. The substrate moduli (dashed lines) of Ecoflex with 5 and 10 wt% oil-T15 match those with 2 and 6.5 wt% Silicone Thinner®, respectively. The error bars represent standard deviation of the mean (n = 5). (b) Barnacle adhesion strength on Ecoflex containing 0%, 2%, and 6.5% Silicone Thinner® as a function of applied strains. (c) Percentage decrease in barnacle adhesion strength from 80.5 kPa for elastomer without oil-additive, with oil-T15 and with Silicone Thinner® at 0%, 12.5% and 50% substrate strains. 80.5 kPa corresponds to the adhesion strength of barnacle on just Ecoflex (i.e., without Silicone Thinner® oil-T15, or applied substrate strain). The errors bar in (b) and (c) represent standard deviation of the mean (n = 15) and * represents $p < 0.01$.

Figure 38a shows the change in Ecoflex modulus for different concentration of oil-T15 and Silicone Thinner® additives, measured after conditioning in seawater for a period of 2 weeks (see Methods section). These data show that the modulus of Ecoflex is reduced with increase in additive (Silicone Thinner® or oil-T15) concentration. The modulus of Ecoflex with 5 wt% oil-T15 was 35.7 kPa, which closely matches with Ecoflex containing 2 wt% Silicone Thinner®. Likewise, the modulus of Ecoflex with 10 wt% oil-T15 was 30.8 kPa, which matches with Ecoflex containing 6.5 wt% Silicone Thinner®. The Ecoflex elastomers with 2 and 6.5 wt% Silicone Thinner® where used as control samples to examine the effect of change in elastomer modulus on barnacle adhesion strength.

Using the procedure detailed in the methods section barnacles were reattached and grown on multiple replicates of Ecoflex elastomer with 2% and 6.5% Silicone Thinner®. The adhesion strength of barnacles was measured on these surfaces before and after application of cyclic substrate strain. The experimental results are summarized in Figure 38b. It can be observed that without deformation (i.e., 0% strain), the barnacle

adhesion strength on Ecoflex decreased slightly (< 5%) upon incorporation of Silicone Thinner®. When substrate deformation was applied (12.5 - 50% strain), the barnacle adhesion strength dramatically decreased with increase in strain on all substrates. Moreover, for any given strain (> 0%), the barnacle adhesion strength was lower on Ecoflex without Silicone Thinner® and increasing amounts of Silicone Thinner® resulted in less decrease in adhesion strength relative to the unstrained control. This indicates that incorporation of Silicone Thinner® increases the amount of substrate strain needed to detach barnacles. Given that Silicone Thinner® lowers the modulus of Ecoflex (Figure 38a) and under the assumption that Silicone Thinner® has minimal effect of surface action on barnacle glue properties, the results from Figure 38b suggest that a softer substrate (i.e., lower modulus) requires larger amount of substrate strain to detach barnacles.

Since the moduli of Ecoflex with 2 and 6.5 wt% Silicone Thinner® match with those of Ecoflex with 5 and 10 wt% oil-T15, respectively (see Figure 38a), a comparison of data in Figure 37b and Figure 38b allow us to quantitatively de-couple the two major effects (i.e., substrate modulus and surface-action of oils) of silicone-oils on the barnacle adhesion strength. This comparison is shown in Figure 38c in terms of percentage decrease in barnacle adhesion strength compared to the unstrained Ecoflex control. That is, the percentage values were calculated by considering the barnacle adhesion strength on just Ecoflex (i.e., without Silicone Thinner® oil-T15, or applied substrate strain) as

reference. Under no substrate deformation (i.e., 0% strain), the barnacle adhesion strength on Ecoflex with Silicone Thinner® decreased by < 5%, whereas on Elastomer with oil-T15 the adhesion strength decreased by ≈7.5% (for 5 wt% oil-T15) and ≈16% (for 10 wt% oil-T15). This implies that, in the absence of deliberate substrate deformation, the decrease in barnacle adhesion strength due to silicone-oils is partly contributed by decrease of elastomer modulus and partly by surface-action (e.g., inhibition of enzymatic curing of bioadhesives of oil eluted to the surface).

When substrate deformation (cyclic strain > 0%) was applied (Figure 38c), the percentage decrease in barnacle adhesion strength was higher on Ecoflex without additives as compared to Ecoflex with Silicone Thinner®. For instance, after 50% cyclic strain, the barnacle adhesion strength on Ecoflex (without oil or Silicone Thinner® additive) was decreased by ≈47%, but for Ecoflex with 6.5 wt% Silicone Thinner® it was decreased by only ≈30%. Also, for any given strain, the decrease in barnacle adhesion strength was highest on Ecoflex with oil-T15. Taken together, this comparison suggests that decrease in elastomer modulus (due to silicone-oils) increases the strain required to detach barnacles, while the surface-action of silicone-oils dramatically reduces the barnacle adhesion strength upon substrate deformation so that the overall strain required to detach barnacles is lowered.

6.4.3 FEM model for barnacle detachment using substrate deformation

Fracture mechanics models are often used to study the forces involved in the mechanical debonding of bioadhesives. Kendall [241], Chaudhury [260] and others considered pseudo-barnacles (i.e., rigid studs glued to test surfaces) to gain insight into the fracture mechanics involved in the detachment of barnacles. In those studies, the barnacle detachment force was applied perpendicular to the surface, which leads to a tensile-mode crack, which is not applicable here because the current study is based on shear-mode cracks, generated by applying force parallel to the Ecoflex surface. To better understand the effect of substrate modulus and applied strain on barnacle detachment, a finite element method (FEM) model was developed to calculate the energy release rate during the strain-enhanced detachment process. The energy release (i.e., the decrease of the system's elastic energy per unit area when the crack propagates) is affected by the elastic mismatch, the barnacle contact area and the lengths of cracks generated at the barnacle-substrate interface.

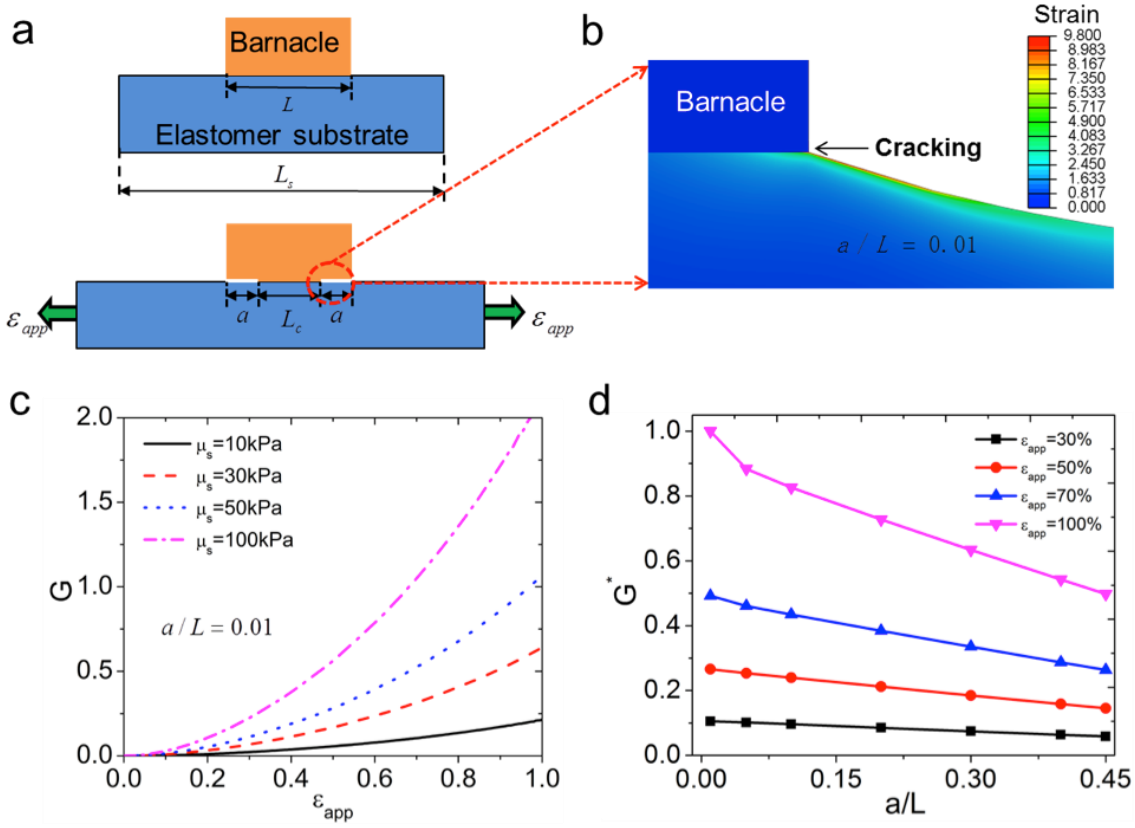

Figure 39: FEM model of barnacle detachment using substrate deformation. (a) Schematic illustration of the debonding process. L represents the length of the substrate and a represents the length of the symmetric crack formed at the interface. (b) Contour plot of the strain distribution in the substrate from the FEM simulation for a/L = 0.01. (c) Energy release rate (G) of the barnacle-substrate system as a function of the applied strain (ε_{app}) for different substrate modulus and a/L = 0.01. (d) Normalized energy release rate (G*) of the barnacle-substrate system as a function of the crack length for different applied strains.

Considering a 2D plane-strain model as shown in Figure 39a, when substrate strain is applied to the elastomer, it is assumed that two cracks develop at the periphery of the interface between the barnacle baseplate and elastomer surface, and symmetrically propagate inward with increase in substrate strain (the 2D schematic in Figure 5a has resemblance to digital photographs of barnacle base plate shown in Figure

3a). The crack-propagation happens when the decrease of the interfacial elastic energy due to applied strain exceeds the adhesion energy between the barnacle and the elastomer [257]. As seen in the calculated strain distribution in the elastomer substrate (Figure 39b), the crack tip has a high stress and strain concentration which indicates that crack is initiated from the edge of the barnacle baseplate. As the baseplate of the barnacle is stiffer than the elastomer substrate, the barnacle is relatively rigid [241]. Following the work done by Lu et al. [257] for studying the delamination of rigid metal island on soft substrate, the energy release rate (G) for crack propagation at the interface of barnacle and strained elastomer substrate can be calculated as

$$G = \frac{1}{2}\mu_s \varepsilon_{app}^2 L_s \tan\left(\frac{\pi L_c}{2L_s}\right) \tag{16}$$

where μ_s is the shear modulus of the elastomer substrate, L is the length of the barnacle baseplate adhered on the substrate, L_s is the length of the substrate at 0% strain, $L_c = L - 2a$ is the contact area length, and ε_{app} is the applied strain upon active deformation. This model can be used to explain the effect of the applied strain and the substrate modulus on the performance of detaching barnacle from substrate surfaces via the active strain method. Taken a small crack (a/L=1%) as an example, it is apparent from Equation (1) and Figure 39c, that for a specific strain, a stiffer substrate will generate a larger energy release rate, i.e., a rigid substrate will be more efficient in releasing the barnacles. This result agrees with the experimental observations with

Ecoflex with and without Silicone Thinner® (Figure 38a and 37b). Figure 39d shows the normalized energy release rate as a function of crack size, *a*/*L*, for different applied substrate strains. The interfacial crack propagates as the energy release rate equals the value of adhesion strength of barnacle on the surface, i.e., for an applied external strain, the barnacle will not debond at the edge if the adhesion strength is above the curve in Figure 39d. It can be seen from Figure 39d that the energy release rate decreases with the increase in crack length, in which the energy release rate is normalized with respect to the energy release rate of zero crack length and 100% strain. This indicates that the larger the barnacle baseplate, the easier it will be to detach the barnacle using substrate strain although we have no data available for barnacles of a variety of different sizes. It can also be observed that for a specific crack length, *a*/*L*, the larger the strain is applied, the higher is the energy release rate and the easier it will be to detach the barnacle. This is in agreement with the observed changes in barnacle adhesion strength due to change in modulus (Figure 38b). While this model is consistent with the experimental results observed in the case of Ecoflex with Silicone Thinner®, it fails to explain the more significant reduction of the experimental results obtained for silicone-oil additives (Figure 37b and 36c). We thus conclude that, in case of silicone-oil additives, their surface-action (i.e., presence of the oils at the interface) can result in reduction in the adhesion strength due to due to physical or chemical effects (e.g., interference of

silicone-oil with the enzymatic curing process of barnacle's glue), since they are not accounted for in this model.

6.5 Conclusions

Incorporation of silicone-oil additives and intentional surface deformation (i.e., active-strain) are two distinct approaches that enhance detachment of barnacle form silicone-based elastomers. This study combined both these approaches and investigated the synergistic dual-effect of silicone-oil additives and substrate strain on barnacle detachment from silicone-based Ecoflex elastomer. Control samples included Ecoflex without silicone-oil, while Ecoflex with silicone-oils consisted of four sample types – two different oils (oil-T15 and oil-T05) at different concentration (5 and 10 wt%). The adhesion strength of barnacles on Ecoflex elastomers (with and without silicone-oil) was determined before and after the applying varied amounts (0 – 50%) of cyclic strain. On Ecoflex without silicone-oil, surface strain reduced the barnacle adhesion strength up ≈45 kPa, but on Ecoflex with 10 wt% silicone-oil (oil-T15), the barnacle was completely detached. These results confirmed our hypothesis that incorporation of silicone-oil reduces the substrate strain needed to detach barnacles. The modulus of Ecoflex was also measured and it was observed that incorporation of silicone-oil additives (up to 10 wt%) reduced the modulus from ≈41.8 to ≈31.8 kPa. Since the modulus of elastomers is known to influence the adhesion strength of barnacles (Brady and Singer 2000), the effect of change in the Ecoflex modulus (due to silicone-oil) on barnacle detachment

using strain was investigated. To de-couple the effect of surface-action of oil-additives, Silicone Thinner® was used to increase the mesh size of the elastomer and thus lower its modulus. It was observed that the decrease in Ecoflex modulus obtained using Silicone Thinner® increased the amount of strain needed to detach barnacles, which is in contrast to the silicone-oil additives, which enabled easier detachment of barnacles. This suggests that surface-activity of the silicone-oils, which are known to elute to the elastomer's surface, has a major contribution towards reducing the amount of strain required to detach barnacles. Analysis based on a FEM model was employed to elucidate the effect of strain on barnacle detachment. The model agrees with the observed experimental data for the effect of substrate modulus, but cannot be used to interpret the experiments with silicone-oil because the model does not account for the surface-action of silicone-oils.

In conclusion, adding silicone oils into elastomers can dramatically reduce the amount of strain needed to detach barnacles. Thus, this report provides a potential, new, bifunctional approach to mitigate biofouling in marine and biomedical [261] applications. The use of surface deformation technology has been already demonstrated (using electro-actuation [117] and pneumatic-actuation [208] techniques) and use of silicone-oil additives may improve such approaches to biofouling management.

6.6 Chapter Acknowledgements

The work presented in this chapter was supported by the Office of Naval Research (Grant N000141310828) and the NSF's Research Triangle Materials Research Science and Engineering Center (Grant DMR-1121107).

7. Chapter 7: Dynamic surface deformation for biofouling management: Conclusions and future directions

7.1 Summary

Biofouling is a natural phenomenon, encountered in an extremely wide range of situations, and is generally problematic in all human endeavors where water based liquids are in contact with other materials. Examples include: (i) the high cost of mitigation of biofouling on maritime vessels [262], (ii) the growing significance of infectious biofilms (matrix-enclosed microbial adlayers) as a failure mode of implanted materials and devices [11], and (iii) the adaptation of antibiotic-resistant bacterial strains within biofilms in medical and industrial settings [121]. In this work (in Chapters 3 and 4), we pioneered the use of dynamic surface deformation of elastomers as a general, non-toxic, fouling release approach for management of marine biofouling. Further, we demonstrated (Chapters 5 and 6) the application of dynamic deformation technology as a complementary approach to existing antifouling and fouling-release strategies.

In Chapter 3, we demonstrated at least three different approaches (direct mechanical stretching, electro-actuation and pneumatic-actuation) to generate dynamic surface deformation of elastomers. Employing these different deformation techniques, we showed that active surface strain effectively detaches two types of model bacterial biofilms and barnacles from silicone-based elastomers. In the case of bacterial biofilms, when the applied surface strain was above a certain critical threshold, effective triggered

detachment (> 90% removal) of biofilm was observed. Also, the critical strain required to detach a biofilm decreased with increase in biofilm thickness. For example, *C. marina* biofilm of ≈36 μm thickness (grown for 3 days on PDMS elastomer using laboratory conditions) required a critical strain of ≈15%, whereas a critical strain of < 5% was enough to detach *C. marina* biofilm of ≈78 μm thickness (grown for 7 days). We interpreted the detachment of biofilm under surface strain as a debonding process. By assuming the biofilm to be uniform and linearly elastic, we surmised that debonding occurs when the elastic energy of the biofilm exceeds the adhesion energy between biofilm and the substrate. Based on these results we developed a theoretical relation for critical strain given by

$$e_c = \sqrt{\frac{2\Gamma}{HY}} \qquad (7)$$

where Γ, H, and Y represent the thickness, adhesion strength and modulus of the biofilm.

In the case of barnacles, we observed that application of surface strain reduced the adhesion strength, however, no threshold behavior was observed and the strain required to completely detach a barnacle was several times higher than that of slimy biofilms. For example, a surface strain of ≈100% was required to completely detach a barnacle from a PDMS substrate (Sylgard 184, 155 kPa modulus). The higher substrate strain required for barnacle detachment is likely due to a combination of their different attachment geometry and the greater adhesion strength of the barnacles' glue as

compared to that of slimy bacterial biofilms. We employed a 2D fracture mechanics model to explain the detachment of barnacle under substrate deformation. Due to mismatch in the elastic modulus (i.e., base plate of the barnacle is much more rigid than the elastomer substrate), externally applied substrate strain produces an inward crack at the interface between the barnacle baseplate and elastomer substrate. This crack length increases with increase the amount of substrate strain and thereby decreases the adhesion strength of the barnacle.

In Chapter 4, we investigated the application of surface deformation technology for biofouling management in natural marine environment. In this study, dynamic surface deformation via pneumatic actuation was used to examine the effect of surface strain on the detachment of natural biofilms in field studies and then compared with model microbial biofilms under laboratory conditions. Both laboratory and field studies showed that effective triggered detachment of biofilms occurs above a critical substratum strain. It was also found that the substratum modulus affected the strain needed to detach biofilm with higher modulus silicone substrata requiring less maximal strain for efficient detachment.

In summary, the work presented in Chapter 3 and 4, clearly demonstrated the significance and efficacy of dynamic surface deformation of elastomers as a promising technology for biofouling management. Since silicone-based surfaces are widely used in efforts to manage biofouling, the dynamic surface deformation technique can be

complementary to existing commercial methods for biofouling management. Based on this recognition, we focused our work towards developing multi-functional active surfaces for biofouling control. To this end, we studied two different approaches: (i) modification of elastomer surfaces with antifouling zwitterionic polymers, and (ii) incorporation of silicone-oil additives into elastomers.

For approach (i), presented in Chapter 5, we employed a chemical approach to modify the surface of PVMS elastomers with fouling resistant zwitterionic polymers. In this approach, we prepared PVMS elastomer and briefly exposed its surface to UV-light, in presence of thiol-based ATRP initiator solution, to covalently link the sulfhydryl (-SH) groups of initiator molecules with the vinyl (-CH=CH_2) groups present on the PVMS surface. The initiator functionalized PVMS was then used to graft zwitterionic PSBMA using ARGET-ATRP. We used XPS, FTIR and contact angle goniometry to characterize PSBMA modified PVMS elastomer substrate. The results obtained from surface characterization analysis confirmed that we were able to successfully modify the surface of PVMS with zwitterionic polymer grafts. Unlike other existing methods, this above chemical approach has the advantage of modifying the elastomeric surfaces with polymer grafts without dramatically increasing the substrates' surface modulus.

We used the above as-prepared surfaces for biofouling studies. Because of the antifouling properties of zwitterionic PSBMA, PVMS-PSBMA (i.e. PVMS modified with PSBMA) exhibited excellent resistance against protein adsorption, barnacle larvae

settlement, and bacterial adhesion over short-term exposure (up to 5 days). Upon long-term fouling exposure (after 12 days) however, biofilm accumulated on the entire surface of PVMS-PSBMA. In general, this is one of the major drawbacks of all existing fouling-resistant surfaces – they all get fouled eventually due to the robust conditions in the natural environment, which hosts' wide variety of opportunistic fouling species.

In our approach however, we applied dynamic deformation, which effectively detached the accumulated biofilm and reactivated the fouling-resistant properties of PVMS-PSBMA. In summary, the results from this study prove that these types of dual-functional surfaces are applicable for pro-active biofouling management on marine equipment and biomedical devices.

For approach (ii), presented in Chapter 6, we investigated the synergistic dual-effect of silicone-oil additives and substrate strain on barnacle detachment. In this study, control samples included Ecoflex without silicone-oil, while Ecoflex with silicone-oils consisted of four sample types – two different oils (oil-T15 and oil-T05) at different concentration (5 and 10 wt%). The adhesion strength of barnacles on Ecoflex elastomers (with and without silicone-oil) was determined before and after the applying varied amounts (0 – 50%) of cyclic strain. Since the modulus of elastomers is known to influence the adhesion strength of barnacles [79], the effect of change in the Ecoflex modulus (due to silicone-oil) on barnacle detachment using strain was investigated. To de-couple the effect of surface-action of oil-additives, Silicone Thinner® was used to

increase the mesh size of the elastomer and thus lower its modulus. It was observed that the decrease in Ecoflex modulus obtained using Silicone Thinner® increased the amount of strain needed to detach barnacles, which is in contrast to the silicone-oil additives, which enabled easier detachment of barnacles. This suggests that surface-activity of the silicone-oils, which are known to elute to the elastomer's surface, has a major contribution towards reducing the amount of strain required to detach barnacles. In summary, adding silicone oils into elastomers can dramatically reduce the amount of strain needed to detach barnacles. Taken together, the studies presented in Chapter 5 and 6, provide a promising proof-of-concepts for the application of dynamic surface deformation as a complementary approach to existing antifouling strategies used for biofouling control. Since elastomeric coatings are heavily used on various types of substrates (e.g., ship-hulls, industrial pipes and urinary catheters) that are target for biofouling, the dynamic surface deformation by itself and as a dual-approach can be advantageous for biofouling management.

7.2 Future Directions

7.2.1 Stimuli-responsive polymer modified elastomer surfaces for short-term and long-term fouling-release

In Chapter 5, we presented a chemical approach (thiol-ene click chemistry followed by ARGET-ATRP) to modify the surface of PVMS elastomer with antifouling zwitterionic polymeric grafts. In principal, that chemical approach should be applicable to graft other types of bioactive polymers as well. We are interested in modifying PVMS

elastomer surface with poly(*N*-ispropylacrylamide) (PNIPAAm) polymer. PNIPAAm is a thermo-responsive polymer that has a lower critical solution temperature (LCST) in water at ≈32 °C. PNIPAAm undergoes a triggered reversible change in its physical conformation (from hydrophilic to relative hydrophobic state) in aqueous solutions by simply altering the temperature from below to above its LCST. We have previously reported that substrates (such as glass and Au) modified with PNIPAAm polymer can reversible control the attachment and release of marine bacteria by changing the temperature of grafted PNIPAAm from above to below (or below to above) the LCST (≈ 32 °C) of PNIPAAM [1, 2]. This behavior is due to the reversible swelling and shrinking of the grafted PNIPAAm layer above and below 32 °C. Though PNIPAAm polymers grafted from glass or Au substrates are effective against short-term (hrs.) fouling release, they fail against long-term (days) exposure to fouling environment [2].

In this proposed project we hypothesize that elastomer surfaces modified with PNIPAAm allows both short-term and long-term fouling release. We propose that microbes that adhere over short-term (hrs.) can be released via the thermo-responsive behavior of PNIPAAm, and if the surfaces are allowed to bioaccumulate over long-term (days), dynamic surface deformation of elastomers can be employed for detachment the fouling species and thereby again reactive the short-term fouling-release properties of PNIPAAm polymer.

Preliminary results:

As a first step for this proposed project, we attempted to graft PNIPAAm polymer from PVMS using the method described in Chapter 5. In brief, PVMS elastomer surface was functionalized with ATRP initiator using UV assisted thiol-ene click chemistry and then followed by the ARGET-ATRP reaction. The product of this reaction is referred here as PVMS-PNIPAAm. PVMS-PNIPAAm surface was characterized using FTIR and static water CA measurements. The FTIR absorbance spectrum (Figure 39a) of PVMS-PNIPAAm showed C=O (1670 cm^{-1}) and N-H (3310 cm^{-1}) peaks that are characteristic to PNIPAAm [15]. The static water CA measured on PVMS-PNIPAAm (Figure 39b) showed a change of 28 ± 2 degrees with change in surface temperature from 37 °C to 22 °C, while PVMS (control) showed no such significant change in CA. The changes in CA with temperature on PVMS-PNIPAAm are due to the difference in hydration/wetting of the PNIPAAm above and below its LCST (≈ 32 °C) [15, 107, 263]. These results confirmed the successful grafting of PNIPAAm polymer from PVMS.

The fouling-release properties of PVMS-PNIPAAm over short term were examined using bacterial attachment and release assays. PVMS-PNIPAAm and PVMS (control) were incubated in a *C. marina* (1×10^7 cells/mL in 0.85% NaCl) suspension for 2 hr. at 37 °C and then gently rinsed (estimated shear rate = 0.04 Pa) at 22 °C with 60 mL 0.85% NaCl solution. Both PVMS and PVMS-PNIPAAm (Figure 39c) showed similar cell density (~ 6,000 cells/mm^2) prior to rinsing, indicating that PNIPAAm did not reduce *C.*

marina attachment relative to PVMS (control). However, upon rinsing the surface at the same shear rate at 22 °C (a temperature well below the LCST of PNIPAAm), nearly 86% of the attached cells released from PVMS-PNIPAAm, while the PVMS (control) showed no significant (< 10%) cell release ($P > 0.05$). This significant degree of cell release from PVMS-PNIPAAM is due to the thermo-responsive behavior of the PNIPAAm. PNIPAAm undergoes a hydration transition during the rinsing cycle, which causes it to become more hydrated and swell, and thus reduces the adhesion strength of the cells, which detach upon rinsing-induced fluid shear [15, 109]. These results are in agreement with previously reported results for PNIPAAm polymer grafted from glass and gold surfaces [106-109]. We expect that biofilms, which accumulate on PVMS-PNIPAAm over prolonged exposure to fouling environment, can debonded using active surface deformation.

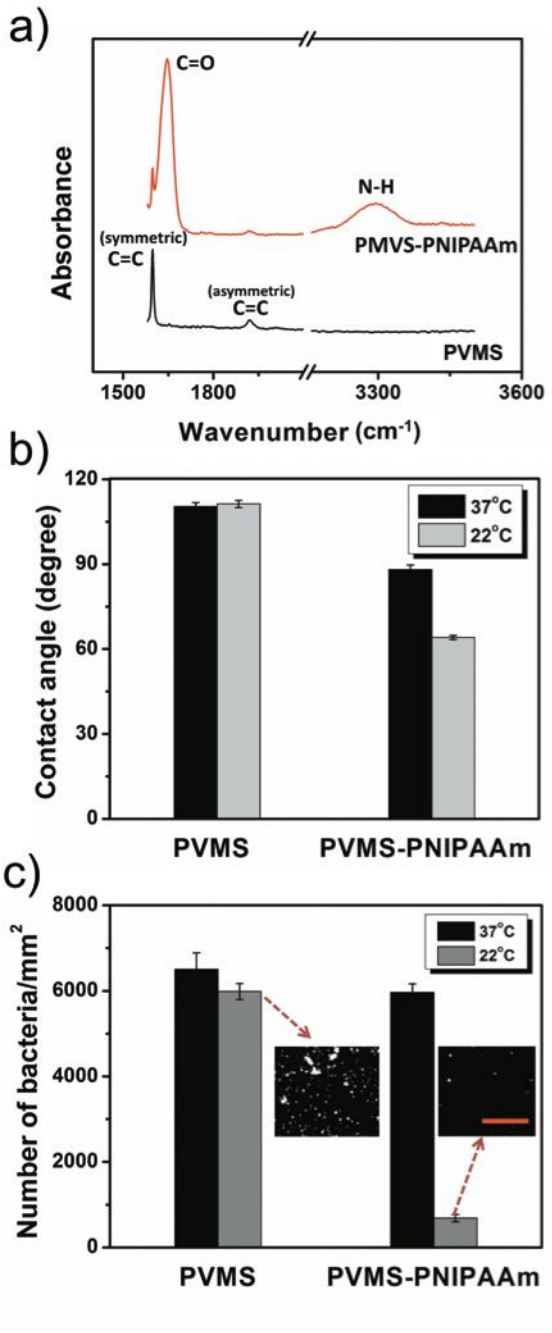

Figure 40: (a) FITR absorbance spectra of PVMS and PVMS-PNIPAAm surfaces. (b) Static water contact angle measurements on PVMS and PVMS-PNIPAAM surfaces at 22 and 37 °C. (c) Surface density of C. marina on PVMS and PVMS-PNIPAAm surfaces after 2 hr. attachment at 37 °C and after gentle rinsing of those surfaces at 22

°C using 0.85% NaCl solution. The inset images are representative phase contrast microscopy images that show the attached C. marina cells (seen as white dots/clusters) on PVMS and PVMS-PNIPAAm surfaces after the rinse cycle; the scale bar corresponds to 500 μm. Each of the error bars on (b) and (c) correspond to the standard deviation of the mean (n = 5).

7.2.2 Application of pneumatic de-icing boots for biofouling management

Formation of ice on aircraft wings is a serious concern for aviation industry because it increases drag, destroys the smooth flow of air, and effects the control of the aircrafts' operation [264]. To overcome this problem aviation aircrafts are often equipped with pneumatic de-icing boots. Pneumatic de-icing boots are inflatable rubber strips that can be easily affixed to the leading edge of the wing and tail surfaces. When activated, the space inside the rubber stripes is pressurized with air and cause the surface to stretch as shown in Figure 41. The surface strain generated due to stretching helps to breaks the ice from the surface. Applying suction will remove the air and de-pressurize the space inside the rubber strips and allows the surface return to its original shape. In principal, this approach is very similar to the soft-robotic inspired pneumatic-actuation, presented in Chapter 3 and 4, for biofilm and barnacle detachment. The length scale of the samples used in our previous pneumatic-actuation studies was limited to few centimeters and the exposure time to fouling environment was limited to 2 weeks.

In this proposed project we anticipate to use the above-mentioned commercial pneumatic deicing boots for biofouling management in field environment over several months. The commercial pneumatic de-icing boots are of much larger dimension

(typically the size of aircraft wings), so it would help us to investigate the application of de-icing boots for biofouling management in field environments, over prolonged time periods (2 - 6 months). Most of the commercial deicing boots are typically manufactured using neoprene or polyurethane materials. Since silicone fouling-release coatings are favorable for fouling-release application, we plan to partition the surface of deicing boots by 2 feet square meter and coated each section with different types of commercially available standard silicone coatings, such as Intersleek 700 (AkzoNoble, NL), T2-RTV silicone (Dow Corning, USA), Sylgard 184 (Dow Corning, USA), Ecoflex (Smooth-On, Inc., USA). These studies will allow us to examine the performance of dynamic surface deformation technology for biofouling management on wide variety silicone-based coatings, exposed to similar fouling conditions.

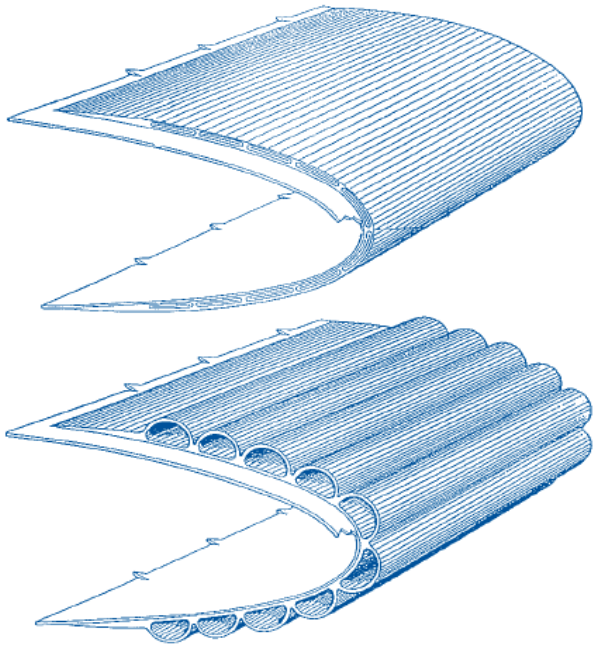

Figure 41: Schematic of deicing boot (fitted on to a curved surface) before (top image) and after (bottom image) pneumatic-actuation. Courtesy: Goodrich pneumatic de-icing systems (UTC Aerospace Systems, USA).

7.2.3 Quantitative Study of Bioadhesion and Triggered Cell and Biofilm Release from Engineered Multifunctional Surfaces

Quantitative measurement of bioadhesion phenomena is of paramount necessity in understanding and preventing a number of deleterious processes in marine biofouling phenomena, medical microbiology, thrombosis and cancer-metastasis. In Chapters 3 – 6, we showed that deformation of elastomers is highly efficacious for detachment of various types of biofilms. Though we have acknowledged in our studies that substrate strain decreases the biofilms' adhesion strength, we did not precisely measure the actual adhesion strengths of biofilm on the substrate (before and after deformation). Traditional methods to characterize adhesion of biofilms on silicone

coatings are problematic and their accuracy is ambiguous due to their incompatibility with in situ biofilm conditions [265]. In this context, we propose that Bioflux instrument (Fluxion Biosciences, Inc., USA) can be used for quantitative biofilm adhesion assays (Figure 42). The Bioflux instrument is equipped with a custom-designed, versatile, microfluidic sample cell and associated pumps and controllers that allow biofilms and cells on engineered surfaces to be subjected to a wide range of precisely controlled shears and a number of triggers for debonding of biofouling. The data collected using the adhesion assays can to precisely determine the adhesion energy of the biofilms (before and after surface deformation) using a newly developed software (SAS) from 4Deep Inc. This approach will enable to characterize biofilm adhesion energy accurately and easily so that one could systematically investigate the effects of surface properties, substrate modulus, and applied strains needed for reduction of adhesion strength and detachment. We believe that a firm understanding of bioadhesion behavior is essential for developing ultra-high-performance, environment-friendly strategies to control biofouling [100].

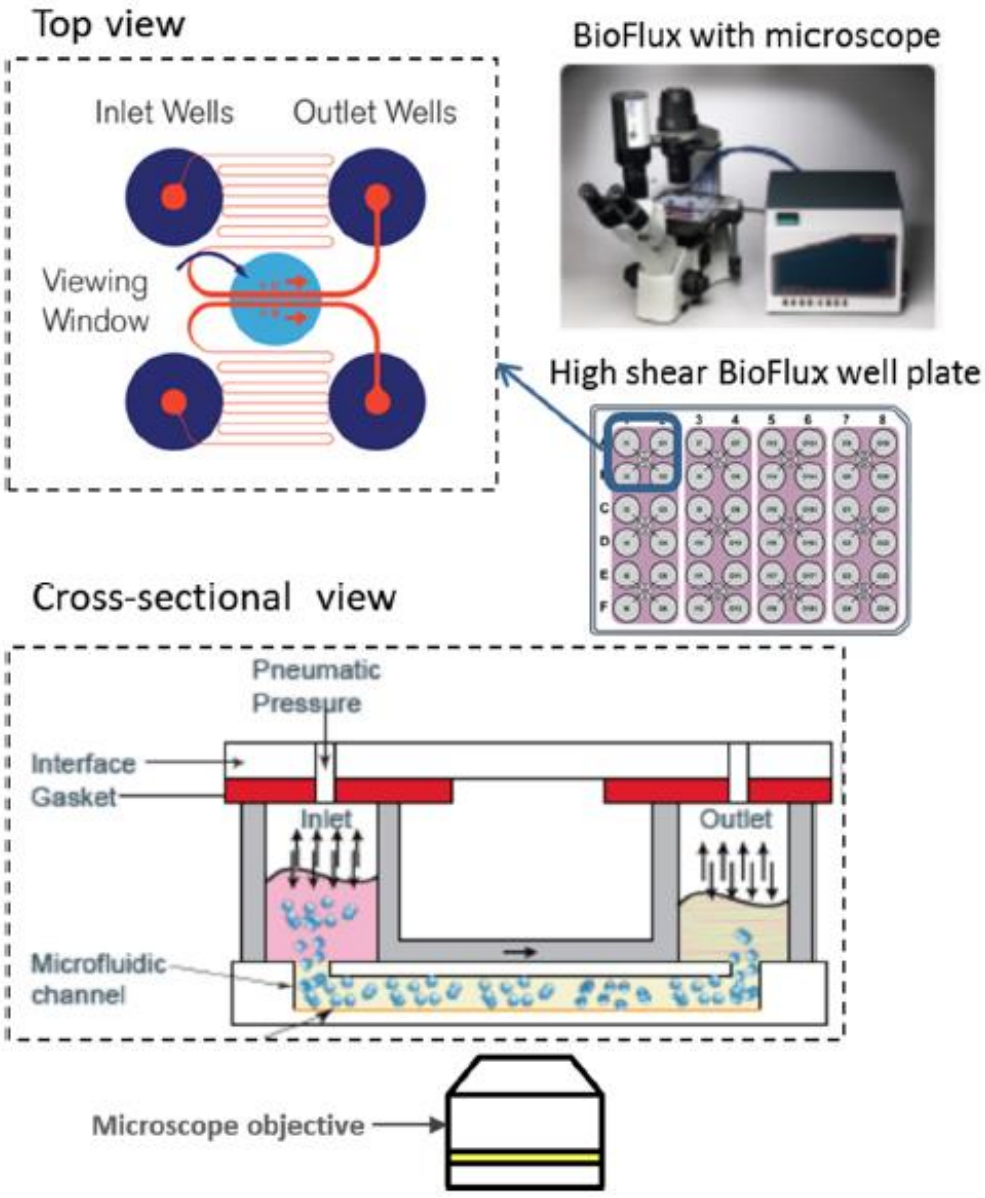

Figure 42: Top view: schematic of the BioFlux well-plate showing the flow path of two inlet and outlet media reservoirs (wells) connected through a microfluidic channel. Cross-sectional view: the microfluidic channel (used for bacterial adhesion and biofilm growth) on a microscope. Middle-right: schematic of the 48-well high shear BioFlux plate. Top-right: automated programmable BioFlux flow control system integrated with well plate and microscope. Courtesy: BioFlux system (Fluxion Biosciences, Inc., USA).

References

1. Costerton J. W., C.K.J., Gessey G. G., Ladd T. I., Nickel J. C., Dasgupta M., Marrie T. J., *Bacterial biofilms in nature and disease.* Annual Reviews Microbiology, 1987. 41: p. 435-464.

2. Stoodley P., S.K., Davies D. G., Costerton J.W., *Biofilms as complex differentiated communities.* Ann. Rev. Microbiol., 2002. 56: p. 187-209.

3. Callow J. A., C.M.E., *Biofilms.* Progress in Molecular Subcellular Biology 2006. 42: p. 141-169.

4. Stoodley L. H., S.P., *Evolving concepts in biofilm infections.* Cellular Microbiology, 2009. 7: p. 1034-1043.

5. Bixler, G.D. and B. Bhushan, *Biofouling: lessons from nature.* Philosophical Transactions of the Royal Society a-Mathematical Physical and Engineering Sciences, 2012. 370: p. 2381-2417.

6. Hellio, C. and D.M. Yebra, *Marine fouling organisms and their impact.* In: Advances in Marine Antifouling Coatings and Technologies, 2009: p. 1-15.

7. Callow, M.E. and J.A. Callow, *Marine biofilms: a sticky problem.* Biologist, 2002. 49: p. 1-4.

8. Flemming H-C, M.P.S., Venkatesan R., Cooksey K., *Marine and industrial biofouling.* Springer Series on Biofilms, 2009. 4: p. 3-328.

9. Callow M. E., C.J.A., Clare A. S., *Some new insights into marine biofouling.* Paints & Coatings, World Super Yatch, 2003. 1: p. 34-39.

10. Stoodley L. H., C.J.W., Stoodley P., *Bacterial biofilms: From the natural environment to infectious diseases.* Nature Reviews, 2004. 2: p. 95-108.

11. Siddiq, D.M. and R.O. Darouiche, *New strategies to prevent catheter-associated urinary tract infections.* Nature Reviews Urology, 2012. 9: p. 305-314.

12. Levering, V., Q. Wang, P. Shivapooja, X. Zhao, and G.P. Lopez, *Soft robotic concepts in catheter design: an on-demand fouling-release urinary catheter.* Advanced Healthcare Materials, 2014. 3: p. 1588-1596.

13. Wang, Q.M., L. Zhang, and X.H. Zhao, *Creasing to cratering instability in polymers under ultrahigh electric fields.* Physical Review Letters, 2011. 106: p. 118301.

14. Efimenko, K., J.A. Crowe, E. Manias, D.W. Schwark, D.A. Fischer, and J. Genzer, *Rapid formation of soft hydrophilic silicone elastomer surfaces.* Polymer, 2005. 46: p. 9329-9341.

15. Shivapooja, P., L.K. Ista, H.E. Canavan, and G.P. Lopez, *ARGET-ATRP synthesis and characterization of PNIPAAm brushes for quantitative cell detachment studies.* Biointerphases, 2012. 7: p. 1-10.

16. Truby, K., C. Wood, J. Stein, J. Cella, J. Carpenter, C. Kavanagh, G. Swain, D. Wiebe, D. Lapota, A. Meyer, E. Holm, D. Wendt, C. Smith, and J. Montemarano, *Evaluation of the performance enhancement of silicone biofouling-release coatings by oil incorporation.* Biofouling, 2000. 15: p. 141-150.

17. Kavanagh, C.J., G.W. Swain, B.S. Kovach, J. Stein, C. Darkangelo-Wood, K. Truby, E. Holm, J. Montemarano, A. Meyer, and D. Wiebe, *The effects of silicone fluid additives and silicone elastomer matrices on barnacle adhesion strength.* Biofouling, 2003. 19: p. 381-390.

18. Rittschof, D., B. Orihuela, T. Harder, S. Stafslien, B. Chisholm, and G.H. Dickinson, *Compounds from silicones alter enzyme activity in curing barnacle glue and model enzymes.* PLoS One, 2011. 6: p. e16487.

19. Ahmed, N., T. Murosaki, A. Kakugo, T. Kurokawa, J.P. Gong, and Y. Nogata, *Long-term in situ observation of barnacle growth on soft substrates with different elasticity and wettability.* Soft Matter, 2011. 7: p. 7281-7290.

20. Lejars, M., A. Margaillan, and C. Bressy, *Fouling release coatings: A nontoxic alternative to biocidal antifouling coatings.* Chemical Reviews, 2012. 112: p. 4347-4390.

21. Rosenhahn, A., S. Schilp, H.J. Kreuzer, and M. Grunze, *The role of "inert'' surface chemistry in marine biofouling prevention.* Physical Chemistry Chemical Physics, 2010. 12: p. 4275-4286.

22. Ista, L.K. and G.P. Lopez, *Interfacial tension analysis of oligo(ethylene glycol)-terminated self-assembled monolayers and their resistance to bacterial attachment.* Langmuir, 2012. 28: p. 12844-12850.

23. Vanoss, C.J., R.J. Good, and M.K. Chaudhury, *Additive and nonadditive surface-tension components and the interpretation of contact angles.* Langmuir, 1988. 4: p. 884-891.

24. Verwey, E.J.W., *Theory of the stability of lyophobic colloids.* Journal of Physical and Colloid Chemistry, 1947. 51: p. 631-636.

25. Aldred, N., G.Z. Li, Y. Gao, A.S. Clare, and S.Y. Jiang, *Modulation of barnacle (Balanus amphitrite Darwin) cyprid settlement behavior by sulfobetaine and carboxybetaine methacrylate polymer coatings.* Biofouling, 2010. 26: p. 673-683.

26. Vater, S.M., S. Weisse, S. Maleschlijski, C. Lotz, F. Koschitzki, T. Schwartz, U. Obst, and A. Rosenhahn, *Swimming behavior of pseudomonas aeruginosa studied by holographic 3D tracking.* Plos One, 2014. 9: p. e87765.

27. Huggett, M.J., J.E. Williamson, R. de Nys, S. Kjelleberg, and P.D. Steinberg, *Larval settlement of the common Australian sea urchin Heliocidaris erythrogramma in response to bacteria from the surface of coralline algae.* Oecologia, 2006. 149: p. 604-619.

28. Magin, C.M., S.P. Cooper, and A.B. Brennan, *Non-toxic antifouling strategies.* Materials Today, 2010. 13: p. 36-44.

29. Chapman, R.G., E. Ostuni, S. Takayama, R.E. Holmlin, L. Yan, and G.M. Whitesides, *Surveying for surfaces that resist the adsorption of proteins.* Journal of the American Chemical Society, 2000. 122: p. 8303-8304.

30. Grunze, M., A. Schertel, R. Uhrig, A. Welle, and C. Woll, *The role of adhesion promoters on the molecular and mesoscopic structure of the interphase.* Journal of Adhesion, 1996. 58: p. 43-67.

31. Yonzon, C.R., E. Jeoungf, S.L. Zou, G.C. Schatz, M. Mrksich, and R.P. Van Duyne, *A comparative analysis of localized and propagating surface plasmon resonance sensors: The binding of concanavalin a to a monosaccharide functionalized self-assembled monolayer.* Journal of the American Chemical Society, 2004. 126: p. 12669-12676.

32. Cao, X.Y., M.E. Pettit, S.L. Conlan, W. Wagner, A.D. Ho, A.S. Clare, J.A. Callow, M.E. Callow, M. Grunze, and A. Rosenhahn, *Resistance of polysaccharide coatings to proteins, hematopoietic cells, and marine organisms.* Biomacromolecules, 2009. 10: p. 907-915.

33. Chen, S.F. and S.Y. Jiang, *A new avenue to nonfouling materials.* Advanced Materials, 2008. 20: p. 335-+.

34. Kind, M. and C. Woll, *Organic surfaces exposed by self-assembled organothiol monolayers: Preparation, characterization, and application.* Progress in Surface Science, 2009. 84: p. 230-278.

35. Rosenhahn, A., J.A. Finlay, M.E. Pettit, A. Ward, W. Wirges, R. Gerhard, M.E. Callow, M. Grunze, and J.A. Callow, *Zeta potential of motile spores of the green alga Ulva linza and the influence of electrostatic interactions on spore settlement and adhesion strength.* Biointerphases, 2009. 4: p. 7-11.

36. Petrone, L., A. Di Fino, N. Aldred, P. Sukkaew, T. Ederth, A.S. Clare, and B. Liedberg, *Effects of surface charge and Gibbs surface energy on the settlement behaviour of barnacle cyprids (Balanus amphitrite).* Biofouling, 2011. 27: p. 1043-1055.

37. Ederth, T., M.E. Pettitt, P. Nygren, C.X. Du, T. Ekblad, Y. Zhou, M. Falk, M.E. Callow, J.A. Callow, and B. Liedberg, *Interactions of Zoospores of Ulva linza with Arginine-Rich Oligopeptide Monolayers.* Langmuir, 2009. 25: p. 9375-9383.

38. Ederth, T., P. Nygren, M.E. Pettitt, M. Ostblom, C.X. Du, K. Broo, M.E. Callow, J. Callow, and B. Liedberg, *Anomalous settlement behavior of Ulva linza zoospores on cationic oligopeptide surfaces.* Biofouling, 2008. 24: p. 303-312.

39. Hejda, F., P. Solar, and J. Kousal, *Surface free energy determination by contact angle measurements - A comparison of vairous approaches.* in WDS'10 Proceedings of Contributed Papers, 2010. Part III: p. 25-30.

40. Zenkiewicz, M., *Methods used for calculation of surface free energy of solids.* Journal of Achievements in Materials and Manufacturing Engineering, 2007. 24: p. 137-145.

41. Vogler, E.A., *Structure and reactivity of water at biomaterial surfaces.* Advances in Colloid and Interface Science, 1998. 74: p. 69-117.

42. Baier, R.E., *Surface properties influencing adhesion properties.* ed. R. S. Manly, In: Adhesion in Biological Systems, 1970. Academic Press Inc., New York: p. 15-48.

43. Baier, R.E. and V.A. DePalma, *in Management of occlusive arterial disease.* ed. W. A. Dale, Year Book Medical Publishers, Inc., 1971. Chicago: p. 147-163.

44. Baier, R.E., *Adsorption of microorganisms of surfaces.* ed. G. Bitton and K. S. Marshall, Wiley-Interscience, 1980. New York: p. 59-104.

45. Absolom, D.R., F.V. Lamberti, Z. Policova, W. Zingg, C.J. Vanoss, and A.W. Neumann, *Surface thermodynamics of bacterial adhesion.* Applied and Environmental Microbiology, 1983. 46: p. 90-97.

46. Ista, L.K., M.E. Callow, J.A. Finlay, S.E. Coleman, A.C. Nolasco, R.H. Simons, J.A. Callow, and G.P. Lopez, *Effect of substratum surface chemistry and surface energy on attachment of marine bacteria and algal spores.* Applied and Environmental Microbiology, 2004. 70: p. 4151-4157.

47. Callow, M.E., J.A. Callow, L.K. Ista, S.E. Coleman, A.C. Nolasco, and G.P. Lopez, *Use of self-assembled monolayers of different wettabilities to study surface selection and primary adhesion processes of green algal (Enteromorpha) zoospores.* Applied and Environmental Microbiology, 2000. 66: p. 3249-3254.

48. Finlay, J.A., M.E. Callow, L.K. Ista, G.P. Lopez, and J.A. Callow, *The influence of surface wettability on the adhesion strength of settled spores of the green alga Enteromorpha and the diatom Amphora.* Integrative and Comparative Biology, 2002. 42: p. 1116-1122.

49. Rittschof, D. and J.D. Costlow, *Bryozoan and barnacle settlement in relation to initial surface wettability: a comparison of laboratory and field studies.* Scientia Marina, 1989. 53: p. 411-416.

50. Huggett, M.J., B.T. Nedved, and M.G. Hadfield, *Effects of initial surface wettability on biofilm formation and subsequent settlement of Hydroides elegans.* Biofouling, 2009. 25: p. 387-399.

51. Liu, Y. and Q. Zhao, *Influence of surface energy of modified surfaces on bacterial adhesion.* Biophysical Chemistry, 2005. 117: p. 39-45.

52. Howell, D. and B. Behrends, *A review of surface roughness in antifouling coatings illustrating the importance of cutoff length.* Biofouling, 2006. 22: p. 401-410.

53. Carman, M.L., T.G. Estes, A.W. Feinberg, J.F. Schumacher, W. Wilkerson, L.H. Wilson, M.E. Callow, J.A. Callow, and A.B. Brennan, *Engineered antifouling microtopographies - correlating wettability with cell attachment.* Biofouling, 2006. 22: p. 11-21.

54. Yebra, D.M., S. Kiil, and K. Dam-Johansen, *Antifouling technology - past, present and future steps towards efficient and environmentally friendly antifouling coatings.* Progress in Organic Coatings, 2004. 50: p. 75-104.

55. Callow, M.E. and J.E. Callow, *Marine biofouling: a sticky problem.* Biologist, 2002. 49: p. 1-5.

56. Yu, J., W. Wei, E. Danner, R.K. Ashley, J.N. Israelachvili, and J.H. Waite, *Mussel protein adhesion depends on interprotein thiol-mediated redox modulation.* Nature Chemical Biology, 2011. 7: p. 588-590.

57. Kamino, K., S. Odo, and T. Maruyama, *Cement proteins of the acorn barnacle, Megabalanus rosa.* Biological Bulletin, 1996. 190: p. 403-409.

58. Marechal, J.P. and C. Hellio, *Challenges for the development of new non-toxic antifouling solutions.* International Journal of Molecular Sciences, 2009. 10: p. 4623-4637.

59. Schultz, M.P., *Effects of coating roughness and biofouling on ship resistance and powering.* Biofouling, 2007. 23: p. 331-41.

60. Salta, M., J.A. Wharton, P. Stoodley, S.P. Dennington, L.R. Goodes, S. Werwinski, U. Mart, R.J.K. Wood, and K.R. Stokes, *Designing biomimetic antifouling surfaces.* Philosophical Transactions of the Royal Society a-Mathematical Physical and Engineering Sciences, 2010. 368: p. 4729-4754.

61. Kiil, S., C.E. Weinell, D.M. Yebra, and K. Dam-Johansen, *Marine biofouling protection: design of controlled release antifouling paints.* Chemical Product Design: Toward a Perspective through Case Studies, 2007. 23: p. 181-238.

62. Piola, R.F., K.A. Dafforn, and E.L. Johnston, *The influence of antifouling practices on marine invasions (vol 332, pg 41, 2007).* Biofouling, 2010. 26: p. 497-497.

63. Characklis, W.G., *Microbial biofouling.* In: Biofilms (John Wiley & Sons), 1990: p. 523-584.

64. Delauney, L., C. Compere, and M. Lehaitre, *Biofouling protection for marine environmental sensors.* Ocean Science, 2010. 6: p. 503-511.

65. Langhamer, O., D. Wilhelmsson, and J. Engstrom, *Artificial reef effect and fouling impacts on offshore wave power foundations and buoys - a pilot study.* Estuarine Coastal and Shelf Science, 2009. 82: p. 426-432.

66. Fitzgerald, J.W., M.S. Davies, and G.B. Hurdle, *Corrosion and fouling of sonar equipment.* Pt. 1. Report no. S2477, Naval Research Laboratory, March, 1947., 1947.

67. Houghton, D.R., *Marine Fouling and Offshore Structures.* Ocean Management, 1978. 4: p. 347-352.

68. Venugopalan, V.P. and A.B. Wagh, *Biofouling of an offshore oil platform - faunal composition and biomass.* Indian Journal of Marine Sciences, 1990. 19: p. 53-56.

69. Paschen, M., U. Rudorf, and C. Dally, *Bio-fouling on underwater cables –results of long-term storage tests of different cable sheathing materials in the Baltic Sea.* European International Journal of Science and Technology, 2014. 3: p. 52-62.

70. Dexter, S.C., H.J. Zhang, and P. Chandrasekaran, *Biofouling effects on corrosion of stainless alloys in seawater.* Biodeterioration Research, 1994. 4: p. 553-571.

71. Teng, F., Y.T. Guan, and W.P. Zhu, *Effect of biofilm on cast iron pipe corrosion in drinking water distribution system: Corrosion scales characterization and microbial community structure investigation.* Corrosion Science, 2008. 50: p. 2816-2823.

72. Hole, W.O.I., *Marine fouling and its prevention.* U.S. Naval Institute: Annapolis, MD, 1952.

73. Thomas, K.V. and S. Brooks, *The environmental fate and effects of antifouling paint biocides.* Biofouling, 2010. 26: p. 73-88.

74. Almeida, E., T.C. Diamantino, and O. de Sousa, *Marine paints: The particular case of antifouling paints.* Progress in Organic Coatings, 2007. 59: p. 2-20.

75. Omae, M., *General aspects of tin-free antifouling paints.* Chemical Reviews, 2003. 103: p. 3431-3448.

76. Callow, J.A. and M.E. Callow, *Trends in the development of environmentally friendly fouling-resistant marine coatings.* Nature communications, 2011. 2: p. 244.

77. Estarlich, F.F., S.A. Lewey, T.G. Nevell, A.A. Thorpe, J. Tsibouklis, and A.C. Upton, *The surface properties of some silicone and fluorosilicone coating materials immersed in seawater.* Biofouling, 2000. 16: p. 263-275.

78. Callow, M.E. and R.L. Fletcher, *The influence of low surface-energy materials on bioadhesion - a review.* International Biodeterioration & Biodegradation, 1994. 34: p. 333-348.

79. Brady, R.F. and I.L. Singer, *Mechanical factors favoring release from fouling release coatings.* Biofouling, 2000. 15: p. 73-81.

80. Stein, J., K. Truby, C.D. Wood, J. Stein, M. Gardner, G. Swain, C. Kavanagh, B. Kovach, M. Schultz, D. Wiebe, E. Holm, J. Montemarano, D. Wendt, C. Smith, and A. Meyer, *Silicone foul release coatings: Effect of the interaction of oil and coating functionalities on the magnitude of macrofouling attachment strengths.* Biofouling, 2003. 19: p. 71-82.

81. Wynne, K.J., G.W. Swain, R.B. Fox, S. Bullock, and J. Uilk, *Two silicone nontoxic fouling release coatings: Hydrosilation cured PDMS and CaCO3 filled, ethoxysiloxane cured RTV11.* Biofouling, 2000. 16: p. 277-+.

82. Bodkhe, R.B., S.J. Stafslien, J. Daniels, N. Cilz, A.J. Muelhbert, S.E.M. Thompson, M.E. Callow, J.A. Callow, and D.C. Webster, *Zwitterionic siloxane-polyurethane fouling-release coatings.* Progress in Organic Coatings, 2015. 78: p. 369-380.

83. Bers, A.V. and M. Wahl, *The influence of natural surface microtopographies on fouling.* Biofouling, 2004. 20: p. 43-51.

84. Schumacher, J.F., N. Aldred, M.E. Callow, J.A. Finlay, J.A. Callow, A.S. Clare, and A.B. Brennan, *Species-specific engineered antifouling topographies: correlations between the settlement of algal zoospores and barnacle cyprids.* Biofouling, 2007. 23: p. 307-317.

85. Schumacher, J.F., M.L. Carman, T.G. Estes, A.W. Feinberg, L.H. Wilson, M.E. Callow, J.A. Callow, J.A. Finlay, and A.B. Brennan, *Engineered antifouling microtopographies - effect of feature size, geometry, and roughness on settlement of zoospores of the green alga Ulva.* Biofouling, 2007. 23: p. 55-62.

86. Berntsson, K.M., P.R. Jonsson, M. Lejhall, and P. Gatenholm, *Analysis of behavioural rejection of micro-textured surfaces and implications for recruitment by the barnacle Balanus improvisus.* Journal of Experimental Marine Biology and Ecology, 2000. 251: p. 59-83.

87. Petronis, S., K. Berntsson, J. Gold, and P. Gatenholm, *Design and microstructuring of PDMS surfaces for improved marine biofouling resistance.* Journal of Biomaterials Science-Polymer Edition, 2000. 11: p. 1051-1072.

88. Quere, D., *Wetting and roughness.* Annual Review of Materials Research, 2008. 38: p. 71-99.

89. Marmur, A., *Super-hydrophobicity fundamentals: implications to biofouling prevention.* Biofouling, 2006. 22: p. 107-115.

90. Genzer, J. and K. Efimenko, *Recent developments in superhydrophobic surfaces and their relevance to marine fouling: a review.* Biofouling, 2006. 22: p. 339-360.

91. Xia, D.Y., L.M. Johnson, and G.P. Lopez, *Anisotropic Wetting Surfaces with One-Dimesional and Directional Structures: Fabrication Approaches, Wetting Properties and Potential Applications.* Advanced Materials, 2012. 24: p. 1287-1302.

92. Scardino, A.J., E. Harvey, and R. De Nys, *Testing attachment point theory: diatom attachment on microtextured polyimide biomimics.* Biofouling, 2006. 22: p. 55-60.

93. Scardino, A.J., J. Guenther, and R. de Nys, *Attachment point theory revisited: the fouling response to a microtextured matrix.* Biofouling, 2008. 24: p. 45-53.

94. Efimenko, K., J. Finlay, M.E. Callow, J.A. Callow, and J. Genzer, *Development and Testing of Hierarchically Wrinkled Coatings for Marine Antifouling.* Acs Applied Materials & Interfaces, 2009. 1: p. 1031-1040.

95. Lin, F.Y., W.Y. Chen, and M.T.W. Hearn, *Thermodynamic analysis of the interaction between proteins and solid surfaces: application to liquid chromatography.* Journal of Molecular Recognition, 2002. 15: p. 55-93.

96. Krishnan, S., R. Ayothi, A. Hexemer, J.A. Finlay, K.E. Sohn, R. Perry, C.K. Ober, E.J. Kramer, M.E. Callow, J.A. Callow, and D.A. Fischer, *Anti-biofouling properties of comblike block copolymers with amphiphilic side chains.* Langmuir, 2006. 22: p. 5075-86.

97. Gudipati, C.S., C.M. Greenlief, J.A. Johnson, P. Prayongpan, and K.L. Wooley, *Hyperbranched fluoropolymer and linear poly(ethylene glycol) based Amphiphilic crosslinked networks as efficient antifouling coatings: An insight into the surface compositions, topographies, and morphologies.* Journal of Polymer Science Part a-Polymer Chemistry, 2004. 42: p. 6193-6208.

98. Martinelli, E., S. Agostini, G. Galli, E. Chiellini, A. Glisenti, M.E. Pettitt, M.E. Callow, J.A. Callow, K. Graf, and F.W. Bartels, *Nanostructured films of amphiphilic fluorinated block copolymers for fouling release application.* Langmuir, 2008. 24: p. 13138-13147.

99. Martinelli, E., S. Menghetti, G. Galli, A. Glisenti, S. Krishnan, M.Y. Paik, C.K. Ober, D.M. Smilgies, and D.A. Fischer, *Surface Engineering of Styrene/PEGylated-Fluoroalkyl Styrene Block Copolymer Thin Films.* Journal of Polymer Science Part a-Polymer Chemistry, 2009. 47: p. 267-284.

100. Krishnan, S., C.J. Weinman, and C.K. Ober, *Advances in polymers for anti-biofouling surfaces.* Journal of Materials Chemistry, 2008. 18: p. 3405-3413.

101. Yang, W.J., K.G. Neoh, E.T. Kang, S.L.M. Teo, and D. Rittschof, *Polymer brush coatings for combating marine biofouling.* Progress in Polymer Science, 2014. 39: p. 1017-1042.

102. Kingshott, P., H. Thissen, and H.J. Griesser, *Effects of cloud-point grafting, chain length, and density of PEG layers on competitive adsorption of ocular proteins.* Biomaterials, 2002. 23: p. 2043-2056.

103. Schilp, S., A. Rosenhahn, M.E. Pettitt, J. Bowen, M.E. Callow, J.A. Callow, and M. Grunze, *Physicochemical properties of (ethylene glycol)-containing self-assembled monolayers relevant for protein and algal cell resistance.* Langmuir, 2009. 25: p. 10077-10082.

104. Harder, P., M. Grunze, R. Dahint, G.M. Whitesides, and P.E. Laibinis, *Molecular conformation in oligo(ethylene glycol)-terminated self-assembled monolayers on gold and*

silver surfaces determines their ability to resist protein adsorption. Journal of Physical Chemistry B, 1998. 102: p. 426-436.

105. Zhang, Z., J.A. Finlay, L.F. Wang, Y. Gao, J.A. Callow, M.E. Callow, and S.Y. Jiang, *Polysulfobetaine-grafted surfaces as environmentally benign ultralow fouling marine coatings.* Langmuir, 2009. 25: p. 13516-13521.

106. Ista L. K., L.G.P., *Lower critical solubility temperature materials as biofouling release agents.* Journal of Industrial Microbiology and Biotechnology, 1998. 20: p. 121-125.

107. Ista L. K., M.S., Perez-Luna V. H., Lopez G. P., *Synthesis of poly(N-isopropylacrylamide) on initiator-modified self-assembled monolayers.* Langmuir, 2001. 17: p. 2552-2555.

108. Ista, L.K., V.H. Pérez-Luna, and G.P. López, *Surface-grafted, environmentally sensitive polymers for biofilm release.* Applied and Environmental Microbiology, 1999. 64: p. 1603-1609.

109. Ista L. K., M.S., Lopez G. P., *Attachment and detachment of bacteria on surfaces with tunable and switchable wettability.* Biofouling, 2010. 26: p. 111-118.

110. Thome, I., S. Bauer, S. Vater, K. Zargiel, J.A. Finlay, M.P. Arpa-Sancet, M. Alles, J.A. Callow, M.E. Callow, G.W. Swain, M. Grunze, and A. Rosenhahn, *Conditioning of Self-assembled Monolayers at Two Static Immersion Test Sites Along the East Coast of Florida and its Effect on Early Fouling Development.* Biofouling, 2014. 30: p. 1011-1021.

111. Callow, M.E., A.R. Jennings, A.B. Brennan, C.E. Seegert, A. Gibson, L. Wilson, A. Feinberg, R. Baney, and J.A. Callow, *Microtopographic cues for settlement of zoospores of the green fouling alga Enteromorpha.* Biofouling, 2002. 18: p. 237-245.

112. Hoipkemeier-Wilson, L., J. Schumacher, M. Carman, A. Gibson, A. Feinberg, M. Callow, J. Finlay, J. Callow, and A. Brennan, *Antifouling potential of lubricious, micro-engineered, PDMS elastomers against zoospores of the green fouling alga Ulva (Enteromorpha).* Biofouling, 2004. 20: p. 53-63.

113. Myan, F.W.Y., J. Walker, and O. Paramor, *The interaction of marine fouling organisms with topography of varied scale and geometry: a review.* Biointerphases, 2013. 8: p. 30.

114. Thome, I., M.E. Pettitt, M.E. Callow, J.A. Callow, M. Grunze, and A. Rosenhahn, *Conditioning of surfaces by macromolecules and its implication for the settlement of zoospores of the green alga Ulva linza.* Biofouling, 2012. 28: p. 501-510.

115. Zhang, H., R. Lamb, and J. Lewis, *Engineering nanoscale roughness on hydrophobic surface - preliminary assessment of fouling behaviour.* Science and Technology of Advanced Materials, 2005. 6: p. 236-239.

116. Xiao, L.L., J.S. Li, S. Mieszkin, A. Di Fino, A.S. Clare, M.E. Callow, J.A. Callow, M. Grunze, A. Rosenhahn, and P.A. Levkin, *Slippery liquid-infused porous surfaces showing marine antibiofouling properties.* Acs Applied Materials & Interfaces, 2013. 5: p. 10074-10080.

117. Shivapooja, P., Q. Wang, B. Orihuela, D. Rittschof, G.P. Lopez, and X. Zhao, *Bioinspired surfaces with dynamic topography for active control of biofouling.* Advanced materials, 2013. 25: p. 1430-4.

118. Fratzl, P., *Biomimetic materials research: what can we really learn from nature's structural materials?* Journal of the Royal Society Interface, 2007. 4: p. 637-42.

119. Hall-Stoodley, L., J.W. Costerton, and P. Stoodley, *Bacterial biofilms: From the natural environment to infectious diseases.* Nature Reviews Microbiology, 2004. 2: p. 95-108.

120. Callow, M.E. and J.A. Callow, *Marine biofouling: a sticky problem.* Biologist, 2002. 49: p. 10-14.

121. Bryers, J.D., *Medical biofilms.* Biotechnology and bioengineering, 2008. 100: p. 1-18.

122. Chung, J.Y. and M.K. Chaudhury, *Soft and hard adhesion.* Journal of Adhesion, 2005. 81: p. 1119-1145.

123. Efimenko, K., M. Rackaitis, E. Manias, A. Vaziri, L. Mahadevan, and J. Genzer, *Nested self-similar wrinkling patterns in skins.* Nature Materials, 2005. 4: p. 293-297.

124. Brady, R.F., *Properties which influence marine fouling resistance in polymers containing silicon and fluorine.* Progress in Organic Coatings, 1999. 35: p. 31-35.

125. Swain, G.W., B. Kovach, A. Touzot, F. Casse, and C. Kavanagh, *Measuring the performance of today's antifouling coatings.* Journal of Ship Production, 2007. 23: p. 164-170.

126. Ralston, E. and G. Swain, *Bioinspiration - the solution for biofouling control?* Bioinspiration & Biomimetics, 2009. 4: p. 1-9.

127. Wanner, A., *Clinical aspects of mucociliary transport.* The American review of respiratory disease, 1977. 116: p. 73-125.

128. Matsui, H., B.R. Grubb, R. Tarran, S.H. Randell, J.T. Gatzy, C.W. Davis, and R.C. Boucher, *Evidence for periciliary liquid layer depletion, not abnormal ion composition, in the pathogenesis of cystic fibrosis airways disease.* Cell, 1998. 95: p. 1005-1015.

129. Sanchez, T., D. Welch, D. Nicastro, and Z. Dogic, *Cilia-like beating of active microtubule bundles.* Science, 2011. 333: p. 456-459.

130. Wahl, M., K. Kroger, and M. Lenz, *Non-toxic protection against epibiosis.* Biofouling, 1998. 12: p. 205-226.

131. Evans, B.A., A.R. Shields, R.L. Carroll, S. Washburn, M.R. Falvo, and R. Superfine, *Magnetically actuated nanorod arrays as biomimetic cilia.* Nano Letters, 2007. 7: p. 1428-1434.

132. Ghosh, R., G.A. Buxton, O.B. Usta, A.C. Balazs, and A. Alexeev, *Designing oscillating cilia that capture or release microscopic particles.* Langmuir, 2010. 26: p. 2963-2968.

133. Dayal, P., O. Kuksenok, A. Bhattacharya, and A.C. Balazs, *Chemically-mediated communication in self-oscillating, biomimetic cilia.* Journal of Materials Chemistry, 2012. 22: p. 241-250.

134. Sidorenko, A., T. Krupenkin, A. Taylor, P. Fratzl, and J. Aizenberg, *Reversible switching of hydrogel-actuated nanostructures into complex micropatterns.* Science, 2007. 315: p. 487-490.

135. D'Souza, F., A. Bruin, R. Biersteker, G. Donnelly, J. Klijnstra, C. Rentrop, and P. Willemsen, *Bacterial assay for the rapid assessment of antifouling and fouling release properties of coatings and materials.* Journal of Industrial Microbiology & Biotechnology, 2010. 37: p. 363-370.

136. Hughes, T.J.R., *The finite element method: linear static and dynamic finite element analysis*, ed. H.T.J. R. Vol. 65. 2000: Dover Publications.

137. Rittschof, D., B. Orihuela, S. Stafslien, J. Daniels, D. Christianson, B. Chisholm, and E. Holm, *Barnacle reattachment: a tool for studying barnacle adhesion.* Biofouling, 2008. 24: p. 1-9.

138. Lu, N., J. Yoon, and Z. Suo, *Delamination of stiff islands patterned on stretchable substrates.* International Journal of Materials Research, 2007. 98: p. 717-722.

139. Williams, J., *Energy release rates for the peeling of flexible membranes and the analysis of blister tests.* International Journal of Fracture, 1997. 87: p. 265-288.

140. Wang, Q., M. Tahir, J. Zang, and X. Zhao, *Dynamic electrostatic lithography: Multiscale on-demand patterning on large-area curved surfaces.* Advanced Materials, 2012. DOI: 10.1002/adma.201200272.

141. Maki, J.S., D. Rittschof, M.-Q. Samuelsson, U. Szewzyk, A.B. Yule, S. I(jelleberg, J.D. Costlow, and R. Mitchell, *Effect of marine bacteria and their expolymers on the attachment of barnacle cypris larvae.* Bulletin of Marine Science, 1990. 46: p. 499-511.

142. Unabia, C.R.C. and M.G. Hadfield, *Role of bacteria in larval settlement and metamorphosis of the polychaete Hydroides elegans.* Marine Biology, 1999. 133: p. 55-64.

143. Shea, C., L.J. Lovelace, and H.E. Smith-Somerville, *Deleya marina as a model organism for studies of bacterial colonization and biofilm formation.* Journal of Microbiology and Biotechnology, 1995. 15.

144. Costerton, J.W., Z. Lewandowski, D.E. Caldwell, D.R. Korber, and H.M. Lappin-Scott, *Microbial Biofilms.* Annual Reviews Microbiology, 1995. 49: p. 711-745.

145. Hutchinson, J.W. and Z. Suo, *Mixed-mode cracking in layered materials.* Advances in Applied Mechanics, 1992. 29: p. 63-191.

146. Shaw, T., M. Winston, C.J. Rupp, I. Klapper, and P. Stoodley, *Commonality of elastic relaxation times in biofilms.* Physical Review Letters, 2004. 93.

147. Lu, N., J. Yoon, and Z. Suo, *Delamination of stiff islands patterned on stretchable substrates.* Int. J. Mater. Res., 2007. 98: p. 717-722.

148. Ramsay, D.B., G.H. Dickinson, B. Orihuela, D. Rittschof, and K.J. Wahl, *Base plate mechanics of the barnacle Balanus amphitrite (=Amphibalanus amphitrite).* Biofouling, 2008. 24: p. 109-118.

149. Chen, S.H. and H.J. Gao, *Non-slipping adhesive contact of an elastic cylinder on stretched substrates.* Preceedings of the Royal Society A-Mathematical Physical and Engineering Sciences, 2006. 462: p. 211-228.

150. Waters, J.F., J. Kalow, H. Gao, and P.R. Guduru, *Axisymmetric adhesive contact under equibiaxial stretching.* Journal of Adhesion, 2012. 88: p. 134-144.

151. Sun, J.-Y., N. Lu, J. Yoon, K.-H. Oh, Z. Suo, and J.J. Vlassak, *Debonding and fracture of ceramic islands on polymer substrates.* Journal of Applied Physics, 2012. 111.

152. Ilievski, F., A.D. Mazzeo, R.E. Shepherd, X. Chen, and G.M. Whitesides, *Soft robotics for chemists.* Angewandte Chemie-International Edition, 2011. 50: p. 1890-1895.

153. Holmes, D.P. and A.J. Crosby, *Snapping surfaces.* Advanced Materials, 2007. 19: p. 3589-+.

154. Thorsen, T., S.J. Maerkl, and S.R. Quake, *Microfluidic large-scale integration.* Science, 2002. 298: p. 580-584.

155. Characklis, W.G., *Fouling biofilm development - a process analysis.* Biotechnology and Bioengineering, 1981. 23: p. 1923-1960.

156. Aftring, R.P. and B.F. Taylor, *Assessment of microbial fouling in an ocean thermal-energy conversion experiment.* Applied and Environmental Microbiology, 1979. 38: p. 734-739.

157. Jain, A. and N. Bhosle, *Biochemical composition of the marine conditioning film: implications for bacterial adhesion.* Biofouling, 2009. 25: p. 13-19.

158. Mieszkin, S., M.E. Callow, and J.A. Callow, *Interactions between microbial biofilms and marine fouling algae: a mini review.* Biofouling, 2013. 29: p. 1097-1113.

159. Schultz, M.P., J.A. Bendick, E.R. Holm, and W.M. Hertel, *Economic impact of biofouling on a naval surface ship.* Biofouling, 2011. 27: p. 87-98.

160. Swain, G.W., B. Kovach, T. Arthur, F. Casse, and C. Kavanagh, *Measuring the performance of today's antifouling coatings.* Journal of Ship Production, 2007. 23: p. 164-170.

161. Casanueva, J.F., J. Sanchez, J.L. Garcia-Morales, T. Casanueva-Robles, J.A. Lopez, J.R. Portela, E. Nebot, and D. Sales, *Portable pilot plant for evaluating marine biofouling growth and control in heat exchangers-condensers.* Water science and technology : a journal of the International Association on Water Pollution Research, 2003. 47: p. 99-104.

162. Nebot, E., J.F. Casanueva, R. Solera, C. Pendon, L.J. Taracido, T. Casanueva-Robles, and C. Lopez-Galindo, *Marine biofouling in heat exchangers.* In Biofouling: Types, Impact and Anti-Fouling, 2010: p. 65-104.

163. Wang, D.C., C.F. Qian, S.X. Cao, Y. Liu, and J.W. Sun, *Effect of different biofouling characteristics on heat transfer of the heat exchanger.* Applied Energy Technology, Pts 1 and 2, 2013. 724-725: p. 1282-1288.

164. Sonak, S., P. Pangam, A. Giriyan, and K. Hawaldar, *Implications of the ban on organotins for protection of global coastal and marine ecology.* Journal of Environmental Management, 2009. 90: p. S96-S108.

165. Voulvoulis, N., M.D. Scrimshaw, and J.N. Lester, *Alternative antifouling biocides.* Applied Organometallic Chemistry, 1999. 13: p. 135-143.

166. Gittens, J.E., T.J. Smith, R. Suleiman, and R. Akid, *Current and emerging environmentally-friendly systems for fouling control in the marine environment.* Biotechnology advances, 2013. 31: p. 1738-1753.

167. Callow, J.A. and M.E. Callow, *Trends in the development of environmentally friendly fouling-resistant marine coatings.* Nature Communications, 2011. 2: p. 1-10.

168. Baier, R.E., *Surface properties influencing biological adhesion.* In: Adhesion in Biological Systems, 1970. R. S. Manly, Ed.: p. 15-48.

169. Chaudhury, M.K., J.A. Finlay, J.Y. Chung, M.E. Callow, and J.A. Callow, *The influence of elastic modulus and thickness on the release of the soft-fouling green alga Ulva linza (syn. Enteromorpha linza) from poly(dimethylsiloxane) (PDMS) model networks.* Biofouling, 2005. 21: p. 41-48.

170. Singer, I.L., J.G. Kohl, and M. Patterson, *Mechanical aspects of silicone coatings for hard foulant control.* Biofouling, 2000. 16: p. 301-309.

171. Kendall, K., *The adhesion and surface energy of elastic solids.* Journal of Physics D: Applied Physics, 1971. 4: p. 1186-1195.

172. Holm, E.R., *Barnacles and biofouling.* Integrative and Comparative Biology, 2012. 52: p. 348-355.

173. Meyer, A., R. Baier, C.D. Wood, J. Stein, K. Truby, E. Holm, J. Montemarano, C. Kavanagh, B. Nedved, C. Smith, G. Swain, and D. Wiebe, *Contact angle anomalies indicate that surface-active eluates from silicone coatings inhibit the adhesive mechanisms of fouling organisms.* Biofouling, 2006. 22: p. 411-423.

174. Stein, J., K. Truby, C.D. Wood, M. Takemori, M. Vallance, G. Swain, C. Kavanagh, B. Kovach, M. Schultz, D. Wiebe, E. Holm, J. Montemarano, D. Wendt, C. Smith, and A. Meyer, *Structure-property relationships of silicone biofouling-release coatings: effect of silicone network architecture on pseudobarnacle attachment strengths.* Biofouling, 2003. 19: p. 87-94.

175. Scardino, A.J. and R. de Nys, *Mini review: Biomimetic models and bioinspired surfaces for fouling control.* Biofouling, 2011. 27: p. 73-86.

176. Halder, P., M. Nasabi, N. Jayasuriya, J. Shimeta, M. Deighton, S. Bhattacharya, A. Mitchell, and M.A. Bhuiyan, *An assessment of the dynamic stability of microorganisms on patterned surfaces in relation to biofouling control.* Biofouling, 2014. 30: p. 695-707.

177. Ling, G.C., M.H. Low, M. Erken, S. Longford, S. Nielsen, A.J. Poole, P. Steinberg, D. McDougald, and S. Kjelleberg, *Micro-fabricated polydimethyl siloxane (PDMS) surfaces regulate the development of marine microbial biofilm communities.* Biofouling, 2014. 30: p. 323-335.

178. Vucko, M.J., A.J. Poole, C. Carl, B.A. Sexton, F.L. Glenn, S. Whalan, and R. de Nys, *Using textured PDMS to prevent settlement and enhance release of marine fouling organisms.* Biofouling, 2014. 30: p. 1-16.

179. Zargiel, K.A. and G.W. Swain, *Static vs dynamic settlement and adhesion of diatoms to ship hull coatings.* Biofouling, 2014. 30: p. 115-129.

180. Majumdar, P., E. Crowley, M. Htet, S.J. Stafslien, J. Daniels, L. VanderWal, and B.J. Chisholm, *Combinatorial materials research applied to the development of new surface coatings XV: An investigation of polysiloxane anti-fouling/fouling-release coatings containing tethered quaternary ammonium salt groups.* Acs Combinatorial Science, 2011. 13: p. 298-309.

181. Shivapooja, P., Q. Wang, B. Orihuela, D. Rittschof, G.P. Lopez, and X. Zhao, *Bioinspired surfaces with dynamic topography for active control of biofouling.* Adv Mater, 2013. 25: p. 1430-1434.

182. Briand, J.F., *Marine antifouling laboratory bioassays: an overview of their diversity.* Biofouling, 2009. 25: p. 297-311.

183. Arruda, E.M. and M.C. Boyce, *A 3-dimensional constitutive model for the large stretch behavior of rubber elastic-materials.* Journal of the Mechanics and Physics of Solids, 1993. 41: p. 389-412.

184. Gerba, C.P. and J.S. McLeod, *Effect of sediments on the survival of Escherichia coli in marine waters.* Applied and environmental microbiology, 1976. 32: p. 114-20.

185. Vogel, V., *Soft robotics: bionic jellyfish.* Nature materials, 2012. 11: p. 841-842.

186. Kim, S., C. Laschi, and B. Trimmer, *Soft robotics: a bioinspired evolution in robotics.* Trends in Biotechnology, 2013. 31: p. 23-30.

187. Shepherd, R.F., F. Ilievski, W. Choi, S.A. Morin, A.A. Stokes, A.D. Mazzeo, X. Chen, M. Wang, and G.M. Whitesides, *Multigait soft robot.* Proceedings of the National Academy of Sciences of the United States of America, 2011. 108: p. 20400-3.

188. Kim, J., E. Nyren-Erickson, S. Stafslien, J. Daniels, J. Bahr, and B.J. Chisholm, *Release characteristics of reattached barnacles to non-toxic silicone coatings.* Biofouling, 2008. 24: p. 313-319.

189. McLean, R.J. and T.R. Simpson, *Preparing for biofilm studies in the field.* Current protocols in microbiology, 2008. Chapter 1: p. Unit 1B 4 1-1B 1 14.

190. Zhang, J.W., C.G. Lin, L. Wang, J.Y. Zheng, F.L. Xu, and Z.Y. Sun, *Study on the correlation of lab assay and field test for fouling-release coatings.* Progress in Organic Coatings, 2013. 76: p. 1430-1434.

191. Ribeiro, E., S.J. Stafslien, F. Casse, J.A. Callow, M.E. Callow, R.J. Pieper, J.W. Daniels, J.A. Bahr, and D.C. Webster, *Automated image-based method for laboratory screening of coating libraries for adhesion of algae and bacterial biofilms.* Journal of Combinatorial Chemistry, 2008. 10: p. 586-594.

192. Holland, R., T.M. Dugdale, R. Wetherbee, A.B. Brennan, J.A. Finlay, J.A. Callow, and M.E. Callow, *Adhesion and motility of fouling diatoms on a silicone elastomer.* Biofouling, 2004. 20: p. 323-329.

193. Cagni, A., C. Chuard, P.E. Vaudaux, J. Schrenzel, and D.P. Lew, *Comparison of sparfloxacin, temafloxacin, and ciprofloxacin for prophylaxis and treatment of experimental foreign-body infection by methicillin-resistant staphylococcus-aureus.* Antimicrobial Agents and Chemotherapy, 1995. 39: p. 1655-1660.

194. Rittschof, D., C.H. Lai, L.M. Kok, and S.L.M. Teo, *Pharmaceuticals as antifoulants: Concept and principles.* Biofouling, 2003. 19: p. 207-212.

195. Jones, G.L., C.T. Muller, M. O'Reilly, and D.J. Stickler, *Effect of triclosan on the development of bacterial biofilms by urinary tract pathogens on urinary catheters.* Journal of Antimicrobial Chemotherapy, 2006. 57: p. 266-272.

196. Bott, T.R., *Introduction to the problem of biofouling in industrial equipment*, in *Biofilms — Science and Technology*, L.F. Melo, et al., Editors. 1992, Springer: Netherlands. p. 3-11.

197. Yebra, D.M., S. Kiil, and K. Dam-Johansen, *Antifouling Technology - Past, Present and Future Steps Towards Efficient and Environmentally Friendly Antifouling Coatings.* Prog. Org. Coat., 2004. 50: p. 75-104.

198. Callow, M.E. and R.L. Fletcher, *The Influence of Low Surface-energy Materials on Bioadhesion - A Review.* Int. Biodeter. Biodegr., 1994. 34: p. 333-348.

199. Brady, R.F. and I.L. Singer, *Mechanical Factors Favoring Release from Fouling Release Coatings.* Biofouling, 2000. 15: p. 73-81.

200. Rittschof, D., B. Orihuela, T. Harder, S. Stafslien, B. Chisholm, and G.H. Dickinson, *Compounds from Silicones Alter Enzyme Activity in Curing Barnacle Glue and Model Enzymes.* Plos One, 2011. 6: p. e16487.

201. Scardino, A.J. and R. de Nys, *Mini Review: Biomimetic Models and Bioinspired Surfaces for Fouling Control.* Biofouling, 2011. 27: p. 73-86.

202. Zhang, Z., J.A. Finlay, L.F. Wang, Y. Gao, J.A. Callow, M.E. Callow, and S.Y. Jiang, *Polysulfobetaine-Grafted Surfaces as Environmentally Benign Ultralow Fouling Marine Coatings.* Langmuir, 2009. 25: p. 13516-13521.

203. Yu, Q., J. Cho, P. Shivapooja, L.K. Ista, and G.P. Lopez, *Nanopatterned smart polymer surfaces for controlled attachment, killing, and release of bacteria.* Acs Applied Materials & Interfaces, 2013. 5: p. 9295-9304.

204. Xiao, L.L., J.S. Li, S. Mieszkin, A. Di Fino, A.S. Clare, M.E. Callow, J.A. Callow, M. Grunze, A. Rosenhahn, and P.A. Levkin, *Slippery Liquid-Infused Porous Surfaces Showing Marine Antibiofouling Properties.* ACS Appl. Mater. Interfaces, 2013. 5: p. 10074-10080.

205. Marechal, J.P. and C. Hellio, *Challenges for the Development of New Non-Toxic Antifouling Solutions.* Int. J. Mol. Sci., 2009. 10: p. 4623-4637.

206. Shivapooja, P., Q. Wang, B. Orihuela, D. Rittschof, G.P. Lopez, and X. Zhao, *Bioinspired Surfaces with Dynamic Topography for Active Control of Biofouling.* Adv. Mater., 2013. 25: p. 1430-1434.

207. Levering, V., Q. Wang, P. Shivapooja, X. Zhao, and G.P. Lopez, *Soft Robotic Concepts in Catheter Design: An On-demand Fouling-release Urinary Catheter.* Adv. Healthc. Mater., 2014. 3: p. 1588-1596.

208. Shivapooja, P., Q.M. Wang, L.M. Szott, B. Orihuela, D. Rittschof, X.H. Zhao, and G.P. Lopez, *Dynamic surface deformation of silicone elastomers for management of marine biofouling: Laboratory and field studies using pneumatic actuation.* Biofouling, 2015. 31: p. 265-274.

209. Jones, D.M., A.A. Brown, and W.T.S. Huck, *Surface-initiated polymerizations in aqueous media: Effect of initiator density.* Langmuir, 2002. 18: p. 1265-1269.

210. Matyjaszewski, K., H. Dong, W. Jakubowski, J. Pietrasik, and A. Kusumo, *Grafting from surfaces for "Everyone": ARGET ATRP in the presence of air.* Langmuir, 2007. 23: p. 4528-4531.

211. Yu, Q., Y.X. Zhang, H. Chen, F. Zhou, Z.Q. Wu, H. Huang, and J.L. Brash, *Protein adsorption and cell adhesion/detachment behavior on dual-responsive silicon surfaces modified with poly(N-isopropylacrylamide)-block-polystyrene copolymer.* Langmuir, 2010. 26: p. 8582-8588.

212. Pitombo, F.B., *Phylogenetic analysis of the balanidae (Cirripedia, Balanomorpha).* Zoologica Scripta, 2004. 33: p. 261-276.

213. Rittschof, D., B. Orihuela, S. Stafslien, J. Daniels, D. Christianson, B. Chisholm, and E. Holm, *Barnacle Reattachment: A Tool for Studying Barnacle Adhesion.* Biofouling, 2008. 24: p. 1-9.

214. Rittschof, D., E.S. Branscomb, and J.D. Costlow, *Settlement and behavior in relation to flow and surface in larval barnacles, balanus-amphitrite Darwin.* Journal of Experimental Marine Biology and Ecology, 1984. 82: p. 131-146.

215. Yu, Q., P. Shivapooja, L.M. Johnson, G. Tizazu, G.J. Leggett, and G.P. Lopez, *Nanopatterned polymer brushes as switchable bioactive interfaces.* Nanoscale, 2013. 5: p. 3632-3637.

216. Ribeiro, E., S.J. Stafslien, F. Casse, J.A. Callow, M.E. Callow, R.J. Pieper, J.W. Daniels, J.A. Bahr, and D.C. Webster, *Automated Image-based Method for Laboratory Screening of Coating Libraries for Adhesion of Algae and Bacterial Biofilms.* J. Comb. Chem., 2008. 10: p. 586-594.

217. Keefe, A.J., N.D. Brault, and S.Y. Jiang, *Suppressing surface reconstruction of superhydrophobic PDMS using a superhydrophilic zwitterionic polymer.* Biomacromolecules, 2012. 13: p. 1683-1687.

218. Yeh, S.B., C.S. Chen, W.Y. Chen, and C.J. Huang, *Modification of silicone elastomer with zwitterionic silane for durable antifouling properties.* Langmuir, 2014. 30: p. 11386-11393.

219. Efimenko, K., W.E. Wallace, and J. Genzer, *Surface modification of Sylgard-184 poly(dimethyl siloxane) networks by ultraviolet and ultraviolet/ozone treatment.* Journal of Colloid and Interface Science, 2002. 254: p. 306-315.

220. Ahmed, S., H.K. Yang, A.E. Ozcam, K. Efimenko, M.C. Weiger, J. Genzer, and J.M. Haugh, *Poly(vinylmethylsiloxane) Elastomer Networks as Functional Materials for Cell Adhesion and Migration Studies.* Biomacromolecules, 2011. 12: p. 1265-1271.

221. Wang, C.H., C.F. Ma, C.D. Mu, and W. Lin, *A novel spproach for dynthesis of zwitterionic polyurethane coating with protein resistance.* Langmuir, 2014. 30: p. 12860-12867.

222. Burden, D.K., D.E. Barlow, C.M. Spillmann, B. Orihuela, D. Rittschof, R.K. Everett, and K.J. Wahl, *Barnacle balanus amphitrite adheres by a stepwise cementing process.* Langmuir, 2012. 28: p. 13364-13372.

223. Pechenik, J.A., D. Rittschof, and A.R. Schmidt, *Influence of delayed metamorphosis on survival and growth of juvenile barnacles balanus-amphitrite.* Marine Biology, 1993. 115: p. 287-294.

224. Aldred, N., G.Z. Li, Y. Gao, A.S. Clare, and S.Y. Jiang, *Modulation of Barnacle (Balanus Amphitrite Darwin) Cyprid Settlement Behavior by Sulfobetaine and Carboxybetaine Methacrylate Polymer Coatings.* Biofouling, 2010. 26: p. 673-683.

225. Quintana, R., M. Gosa, D. Janczewski, E. Kutnyanszky, and G.J. Vancso, *Enhanced stability of low fouling zwitterionic polymer brushes in seawater with diblock architecture.* Langmuir, 2013. 29: p. 10859-10867.

226. Xie, Q., C. Ma, C. Liu, J. Ma, and G. Zhang, *Poly(dimethylsiloxane)-based polyurethane with chemically attached antifoulants for durable marine antibiofouling.* Acs Applied Materials & Interfaces, 2015: p. DOI: 10.1021/acsami.5b07325.

227. Aftring, R.P. and B.F. Taylor, *Assessment of microbial fouling in an ocean thermal-energy conversion experiment.* Appl Environ Microb, 1979. 38: p. 734-739.

228. Callow, M.E. and J.E. Callow, *Marine biofouling: a sticky problem.* Biologist, 2002. 49: p. 1-5.

229. Characklis, W.G., *Fouling biofilm development - a process analysis.* Biotechnol Bioeng, 1981. 23: p. 1923-1960.

230. Bax, N., A. Williamson, M. Aguero, E. Gonzalez, and W. Geeves, *Marine invasive alien species: a threat to global biodiversity.* Marine Policy, 2003. 27: p. 313-323.

231. Sonak, S., P. Pangam, A. Giriyan, and K. Hawaldar, *Implications of the ban on organotins for protection of global coastal and marine ecology.* J Environ Manage, 2009. 90: p. S96-S108.

232. Callow, J.A. and M.E. Callow, *Trends in the development of environmentally friendly fouling-resistant marine coatings.* Nat Commun, 2011. 2: p. 1-10.

233. Truby, K., C. Wood, J. Stein, J. Cella, J. Carpenter, C. Kavanagh, G. Swain, D. Wiebe, D. Lapota, A. Meyer, E. Holm, D. Wendt, C. Smith, and J. Montemarano, *Evaluation of the performance enhancement of silicone biofouling-release coatings by oil incorporation.* Biofouling, 2000. 15: p. 141-+.

234. Kavanagh, C.J., G.W. Swain, B.S. Kovach, J. Stein, C. Darkangelo-Wood, K. Truby, E. Holm, J. Montemarano, A. Meyer, and D. Wiebe, *The effects of silicone fluid additives and silicone elastomer matrices on barnacle adhesion strength.* Biofouling, 2003. 19: p. 381-390.

235. Xiao, L.L., J.S. Li, S. Mieszkin, A. Di Fino, A.S. Clare, M.E. Callow, J.A. Callow, M. Grunze, A. Rosenhahn, and P.A. Levkin, *Slippery Liquid-Infused Porous Surfaces Showing Marine Antibiofouling Properties.* ACS Appl Mater Interfaces, 2013. 5: p. 10074-10080.

236. Carman, M.L., T.G. Estes, A.W. Feinberg, J.F. Schumacher, W. Wilkerson, L.H. Wilson, M.E. Callow, J.A. Callow, and A.B. Brennan, *Engineered antifouling microtopographies - correlating wettability with cell attachment.* Biofouling, 2006. 22: p. 11-21.

237. Fan, X.W., L.J. Lin, J.L. Dalsin, and P.B. Messersmith, *Biomimetic anchor for surface-initiated polymerization from metal substrates.* Journal of the American Chemical Society, 2005. 127: p. 15843-15847.

238. Majumdar, P., E. Crowley, M. Htet, S.J. Stafslien, J. Daniels, L. VanderWal, and B.J. Chisholm, *Combinatorial materials research applied to the development of new surface coatings XV: An investigation of polysiloxane anti-fouling/fouling-release coatings containing tethered auaternary ammonium salt groups.* Acs Combinatorial Science, 2011. 13: p. 298-309.

239. Shivapooja, P., L.K. Ista, H.E. Canavan, and G.P. Lopez, *ARGET-ATRP synthesis and characterization of PNIPAAm brushes for quantitative cell detachment studies.* Biointerphases, 2012. 7: p. 1-10.

240. Wang, C.H., C.F. Ma, C.D. Mu, and W. Lin, *A novel approach for synthesis of zwitterionic polyurethane coating with protein resistance.* Langmuir, 2014. 30: p. 12860-12867.

241. Kendall, K., *Adhesion and Surface Energy of Elastic Solids.* J Phys D Appl Phys, 1971. 4: p. 1186-1195.

242. Brady, R.F. and I.L. Singer, *Mechanical factors favoring release from fouling release coatings.* Biofouling, 2000. 15: p. 73-81.

243. Rittschof, D., B. Orihuela, T. Harder, S. Stafslien, B. Chisholm, and G.H. Dickinson, *Compounds from silicones alter enzyme activity in curing barnacle glue and model enzymes.* PLoS One, 2011. 6: p. e16487.

244. Levering, V., Q.M. Wang, P. Shivapooja, X.H. Zhao, and G.P. Lopez, *Soft robotic concepts in catheter design: an on-demand fouling-release urinary catheter.* Advanced Healthcare Materials, 2014. 3: p. 1588-1596.

245. Naldrett, M.J. and D.L. Kaplan, *Characterization of barnacle (Balanus eburneus and B-cenatus) adhesive proteins.* Marine Biology, 1997. 127: p. 629-635.

246. Sun, Y.J., S.L. Guo, G.C. Walker, C.J. Kavanagh, and G.W. Swain, *Surface elastic modulus of barnacle adhesive and release characteristics from silicone surfaces.* Biofouling, 2004. 20: p. 279-289.

247. Holm, E.R., *Barnacles and biofouling.* Integr Comp Biol, 2012. 52: p. 348-355.

248. Kamino, K., *Mini-review: Barnacle adhesives and adhesion.* Biofouling, 2013. 29: p. 735-749.

249. Nevell, T.G., D.P. Edwards, A.J. Davis, and R.A. Pullin, *The surface properties of silicone elastomers Exposed to seawater.* Biofouling, 1996. 10: p. 199-212.

250. Milne, A., *Coated marine surfaces.* UK Patent 1470465, 1977.

251. Nendza, M., *Hazard assessment of silicone oils (polydimethylsiloxanes, PDMS) used in antifouling-/foul-release-products in the marine environment.* Mar Pollut Bull, 2007. 54: p. 1190-1196.

252. Lejars, M., A. Margaillan, and C. Bressy, *Fouling Release Coatings: A Nontoxic Alternative to Biocidal Antifouling Coatings.* Chem Rev, 2012. 112: p. 4347-4390.

253. Swain, G.W. and M.P. Schultz, *The testing and evaluation of non-toxic antifouling coatings.* Biofouling, 1996. 10: p. 187-197.

254. Watermann, B., H.D. Berger, H. Sonnichsen, and P. Willemsen, *Performance and effectiveness of non-stick coatings in seawater.* Biofouling, 1997. 11: p. 101-118.

255. Wendt, D.E., G.L. Kowalke, J. Kim, and I.L. Singer, *Factors that influence elastomeric coating performance: the effect of coating thickness on basal plate morphology, growth and critical removal stress of the barnacle Balanus amphitrite.* Biofouling, 2006. 22: p. 1-9.

256. Rittschof, D., B. Orihuela, S. Stafslien, J. Daniels, D. Christianson, B. Chisholm, and E. Holm, *Barnacle reattachment: a tool for studying barnacle adhesion.* Biofouling, 2008. 24: p. 1-9.

257. Lu, N., J. Yoon, and Z. Suo, *Delamination of stiff islands patterned on stretchable substrates.* Int J Mater Res, 2007. 98: p. 717-722.

258. Kim, J., B.J. Chisholm, and J. Bahr, *Adhesion study of silicone coatings: the interaction of thickness, modulus and shear rate on adhesion force.* Biofouling, 2007. 23: p. 113-120.

259. Ahmed, N., T. Murosaki, T. Kurokawa, A. Kakugo, S. Yashima, Y. Nogata, and J.P. Gong, *Prolonged morphometric study of barnacles grown on soft substrata of hydrogels and elastomers.* Biofouling, 2014. 30: p. 271-279.

260. Chung, J.Y. and M.K. Chaudhury, *Soft and hard adhesion.* J Adhesion, 2005. 81: p. 1119-1145.

261. Levering, V., C. Cao, P. Shivapooja, H. Levinson, X. Zhao, and G.P. López, *Urinary catheter capable of repeated on-demand removal of infectious biofilms via active deformation.* Biomaterials, 2016. 77: p. 77-86.

262. Callow M. E., C.J.A., *Marine biofouling: a sticky problem.* Biologist, 2002. 49: p. 1-5.

263. Yu, Q., J. Cho, P. Shivapooja, L.K. Ista, and G.P. Lopez, *Nanopatterned Smart Polymer Surfaces for Controlled Attachment, Killing, and Release of Bacteria.* ACS Appl. Mater. Interfaces, 2013. 5: p. 9295-9304.

264. Cao, Y.H., Z.L. Wu, Y. Su, and Z.D. Xu, *Aircraft flight characteristics in icing conditions.* Progress in Aerospace Sciences, 2015. 74: p. 62-80.

265. Chen, M.J., Z. Zhang, and T.R. Bott, *Direct measurement of the adhesive strength of biofilms in pipes by micromanipulation.* Biotechnology Techniques, 1998. 12: p. 875-880.

Biography

Phanindhar Shivapooja was born in Hyderabad, India in 1987. He graduated high school from St. Jude's High School in 2004 and was the topper of his class. Phani received his B.S. in Chemical Engineering from Osmania University (Hyderabad) in 2008 where he conducted research under Dr. V.V. Basava Rao on biodegradation and bioremediation of toxic compounds from industrial wastewater. Phani joined the University of New Mexico in 2008 for the MS program in Chemical Engineering. He joined Dr. Gabriel López's lab and conduced his masters' thesis research on synthesis and applications of stimuli-responsive polymeric films. He graduated his MS in 2010 with a GPA of 4.0 and received a gold medal for Best Graduate Engineering from UNM. Phani began his PhD research in Biomedical Engineering at Duke University in 2010 and worked under Dr. López. As a PhD student research, he conducted basic and applied research on stimuli-responsive synthetic materials for biosensor, biomedical and marine application. His PhD research was closely guided Dr. López and other collaborators including Dr. Xuanhe Zhao and Dr. Daniel Rittschof. Phani's PhD research on active surface deformation for biofouling control was awarded with Triangle MRS Student Chapter's Best Technology Innovation Award. Phani participated in the CBTE and PhD Plus certificate programs at Duke University.

.

Publications

1. Urinary catheter capable of repeated on-demand removal of infectious biofilms via active deformation. V. Levering, C. Cao, **P. Shivapooja**, H. Levinson, X. Zhao, G.P. López, Biomaterials, **2016**, 77, p. 77-86.

2. Modification of silicone elastomer surfaces with zwitterionic polymers: Short term fouling resistance and triggered biofouling release. **P. Shivapooja**, Q. Yu, B. Orihuela, R. Mays, D. Rittschof, J. Genzer, G. P. López, ACS applied materials & interfaces, **2015**, 7 (46), p. 25586-25591.

3. Dynamic surface deformation of silicone elastomers for management of marine biofouling: laboratory and field studies using pneumatic actuation. **P. Shivapooja**, Q. Wang, L. M. Szott, B. Orihuela, D. Rittschof, X. Zhao, G. P. López, Biofouling, **2015**, 31 (3), p. 265-274.

4. Soft robotic concepts in catheter design: an on-demand fouling-release urinary catheter. V. Levering, Q. Wang, **P. Shivapooja**, X. Zhao, G. P. López, Advanced healthcare materials, **2014**, 3 (10), p. 1588-1596.

5. Nanopatterned smart polymer surfaces for controlled attachment, killing, and release of bacteria Q. Yu, J. Cho, **P. Shivapooja**, L. K. Ista, G. P. López, ACS applied materials & interfaces, **2013**, 5 (19), p. 9295-9304.

6. Bioinspired surfaces with dynamic topography for active control of biofouling. **P. Shivapooja**, Q. Wang, B. Orihuela, D. Rittschof, G. P. López, X. Zhao, Advanced Materials, **2013**, 25 (10), p. 1430-1434.

7. Nanopatterned polymer brushes as switchable bioactive interfaces. Q. Yu, **P. Shivapooja*** (*co-first author), L.M. Johnson, G. Tizazu, G.J. Leggett, G. P. López, Nanoscale, **2013**, 5 (9), p. 3632-3637.

8. ARGET–ATRP synthesis and characterization of PNIPAAm brushes for quantitative cell detachment studies. **P. Shivapooja**, L.K. Ista, H.E. Canavan, G. P. López, Biointerphases, **2012**, 7 (1), 32, p. 1-10.

Patent

1. Systems and methods for active biofouling control. Inventors: G. P Lopez, V. W Levering, X. Zhao, **P. Shivapooja**, Q. Wang. AUG 2014, PCT/US2012/058000.

Publications in preparation

1. Dynamic surface deformation of silicone-oil incorporated elastomer for barnacle detachment. **P. Shivapooja,** C. Cao, V. Levering, B. Orihuela, D. Rittschof, X.Zhao, G.P. López, (in preparation for submission to Biofouling journal).